Escuela Técnica Superior de Ingeniería Informática
Departamento de Tecnología Electrónica

Tesis doctoral
Compendio de publicaciones

Procesamiento y caracterización de bioseñales para su uso en interfaces de control y afectividad

Autor: **Manuel Merino Monge**
Ingeniero en Informática

Directores: **Isabel María Goméz González**
Alberto Jesús Molina Cantero

Sevilla, octubre de 2015

Agradecimientos

¡¿Quién me iba a decir cuando estaba terminando los estudios universitarios que acabaría escribiendo una Tesis Doctoral?! Repasar todo este tiempo me hace recordar buenos momentos, y no tan buenos, instantes de desánimo en los que no me veía capaz de avanzar, y otros de euforia por la alegría del trabajo bien hecho. Todo lo logrado hasta el día de hoy está sustentado en el apoyo y el cariño de los que me rodean, en sus palabras de ánimo, en cómo me hacían consciente de mis errores y la paciencia que han mostrado conmigo.

Mi más sincero agradecimiento va dirigido primeramente a mis directores de tesis, Isabel y Alberto, por la capacidad de trabajo, por el conocimiento que me han proporcionado, por las ideas de incuestionable valor que me han aportado, y sobretodo, por el apoyo que me han brindado desde el inicio.

La labor de apoyo del Departamento de Tecnología Electrónica de la Universidad de Sevilla ha sido crucial al facilitarme el material para poder desarrollar mi trabajo, así como de sus miembros que se han prestado a ser cobayas en mis investigaciones. Por ello, muchas gracias.

Gracias a mis amigos por estar ahí de apoyo, aconsejándome y distrayéndome cuando lo necesitaba, por hacer de ratas de laboratorio y por muchísimas más cosas.

Gracias a mi familia por estar a mi lado y soportar mis momentos de mal humor.

Gracias Luis, por guiarme con tu experiencia y consejos, por creer en mí y hacerme mejor persona.

Índice general

Página

Índice de figuras III

Índice de tablas V

Glosario VII

1. Introducción 1

2. Objetivos 5

3. Fisiología de las bioseñales 7
3.1. Electroencefalografía . . . 7
3.1.1. Registro de EEG . . . 9
3.1.2. Características del EEG . . . 10
3.2. Electrooculografía . . . 14
3.2.1. Registro de EOG . . . 17
3.2.2. Características del EOG . . . 18
3.3. Electrocardiografía . . . 20
3.3.1. Registro de ECG . . . 21
3.3.2. Características del ECG . . . 22

4. Resultados 29
4.1. Electrooculografía . . . 29
4.1.1. Procesamiento . . . 29
4.1.2. Análisis y aplicaciones . . . 31
4.1.3. Publicación 1 . . . 34
4.2. Electrocardiografía . . . 58
4.2.1. Procesamiento . . . 58
4.2.2. Análisis y aplicaciones . . . 60
4.2.3. Publicación 2 . . . 61
4.2.4. Publicación 3 . . . 71
4.2.5. Publicación 4 . . . 81
4.3. Electroencefalografía . . . 93
4.3.1. Publicación 5 . . . 94

5. Resumen, conclusiones y líneas futuras 99

A. A method of EOG signal processing to detect the direction of eye movements 103

B. Customizable Software Interface for Monitoring Applications 111

Bibliografía 121

Fe de errores 141

Índice de figuras

2.1. Arquitectura del sistema. 5

3.1. Lóbulos del cerebro. 8
3.2. Esquema de posiciones de los electrodos y etiquetas. Los circulos de color azul corresponden al Sistema Internacional 10-20, y en blanco a las posiciones introducidas a éste en su extensión 10-10. 9
3.3. Registro de un ERP. En la parte superior se muestra los datos correspondientes a las ventanas de la secuencia de presentación del mismo estímulo, y en la parte inferior se obtiene el promedio. 12
3.4. Esquema conceptual de electrooculografía. 14
3.5. Musculatura ocular. 15
3.6. Tipos de movimientos oculares. 15
3.7. Tipos de sobredisparos: arriba se muestra la amplitud del movimiento frente al tiempo y abajo la velocidad; a) sacada sin sobredisparo; b) sobredisparo dinámico; c) infradisparo; d) sobredisparo estático. 16
3.8. Montaje para captar la señal de EOG. Los electrodos H y V registran los movimientos horizontales y verticales respectivamente. 17
3.9. Esquema del corazón (Nódulo SA: nódulo sinusal; Nódulo AV: nódulo ariculoventricular; AD: aurícula derecha; AI: aurícula izquierda; VD: ventrículo derecho; VI: ventrículo izquierdo). 20
3.10. Electrocardiograma. 22
3.11. Ejemplo de dos montajes para captar la señal de ECG. . . . 22

4.1. Señal EOG. Sacadas, pestañeos y sobredisparos. 29
4.2. Algoritmo EFS: filtrado de pestañeos y sobredisparos. . . . 30
4.3. Resultados del procesamiento de datos EOG reales. 32
4.4. Diagrama del algoritmo SFE+K para detectar complejos QRS. 58
4.5. Resultado del algoritmo: a) salida del proceso de filtrado, b) clasificación de datos con K-means. 59
4.6. Coste computacional. La línea continua corresponde a la recta de regresión lineal, mientras que la punteada a un ajuste cuadrático. 68

4.7. Histograma de la desviación en la localización del pico máximo de la onda R para la versiones offline y en tiempo real con longitud de buffer desde 0.3 a 2.1s. 69
4.8. Interpolación de valores RR. 70
4.9. Efecto de la longitud del buffer sobre los resultados de la versión en tiempo real. 70

Índice de tablas

3.1. Parámetros temporales de ECG 26
3.2. Parámetros frecuenciales de ECG 27

4.1. Resumen de la eficiencia de los filtros EFS y mediana para el modelo de EOG. 31
4.2. Resumen de la eficiencia del algoritmo SFE+K. 60

Glosario

AC Affective Computing.

CC correlación cruzada.

dB decibelios.

ECG electrocardiografía.
ECM error cuadrático medio.
EEG electroencefalografía.
EFS envelope filter sequence.
EMG electromiografía.
EOG electrooculografía.
ERP event-related potential.

FE filtro de envolvente.
fHF frecuencia centroide de la banda HF.
fLF frecuencia centroide de la banda LF.
FN falsos negativos.
FP falsos positivos.
fVLF frecuencia centroide de la banda VLF.

HCI Human Computer Interface.
HF frecuencias altas con rango de 0.15 a 4Hz.
HRV heart rate variability.

LF frecuencias bajas con rango de 0.04 a 0.15Hz.
LF/HF razón entre LF y HF.
LPP late positive potential.

Mrr mediana de los segmentos RR.

NAV nódulo ariculoventricular.
NSA nódulo sinusal.

P+ predicción positiva.
PC Physiological Computing.
PDB Physionet.
PDS densidad de espectro de potencia.
pNN50 porcentaje de segmentos RR consecutivos que difieren más de 50ms entre sí.
Pre precisión.

RMSSD raíz cuadrada del valor medio de las diferencias sucesivas al cuadrado de los segmentos RR adyacentes.
RR tiempo entre dos ondas R consecutivas.

SDNN desviación estandar de los segmentos RR.
Se sensibilidad.
Secg entropía de los segmentos RR.
SFE+K secuencia de filtro de envolvente y K-means.
SN sistema nervioso.
SNA sistema nervioso autónomo.
SNC sistema nervioso central.
SNP sistema nervioso periférico.
SNPS sistema nervioso parasimpático.
SNS sistema nervioso simpático.
SNSS sistema nervioso somátosensorial.

TINN ancho de la base del triángulo con error mínimo respecto al histograma de los segmentos RR y cuyo máximo coincide con el del histograma.

ULF frecuencias ultra bajas con rango de 0 a 0.003Hz.

VLF frecuencias muy bajas con rango de 0.003 a 0.04Hz.
VP verdaderos positivos.

Capítulo 1

Introducción

El trabajo de investigación que a continuación se describirá está presentado bajo la modalidad "*compendio de publicaciones*" de la Universidad de Sevilla. Éste es la continuación de los trabajos realizados a lo largo del año 2010, los cuales no forman parte de los elementos a evaluar en esta tesis al no cumplir los requisitos exigidos, pero que, para ayudar a la comprensión de lo que se expondrá a continuación, los explicaré de manera muy resumida. Éstos estaban focalizados en mejorar la comunicación de personas con un alto grado de discapacidad motora y una baja capacidad comunicativa. Así, se desarrollaron dos trabajos consistentes en una interfaz de control basado en movimientos oculares (Merino et al, 2010b), y un teclado virtual que permite manejar un ordenador con un alto grado de personalización (Merino et al, 2010a). Esta aplicación puede controlarse mediante diversas interfaces, entre ellas los movimientos oculares o las contracciones musculares voluntarias. Para más detalles sobre ambos trabajos ver los anexos A y B. En base a estos antecedentes, se procedió a profundizar en la temática que constituye el objetivo de esta tesis.

La investigación y el desarrollo de mecanismos de control e interacción con los sistemas informáticos han propiciado la incorporación de nuevos elementos que facilitan su manejo y la comunicación con ellos, como por ejemplo pantallas táctiles, interfaz basada en gestos, seguimiento de mirada (Kim et al, 2005), acelerómetro (Gómez et al, 2010), joystick de barbilla para personas con escasa movilidad (Bolton and Wytch, 1992), control por comandos de voz, etc. Una de las áreas de investigación relacionada con mejorar la capacidad de interacción y comunicación se denomina Interfaz Hombre-Computador (en inglés HCI, Human Computer Interface). Ésta está centrada en el diseño, implementación y evaluación de los mecanismos que hacen posible que las personas interactúen con las computadoras (Olson and Olson, 2003), de manera que una de las principales líneas de investigación es el desarrollo de software y hardware útil, de fácil uso y estéticamente agradable.

Las bioseñales (señales de origen fisiológico) pueden ser una alternativa de control con grandes posibilidades y múltiples aplicaciones en el campo de HCI, sin necesidad de requerir un grado de movilidad alto por parte del usuario. El estudio y análisis de las bioseñales ha logrado importantes avances, en concreto, la electrooculografía (EOG), señal eléctrica causada por los movimientos oculares, ha sido ampliamente usada como elemento

de comunicación, control de un ordenador (Estrany et al, 2009), teclados virtuales (Dhillon et al, 2009; Ashtiani and Mackenzie, 2010; Merino et al, 2010b; MacKenzie and Ashtiani, 2011; Merino et al, 2012), sillas de ruedas (Barea et al, 2000; Yathunanthan et al, 2008), reconocedores de actividad (Bulling et al, 2008, 2009, 2011), y un largo etcétera donde se pueden apreciar sus posibilidades. Otra bioseñal ampliamente estudiada en el campo de HCI es la señal eléctrica resultante de la contracción muscular, denominada electromiografía (EMG). Ésta ha sido aplicada al control de prótesis (Chan et al, 2000; Khushaba et al, 2012), pinzas (Nussbaum et al, 2009), teclados virtuales (Dhillon et al, 2009; Merino et al, 2010a, 2012), etc. Otro ejemplo es la señal eléctrica generada por la actividad neuronal del cerebro (electroencefalografía - EEG). Su estudio ha permitido la edición de texto mediante el paradigma P300 (Nam et al, 2009; Klobassa et al, 2009), el control de un cursor en base al paradigma del ritmo μ, de manera que el usuario pueda desplazarlo en la dirección deseada (Mattiocco et al, 2006), o seleccionar un objeto/acción mediante potenciales visuales evocados (Parini et al, 2009).

Todas las bioseñales anteriormente citadas tienen en común que son usadas para interpretar acciones voluntarias del usuario. Conjuntamente a éstas, el cuerpo humano genera otras que escapan, por lo general, al control del sujeto y que pueden ser usadas para interpretar el contexto y la situación en la que se desarrolla la acción, y actuar sobre el sistema para conseguir una mejor experiencia de uso (Picard, 1997). Desde finales del siglo XX, el interés sobre el estado emocional de los usuarios ha ido creciendo hasta generar un prometedor campo de investigación denominado Computación Afectiva (en inglés AC, Affective Computing). Se puede definir AC como la adaptación de una aplicación sin la intervención explícita de agentes externos, para mejorar la experiencia de uso, basándose en la información de contexto que rodea la actividad que está en desarrollo, y el estado emocional del usuario (Picard, 1997; Ward and Marsden, 2004; El Kaliouby et al, 2006; Calvo and D'Mello, 2010). Un subcampo de AC es la Computación Fisiológica (en inglés PC, Physiological Computing) basada en el uso de bioseñales y cómo éstas cambian para "monitorizar, cuantificar y representar el contexto del usuario, habilitando una adaptación proactiva e implícita en tiempo real" (Fairclough, 2009).

La introducción de información subjetiva del estado del usuario se puede realizar de dos formas diferentes no excluyentes: manual y/o automática. En la primera, es el propio individuo el que inserta dicha información para que se actúe en consecuencia. Este mecanismo supone que el sistema sea totalmente pasivo, de manera que no modificará su comportamiento hasta que el usuario se lo indique. La segunda forma de obtención del estado del usuario transforma al individuo en un elemento pasivo, del cual obtener datos y variar el comportamiento del sistema en función de éstos. La información emocional puede extraerse mediante el análisis de la expresión facial (Kappas, 2010), características no verbales del habla (Pfister and Robinson,

2011), imágenes de resonancia magnética (Han et al, 2015), ritmo cardíaco (Conjeti et al, 2012), electroencefalografía (Nasoz et al, 2010), etc.

El estado emocional de un individuo puede clasificarse con 6 posibles términos: felicidad, sorpresa, tristeza, disgusto, miedo e ira (Ekman et al, 1987). La identificación de estos estados o un subconjunto de los mismos ha sido ampliamente estudiada (Kim et al, 2004; Soleymani et al, 2008; Laparra-Hernández et al, 2009; Petrantonakis and Hadjileontiadis, 2009, 2010a,b), no obstante, otros autores se han centrado en identificar el grado de agitación, estrés, carga de trabajo y/o fatiga mental (Iwanaga et al, 2000; Dedovic et al, 2005; Pfurtscheller et al, 2007; Shi et al, 2007; Luttmann et al, 2010; Setz et al, 2010; Steven A. et al, 2010; Sun et al, 2012). Esto puede ser usado para mejorar la capacidad de un sistema (Norman, 2007), como por ejemplo la regulación de notificaciones (Chen and Vertegaal, 2004), la reducción de la frustración, el nerviosismo y bloqueos mentales durante la conducción de un automóvil (Nasoz et al, 2010; Wu et al, 2010; Singh et al, 2011; Conjeti et al, 2012), prevenir el aburrimiento en videojuegos mediante el mantenimiento del nivel de dificultad (Chanel et al, 2011; Giakoumis et al, 2011), o el refuerzo de emociones positivas (Janssen et al, 2012).

En base a los conceptos citados anteriormente, se ha desarrollado la presente tesis. Ésta comprende dos técnicas de procesamiento de bioseñales, constituida por dos artículos centrados en electrocardiografía y electrooculografía (Merino et al (2015b,a) - secciones 4.1.3 y 4.2.3), en los cuales se trata de eliminar aquellas interferencias que pueden perjudicar el correcto funcionamiento de los sistemas HCI y PC, o destacar los transitorios que son objeto de estudio. Asimismo, se ha analizado las variaciones de diferentes parámetros de electrocardiografía y electroencefalografía en tres artículos de congresos (Merino et al (2012); Monge et al (2014); Merino et al (in press 2015) - secciones 4.2.4, 4.2.5 y 4.3.1), con el objetivo de caracterizar estos cambios para una futura aplicación capaz de detectar el estado emocional del sujeto.

Capítulo 2

Objetivos

El diseño de una interfaz de usuario puede separarse en tres niveles: captación de los datos, procesamiento de la información y actuación sobre el sistema (figura 2.1). El primero de los niveles es responsable de registrar las señales, independientemente de la naturaleza de éstas (movimiento ocular, contracción muscular, frecuencia cardíaca, etc.). Una vez captadas las señales, el segundo bloque lleva a cabo la extracción de información de las mismas, la cual será usada en el tercer nivel para interactuar con el sistema, cuya interpretación puede relacionarse con el control voluntario del computador y/o con el estado emocional del sujeto.

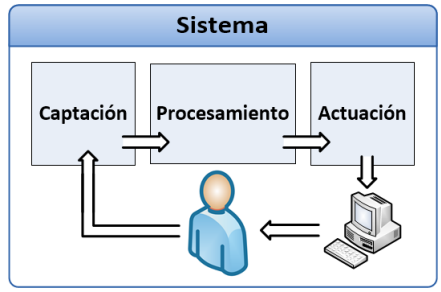

Figura 2.1: Arquitectura del sistema.

El amplio espectro de señales corporales, así como su naturaleza y origen, impone diferentes métodos de captación y procesamiento. De las diferentes técnicas de registro de señales fisiológicas, nos centraremos en las que son poco invasivas, aquellas que usan electrodos de superficie. Asimismo, la información proporcionada por las bioseñales varía de una a otra, de manera que algunas son más adecuadas para determinar diversas características frente a las otras. Esto hace necesario realizar un estudio comparativo entre las diferentes alternativas para determinar qué bioseñales son las más adecuadas en cada caso. Esta tesis se centra en:

- Electroencefalografía (EEG): registro de la señal generada por las neuronas cerebrales.

- Electrooculografía (EOG): registro de la señal asociada al movimiento ocular.

- Electrocardiografía (ECG): registro de la señal resultante de actividad eléctrica del corazón.

La meta principal que pretende este trabajo de investigación es evaluar el uso de las bioseñales para el diseño de interfaces que permitan la interacción con un computador. Se trata de analizar distintas bioseñales para su incorporación a un sistema abierto y flexible, el cual permita elegir la que mejor se adapte al sujeto y su entorno. Para ello, es necesario determinar cuál es el procesamiento más adecuado, y qué parámetros son más robustos y significativos a la hora de inferir una determinada acción o el estado emocional del individuo.

Capítulo 3

Fisiología de las bioseñales

El estudio de las bioseñales requiere conocer la base fisiológica de cada una de ellas. Por ello, a continuación, se va a presentar los mecanismos biológicos que se producen en el cuerpo humano asociados a las diferentes bioseñales en las que se centra esta tesis, y qué información se puede extraer.

Primero se describe la base de la actividad cerebral, seguido de los movimientos oculares, y se finaliza con la actividad cardíaca.

3.1. Electroencefalografía

El sistema nervioso (SN) es el responsable de la coordinación y control de los diferentes órganos que componen el cuerpo humano, cuyo componente básico es la neurona (Carretié Arangüena and Iglesia Dorado, 2000; Nunez and Srinivasan, 2006; Sörnmo et al, 2014). Éste se divide en sistema nervioso central (SNC) y sistema nervioso periférico (SNP). El primero, constituido por el cerebro y la médula, es responsable de llevar a cabo la coordinación muscular, control respiratorio, regulación hormonal, control del ciclo vigilia-sueño, procesar e interpretar la información visual, auditiva, olfativa, y somática (tacto, temperatura, dolor), así como funciones relacionadas con procesos emocionales, motivacionales, aprendizaje y memoria. El segundo, constituido por el resto de componentes de SN que no forman parte del SNC, es responsable de transmitir la información del SNC a músculos y glándulas, y de los receptores sensoriales al SNC. El SNP puede subdividirse en sistema nervioso somátosensorial (SNSS), responsable principal de enviar a la musculatura estriada las ordenes provenientes del SNC y remitir a éste la información sensorial desde los receptores, y sistema nervioso autónomo (SNA) cuya actividad está relacionada con las glándulas, musculatura lisa y cardíaca, cuyo funcionamiento, en general, es involuntario o autónomo. El SNA se divide en dos partes antagonistas, esto es, producen reacciones contrarias: sistema nervioso simpático (SNS) y sistema nervioso parasimpático (SNPS). El primero actúa sobre todo el organismo preparándolo para realizar alguna acción motora, lo que supone un gasto energético, traduciéndose en un aumento de la tasa cardíaca, dilatación de los bronquiolos, contracción de vasos sanguíneos en ciertas zonas, aumento de la sudoración, etc. El segundo aumenta la energía almacenada en el organismo, y tiene la capacidad de actuar por zonas, esto es, limitar su acción a áreas concretas del organismos, por ejemplo, incrementando la actividad digestiva (el SNS

la reduce), disminuyendo el ritmo cardíaco, contrayendo los bronquiolos, etc. De esta forma, la influencia ejercida por el SNA tiene su reflejo en otras bioseñales, por ejemplo el ECG, de manera que a partir de ellas se puede obtener un índice del nivel de acción (SNS) y reposo (SNPS) del individuo.

El cerebro humano puede dividirse en dos partes denominadas hemisferios, los cuales realizan un control cruzado del sistema visual y las actividades motoras del cuerpo, es decir, el hemisferio izquierdo controla la parte derecha del cuerpo y el derecho la parte izquierda. De forma genérica, cada hemisferio puede dividirse en 4 lóbulos diferentes (figura 3.1):

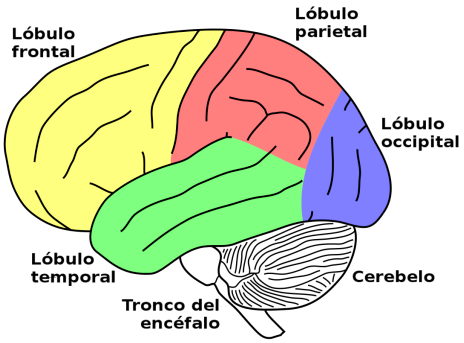

Figura 3.1: Lóbulos del cerebro.[1]

- *Lóbulo frontal*: responsable de la planificación, coordinación, control y ejecución de la conducta (socialización, comportamiento sexual, espontaneidad, control de impulsos y raciocinio), funciones motoras (incluye los movimientos oculares que es independiente de los estímulos visuales), la comunicación mediante la generación y emisión del lenguaje, y memoria a corto plazo. Esta área es responsable de recopilar la información de las restantes estructuras del cerebro para coordinar una respuesta conjunta.
- *Lóbulo parietal*: encargado de procesar la información somática (tacto, presión, dolor, temperatura), el conocimiento de los números y sus relaciones y la manipulación de los objetos.
- *Lóbulo occipital*: centra principalmente el análisis e interpretación de la información visual.
- *Lóbulo temporal*: descifra la información auditivas, afianza la memoria a largo plazo (por ejemplo recuerdo de palabras y nombres de objetos), y realiza tareas visuales complejas como el reconocimiento de rostros, imágenes, objetos, etc.

[1] La imagen es una modificación de otra con licencia copyleft. La original: "Gehirn, lateral - Lobi eng" por NEUROtiker - Trabajo propio. Licencia bajo CC BY-SA 3.0 a través de Wikimedia Commons.

Esta división de funcionalidades de los diferentes lóbulos proporciona una idea general de las acciones que realiza cada uno de ellos. No obstante, el procesamiento de la información es más difuso, como apunta en la capacidad del cerebro de recomponerse y suplir las funciones de ciertas áreas tras una lesión (Bova et al, 2008).

3.1.1. Registro de EEG

La electroencefalografía (EEG) es una técnica de registro de la actividad eléctrica del cerebro que emplea electrodos de superficies repartidos por el cuero cabelludo, que permite el estudio del funcionamiento general del cerebro. Se sabe que el origen de esta actividad no está en los potenciales de acción en los axones de las neuronas (Li and Jasper, 1953) ni es causada por estructuras neuronales cerradas (grupos de neuronas en las que los cuerpos celulares se sitúan en el centro y sus axones se dirigen hacia la periferia, conformando una especie de esfera), como por ejemplo el tronco cerebral, puesto que las corrientes generadas se anulan entre sí cuando se intentan registrar desde el exterior (Lorente De Nó, 1947). No obstante, parece que los potenciales de acción de las dendritas y los cuerpos celulares, principalmente de la corteza cerebral (parte más externa del cerebro y más próxima al cuero cabelludo) son las principales fuentes del EEG (Lorente De Nó, 1947; Cooper et al, 1974; Lutzenberger et al, 1987; Molnár, 1994; Nunez and Srinivasan, 2006).

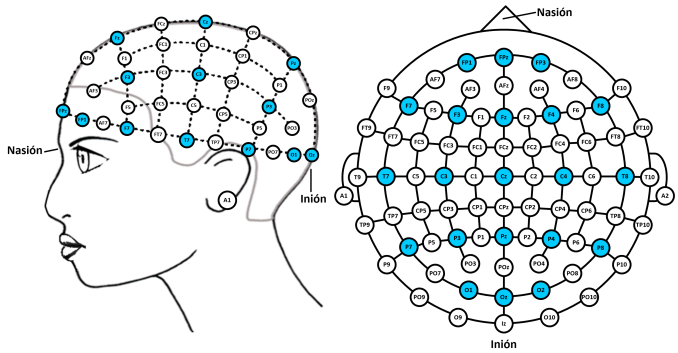

Figura 3.2: Esquema de posiciones de los electrodos y etiquetas. Los circulos de color azul corresponden al Sistema Internacional 10-20, y en blanco a las posiciones introducidas a éste en su extensión 10-10.

El esquema seguido a la hora de situar los electrodos sobre el cuero cabelludo es el mostrado en la figura 3.2 (Jasper, 1958). Éste es un esquema estándar reconocido internacionalmente denominado 10-20 debido a que la distancia entre los electrodos es de un 10% o un 20% el perímetro del cráneo, lo que permite que éstos se sitúen en zonas equivalentes independientemente de la dimensión del cráneo. Existen dos extensiones de este montaje: el sistema 10-10 y el sistema 10-5. En éstos la distancia entre los electrodos se

han disminuido. En el primero la separación se ha reducido a un 10% de la medida del cráneo, mientras que el segundo el espacio es un 10% o un 5% (Chatrian et al, 1985; Oostenveld and Praamstra, 2001).

En estos montajes hay que destacar dos ejes fundamentales: el eje sagital, que se dirige desde el nasión (punto de comienzo del hueso nasal) hasta el inión (protuberancia externa del hueso occipital), que permite diferenciar entre hemisferios cerebrales, y el eje transversal, que va desde un conducto auditivo hasta el otro. Los nombres de las posiciones están asociados al lóbulo sobre el que se sitúan, así el lóbulo occipital tiene asociado la etiqueta *O*, el parietal se identifica como *P* y el temporal se corresponde con la letra *T*. El lóbulo frontal, al ser el más extenso ha sido dividido en zona anterior, media y surco central identificadas como *FP*, *F* y *C*. Las áreas intermedias en el sistema 10-10, al recaer en regiones limítrofes entre lóbulos, están identificadas con la unión de las etiquetas de los lóbulos entre los que se sitúa, por ejemplo, *FC* hace referencia a la zona media y el surco central del lóbulo frontal, *TP* identifica al área temporal-parietal, etc. Los subíndices permiten determinar en qué hemisferio se encuentran situados los electrodos: valores *impares* corresponden al izquierdo, mientras que los casos *pares* se asocian con el derecho. El subíndice *z* indica que el electrodo está situado sobre el eje sagital. Por otro lado, es necesario emplear un electrodo de derivación a tierra, el cual se suele situar en la posición *FPz*, y uno que actúe como referencia, pudiendo situarse sobre los mastoides (detrás de la oreja), lóbulo de las orejas o la punta de la nariz, puesto que estas localizaciones están alejadas de la influencia del EEG y artefactos causados por la actividad muscular.

3.1.2. Características del EEG

A continuación se exponen las características eléctricas y frecuenciales de mayor relevancia de los datos EEG, y se detallan qué información se puede extraer que permita determinar el estado emocional de un individuo.

Características generales

Los datos de EEG muestran un patrón sinusoidal u oscilatorio muy sensible a artefactos debido a su baja potencia, siendo escasamente superior a las interferencias o incluso inferior en algunos casos, destacando los artefactos provenientes de las contracciones de los músculos faciales, los movimientos oculares y parpadeos, ya que pueden afectar a cualquier posición del sistema 10-10. Por ello, se recomienda relajar al sujeto antes de las pruebas, evitar la verbalización, y realizar un registro EOG para usarlo en un proceso posterior de filtrado.

El análisis de la actividad de las ondas EEG se centra básicamente en el estudio de diferentes bandas de frecuencias, asumiéndose que a mayor

actividad cerebral se tiene una mayor frecuencia y una menor amplitud (existe una relación inversa entre ambas características). En termino general, los datos de EEG se dividen en 5 bandas diferentes (Carretié Arangüena and Iglesia Dorado, 2000; Nunez and Srinivasan, 2006; Sörnmo et al, 2014):

- *Onda delta (δ)*: su rango de frecuencia se sitúa entre 0.5 y 4Hz con una amplitud que va de los 100 a los 200μV. Está asociada a una importante atenuación del nivel general de actividad, como sueño profundo. Ésta desaparece durante la vigilia en sujetos sanos, y puede ser indicativo de zonas tumorales o con lesiones ya que se suele captar actividad delta en dichas áreas.

- *Onda theta (θ)*: su rango de frecuencia se sitúa entre 4 y 8Hz con un rango de amplitud situado entre 50 y 100μV y está asociada a una disminución del nivel de actividad, como somnolencia, primeras fases del sueño, meditación o en determinadas tareas que requieren una alta concentración.

- *Onda alfa (α)*: su rango de frecuencia se sitúa entre 8 y 12Hz cuya amplitud varía entre 20 y 50μV. Es el ritmo predominante en sujetos sanos, despiertos y relajados, observándose mejor cuando los ojos están cerrados. Es apreciable en todo el cuero cabelludo, aunque predomina en la región occipital. La aplicación de un estímulo o la realización de una tarea, por sencilla que sea, hace que esta onda desaparezca y aparezca la actividad en la banda beta.

- *Onda beta (β)*: su rango de frecuencia se sitúa entre 12 y 30Hz oscilando entre 10 y 20μV de amplitud. Se asocia a niveles de actividad moderado, de modo que la frecuencia se incrementará según aumenten los requisitos cognitivos o implicaciones afectivas de la tarea. Este ritmo se localiza principalmente en las regiones frontal y central.

- *Onda gamma (γ)*: su rango de frecuencia se sitúa entre 30 y 50Hz con una amplitud inferior a 10μV. Está relacionada con el procesamiento de información y requerimientos cognitivos elevados.

La separación en 5 bandas es la más aceptada, aunque existen subdivisiones de éstas, así como otras ondas que sólo aparecen en ciertas áreas o situaciones especiales. Por ejemplo, algunos autores dividen la onda α en baja, de 8 a 10Hz, y alta, de 10 a 12Hz (Lorenzo et al, 1995; Klimesch, 1999); otros hacen lo mismo pero con la banda β, diferenciando entre ritmo lento (12-18Hz) y rápido (18-30Hz) (Lorenzo et al, 1995); en ciertos estudios consideran la banda γ como una ampliación de la banda β (Cooper and Osselton, 1980); el ritmo μ (8-13Hz) se relacionada con la actividad de las neuronas espejo (Rizzolatti and Craighero, 2004; Oberman et al, 2005),

y el ritmo σ, con frecuencias entre 12 y 15Hz, se relaciona con la fase REM del sueño (Uchida et al, 1994).

Además de los ritmos anteriormente apuntados, que están relacionados con la actividad espontánea del cerebro, existen otros asociados a acontecimientos discretos que se caracterizan por cambios rápidos (respuestas) y de corta duración que se estudian en el dominio temporal. Éstos suelen denominarse potenciales evocados relacionados a eventos (en inglés ERP, event-related potential) y quedan enmascarados por la actividad espontánea del cerebro ya que la amplitud éstos es muy inferior (por lo general menor a 1μV). Para hacerlos visibles se trabaja con promedios de ventanas temporales, que no superan el segundo de longitud, y siguen a una secuencia repetida del mismo estímulo (Dawson, 1947). Se basa en una propiedad de los procesos estocásticos: el promedio de señales aleatorias tiende a cero. Así, la media de los diferentes segmentos revelará las desviaciones relacionadas con ERP y eliminará los elementos no relacionados con ellos (figura 3.3). No obstante, el fenómeno de habituación al estímulo, el cansancio del sujeto y otros elementos pueden mermar la amplitud del ERP, por lo que se aconseja que el número de repeticiones del estímulo no sea excesivamente elevado.

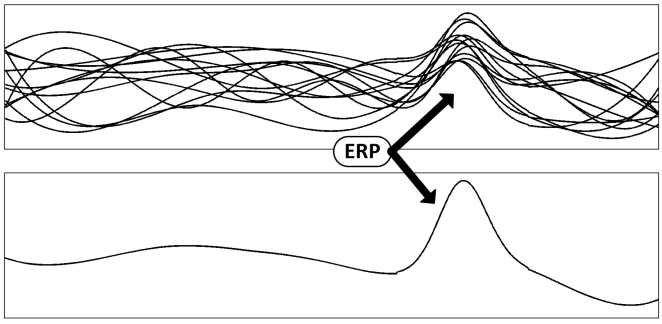

Figura 3.3: Registro de un ERP. En la parte superior se muestra los datos correspondientes a las ventanas de la secuencia de presentación del mismo estímulo, y en la parte inferior se obtiene el promedio.

Características psicofisilógicas

El estudio de las variaciones del EEG ha permitido diferenciar áreas relacionadas con diferentes características psicológicas. Las tareas de tipo analítico (atendiendo más a los detalles), verbales y emociones positivas afectan preferentemente en el hemisferio izquierdo, mientras que el derecho centra las tareas de visión espacial, las actividades de síntesis (atendiendo más al cómputo global) y emociones negativas (Davidson and Fox, 1982; Ahern and Schwartz, 1985; Ray, 1990).

La realización de tareas cognitivas que requieren una demanda alta de atención de los sujetos, como memoria o aritmética, han mostrado una ga-

nancia en la banda θ y una atenuación en la α con respecto al intervalo de reposo inicial y el incremento de la demanda requerida en la actividad (Glass, 1966; Fernández et al, 1995; Gevins et al, 1997; Klimesch, 1997; Gevins et al, 1998), observándose a su vez, que la realización de prácticas, que permiten mejorar el rendimiento obtenido, se traduce en un aumento en ambas bandas (Gevins et al, 1997). También se ha descrito de un incremento de la potencia en la banda δ en las áreas frontal y central causado por tareas aritméticas de diferentes dificultades y requerimientos de concentración (Etevenon, 1986; Valentino et al, 1993; Fernández et al, 1993, 1995). En referencia a la banda β, se ha observado una tendencia creciente en el región frontal del cerebro y decreciente en la restantes zonas, que se agudiza con el aumento de la complejidad de la actividad realizada y la carga cognitiva (Ray and Cole, 1985; Petsche et al, 1986; Fernández et al, 1995). Por otro lado, se ha relacionado el incremento de la demanda de atención con un aumento en la potencia de banda γ, en especial en la región parietal (Gruber et al, 1999).

Los ERP han sido empleados en estudios psicofisiológicos, por ejemplo, como índice de atención (Graham and Hackley, 1991). Aquí se centrará la atención en algunos de ellos que han sido relacionados con diferentes estados psicológicos. Uno de los más importantes ERP es el P300, que sucede entre 300 y 500ms después de observar un estímulo de interés entre un conjunto de estímulos diferentes. Uno de ellos, el que debe captar la atención del individuo, es menos frecuente que el resto, de manera que el sujeto debe atender a este estímulo infrecuente. Esto permite que este ERP pueda ser aplicado en HCI, y además facilita evaluar la relevancia o significado que se le concede a un estímulo (Picton and Hillyard, 1988; Johnson, 1993; Nam et al, 2009; Klobassa et al, 2009). Los ERP también han sido observados como consecuencia de estímulos afectivos. El P300 ha mostrado mayor amplitud en la regiones parietal y temporal ante estímulos que suscitan una mayor agitación a los individuos, frente a aquéllos que inducen relajación (Molnár, 1994; Carretié, 1995). Otro ERP que ha sido usado es el potencial positivo posterior (en inglés LPP, late positive potential), que se produce entre 400 y 500ms después del estímulo. Éste ha mostrado un incremento positivo más relevante cuando se observan emociones positivas que cuando se percibe estímulos negativos (Cacioppo et al, 1994; Bradley et al, 2007; Pastor et al, 2008).

Por último, se ha estudiado el efecto de la somnolencia sobre la actividad cerebral. Los sujetos han mostrado que la banda θ experimenta una desincronización durante la privación de sueño (disminución de la amplitud), principalmente en la región posterior de la corteza cerebral, mientras que la potencia de la banda α, principalmente en el área frontal, experimenta una suave atenuación durante la vigilia o los periodos de privación de sueño, y un aumento significativo (sincronización) después del sueño (Manganotti et al, 2012, 2013).

3.2. Electrooculografía

El sistema muscular ocular tiene como principal objetivo dirigir la fóvea (área de la retina donde se proyectan los haces luminosos) hacia aquellos objetos o escenas que resultan de mayor interés para el individuo. No obstante, este comportamiento constituye una las organizaciones neuronales más complejas del sistema nervioso, ya que los ojos pueden ser dirigidos voluntariamente, cambiando el foco de atención, y a su vez éstos experimentan diferentes movimientos reflejos con el objetivo de mantener la escena visual de interés centrada en la fóvea. Así estos movimientos reflejos compensan los desplazamientos que acontecen al girar la cabeza, al desplazar el cuerpo, cuando se mueve la escena que se está observando o todos ellos a la vez.

El registro de los movimientos oculares no se basa en captar la actividad eléctrica de la musculatura ocular, sino que consiste en medir las variaciones del potencial eléctrico que crea el dipolo ocular córnea-retina con los cambios de fijación en la mirada. Hasta 1922 no se obtendrían los primeros registros EOG humanos, siendo en 1936 cuando se demostraría que la actividad EOG está provocada por el potencial entre la córnea y la retina, y no por la contracción de la musculatura ocular, como se pensaba hasta entonces. Este potencial eléctrico oscila alrededor de ±1mV (Nikara et al, 1976; Scerbo et al, 1992), aunque su valor varía con la intensidad luminosa (Denney and Denney, 1984). Los electrodos situados en las vecindades de los ojos pueden captar la orientación del dipolo ocular, de manera que cada electrodo registrará un potencial más positivo cuando el ojo gire hacia él, y más negativo en caso contrario. Asimismo, si la córnea y la retina están equidistantes a ambos electrodos, la actividad eléctrica captada será nula (figura 3.4).

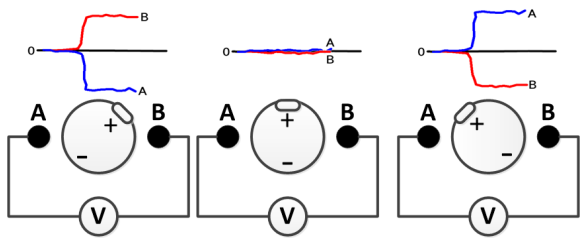

Figura 3.4: Esquema conceptual de electrooculografía.

Los movimientos de los ojos y párpados son el resultado de la actividad de siete músculos que constituyen la musculatura ocular (figura 3.5):

- *Elevador del parpado*: responsable de abrir y cerrar los parpados.
- *Recto lateral* y *medial*: responsables de los movimientos horizontales. El recto lateral aleja la retina del tabique nasal, mientras que el recto medial la aproxima.

- *Recto superior* e *inferior*: responsables de los movimientos verticales. El recto superior gira el ojo hacia arriba y levemente hacia fuera, y el recto inferior lo mueve hacia abajo y someramente hacia adentro.
- *Oblicuo superior* e *inferior*: responsables de los involuntarios movimientos de torsión, esto es, desplazamientos de poca amplitud que permiten que los ojos mantengan cierta horizontalidad cuando la cabeza se inclina a un lado. El oblicuo superior hace girar el ojo de forma que la córnea se dirige hacia abajo y al exterior, y el oblicuo inferior la orienta hacia arriba y afuera.

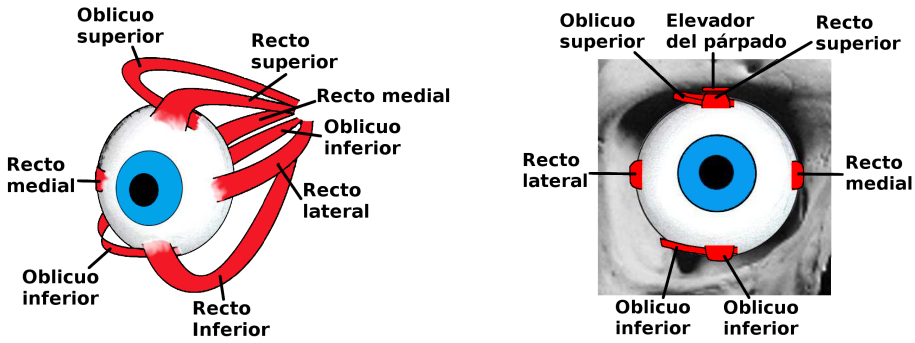

Figura 3.5: Musculatura ocular.

Estos músculos serán los encargados de mover el globo ocular de forma que, en función del músculo o conjunto de músculos que se activen, se tendrá un movimiento u otro. Así, se llama elevación cuando el ojo gira hacia arriba y abatimiento cuando gira hacia abajo, aducción cuando el ojo se dirige hacia la zona nasal y abducción cuando se aleja de ella, y torsión a los desplazamiento involuntarios de compensación de horizontalidad cuando se inclina la cabeza a un lado (figura 3.6).

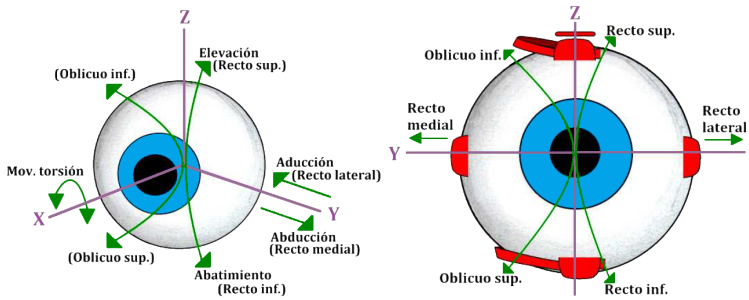

Figura 3.6: Tipos de movimientos oculares.

Además de los movimientos oculares citados, existen los movimientos de vergencias, que hacen que los ojos converjan o diverjan en función de si

se enfocan objetos cercanos o lejanos, y los nistagmoides, consistentes en movimientos intermitentes de poco amplitud y rápida oscilación en torno al centro de visión, que pueden aparecer tras varios giros de un sujeto sobre sí, por consumo de droga, problemas cerebrales, patologías en el sistema visual, etc.

Los movimientos oculares pueden ser agrupados en dos tipos: lentos y rápidos (Carretié Arangüena and Iglesia Dorado, 2000). El primero es responsable de mantener la proyección del objeto de interés sobre la fóvea ocular cuando la escena observada no es estática y su velocidad no sobrepasa los 30°/s. Los movimientos rápidos pueden dividirse en dos tipos: sacadas, con desplazamientos de hasta 700°/s, permiten cambios rápidos del punto de fijación de la mirada, y microsacadas, cuya velocidad es inferior a 0.25°/s, previenen que una escena deje de percibirse debido al efecto de acomodación por la proyección continuada de un objeto en el mismo punto de la retina durante las fijaciones (tiempo que va de una sacada a otra). A menudo el movimiento sacádico no logra alcanzar correctamente el nuevo punto de fijación, de forma que se producen movimientos sacádicos adicionales de "corrección", lo que en la señal se traducen en desviaciones situadas al final de la sacada principal llamadas sobredisparos (Weber and Daroff, 1971; Bahill et al, 1975). En la literatura existen tres tipos de sobredisparos (figura 3.7), de los cuales el denominado como *sobredisparo estático*, que es visible a simple vista, es objeto de análisis. De esta manera, a lo largo de esta tesis, cuando se use el termino sobredisparo se estará haciendo referencia al tipo estático.

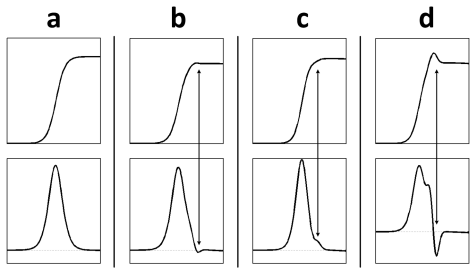

Figura 3.7: Tipos de sobredisparos: arriba se muestra la amplitud del movimiento frente al tiempo y abajo la velocidad; a) sacada sin sobredisparo; b) sobredisparo dinámico; c) infradisparo; d) sobredisparo estático.

Otro aspecto importante de la actividad ocular es el parpadeo. Los parpados son dos membranas móviles que cubren los globos oculares, que propician la limpieza e hidratación de éstos, y los defienden de agentes físicos externos. La apertura y cierre de los mismos causan un interferencia relevante en forma de campana en los datos de EOG que puede dificultar el procesamiento automático de esta señal.

3.2.1. Registro de EOG

La técnica de registro EOG emplea electrodos superficiales cuya localización más común se muestra en la figura 3.8. Suelen situarse alineados con la pupila de los ojos en su posición central mirando al frente. El registro de los movimientos horizontales se realiza con electrodos situados en la comisura externa de ambos ojos, debido a que en la comisura interna puede ser captada parte de la actividad eléctrica del otro ojo. Este tipo de montaje, que usa los dos ojos para registrar la actividad horizontal, se denomina binocular. Los movimientos verticales se suelen estudiar mediante un montaje monocular, es decir, sobre uno de los ojos, situando un electrodo por encima de la ceja, en un área próxima a ésta, y el otro se fija por debajo del parpado inferior, próximo al ojo pero sin resultar molesto, y alineado con el otro electrodo. Al contrario de los movimientos horizontales, estas localizaciones minimizan las interferencias producidas por el otro ojo. Usar el ojo izquierdo o derecho dependerá únicamente del experimentador o la comodidad del sujeto y sus limitaciones. Asimismo, es conveniente situarlos de manera que la tensión captada indique cuál es la dirección del movimiento con el fin de facilitar la interpretación de los datos. Por ello, es común que los movimientos a la derecha y arriba se registren como una desviación de tensión más positiva.

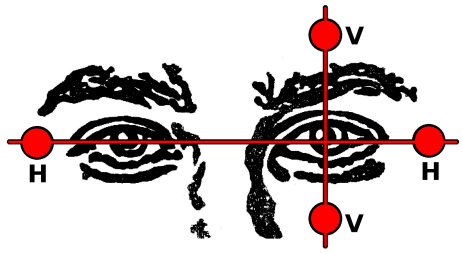

Figura 3.8: Montaje para captar la señal de EOG. Los electrodos H y V registran los movimientos horizontales y verticales respectivamente.

El registro simultáneo de los movimientos verticales y horizontales va a permitir tener un mapa bidimensional de los desplazamientos oculares, tal como ocurre en sistemas basados en localización de la mirada, donde es fundamental calibrar con precisión la señal, de manera que en función del voltaje acontecido al realizar un movimiento se puede determinar cuántos grados se ha desplazado la mirada en una determinada dirección. No obstante, el montaje de los sensores dependerá del estudio que se esté realizando. De hecho, si se está interesado en los movimientos oculares que ocurren durante la lectura de un texto, basta con usar solo el montaje horizontal, o si lo que se quiere es analizar los parpadeos, es suficiente con el montaje vertical.

3.2.2. Características del EOG

A continuación se expone las características eléctricas y temporales asociada al registro de movimientos oculares mediante la técnica EOG, y se detalla qué información se puede extraer que permita determinar el estado emocional de un individuo.

Características generales

La electrooculografía permite el registro de los desplazamiento de los globos oculares mediante las variaciones que se producen en el dipolo córnea-retina. Su análisis muestra que los valores de tensión asociados a los movimientos oculares oscilan entre 5 y 20μV/°, cuasi lineal para desplazamientos de ±30° desde la posición central de los ojos (Singh and Singh, 2012), con una amplitud que va desde 50 a 3500μV según los desplazamientos, y con un rango frecuenciales principales situado entre 0 y 30Hz (Brown et al, 2006). La duración de las sacadas dependen del ángulo del movimiento, siendo los desplazamientos más comunes inferiores a 20°, y con una duración de hasta 100ms (Duchowski, 2007). El periodo de fijación, esto es, el intervalo de tiempo entre dos sacadas consecutivas, oscila entre 100 y 200ms (Manor and Gordon, 2003).

De los diferentes elementos que pueden dificultar el procesamiento automático de los datos de EOG, destacan cuatro: ruido de ambiente, desplazamiento de su línea base o deriva, pestañeos y sobredisparos. El primero es provocado por el entorno que rodea al sujeto durante el registro de datos. En él influye la señal de potencia de la red eléctrica, los equipos eléctricos, la interfaz de contacto entre el electrodo y la piel, etc. La segunda fuente de perturbación, la deriva, es causada por la variabilidad de la componente de continua, que puede verse influida por interferencias de otras bioseñales (EEG, EMG, etc.), el nivel de luminosidad que modifica el potencial corneo-retinal (Nikara et al, 1976; Scerbo et al, 1992), el sexo y la edad (Höhne, 1974), y movimientos corporales del sujeto. Finalmente, los pestañeos y sobredisparos provocan perturbaciones en forma de campana que puede ser confundido con sacadas por las técnicas de procesamiento automáticos, por lo que es conveniente su eliminación. La duración del parpadeo oscila entre 100 y 400ms (Schiffman, 2001), con una frecuencia entre 12 y 19 ocurrencias por minuto para parpadeos espontáneos en individuos relajados, mientras que los sobredisparos son la consecuencia de un movimiento sacádico secundario para corregir un error en la detección del foco de interés, y los cuales son apreciables a simple vista cuando los desplazamientos son grandes (Bahill et al, 1975).

Características psicofisilógicas

Los movimientos oculares y pestañeos han sido principalmente relacionados con la fatiga mental, la privación parcial o total de sueño y sus diferentes fases (Hori, 1982; Hasan, 1996; Sallinen et al, 2004). La fatiga leve, así como la degeneración de éste en somnolencia cuando se extiende en el tiempo, lleva asociado variaciones en diferentes parámetros (Morris and Miller, 1996; Sirevaag and Stern, 2000; Caffier et al, 2003; De Gennaro et al, 2005). Un cansancio severo trae consigo una disminución de la frecuencia de los parpadeos, mientras que la fatiga leve la incrementa. Asimismo, ambos estados producen que la duración del pestañeo aumente, siendo mayor cuando el cansancio es más severo. Por otro lado, la somnolencia produce una ralentización significativa de los movimientos oculares, llegando a ser propios de los primeros estados de sueño (Galley, 1989, 1998; De Gennaro et al, 2000, 2001, 2005; Magosso et al, 2007). La privación total o parcial de sueño, por lo general mayores a 24 horas o con periodos de sueños inferiores a 5 horas, afecta negativamente a las sacadas, disminuyendo su velocidad y precisión, y aumentando su latencia (intervalo de tiempo que va desde el instante que se presenta un estímulo hasta que se inicia el movimiento ocular), sugiriendo una disfunción en la actividad cerebral (Porcu et al, 1998; App and Debus, 1998; Russo et al, 2003; Zils et al, 2005; Rowland et al, 2005; Bocca and Denise, 2006; Schleicher et al, 2008; Hirvonen et al, 2010). La privación de sueño provoca la disminución de la metabolización de la glucosa en el cerebro (Thomas et al, 2000), de manera que puede ser ésta la causa de la variación de la velocidad de la sacada y demás variables oculares.

La realización de tareas monótonas que requieren poca actividad física/mental puede provocar situaciones de somnolencia similares a las producidas con déficit de sueño (Sallinen et al, 2004). La realización de un trabajo monótono y poco estimulante, precedido de un periodo de sueño adecuado y reparador, genera resultados similares a los producidos cuando se experimenta privación parcial del sueño y la tarea requiere cierto nivel de atención. La falta de sueño supone un aumento de la fatiga que provoca un deterioro psicomotor, que afecta a las actividades cognitivas, así como a la coordinación y precisión de movimientos en el individuo, aumentando la probabilidad de accidentes, errores y disminuyendo la productividad (Horne and Reyner, 1995; Harrison and Horne, 2000; Dorrian et al, 2008).

Aunque los movimientos oculares se han relacionado principalmente con la somnolencia, como se ha expuesto anteriormente, ciertos trabajos han estudiado el efecto de la carga cognitiva. El incremento en la complejidad de la tarea lleva asociado una reducción de la frecuencia de pestañeos (Freudenthaler et al, 2003; Himebaugh et al, 2009), y aumento del número de sacadas de amplitud mayores de 10°, las cuales, mayoritariamente, están acompañadas por un parpadeo (Cardona and Quevedo, 2014). Por otro lado, la proporción de fijaciones de entre 150 y 900ms se reducen significativamente,

mientras que aumenta para aquéllas con duración inferior a 150ms o superior a 900ms (Findlay and Walker, 1999; Schleicher et al, 2008). Sin embargo, no se puede establecer una relación inequívoca entre este parámetro y la carga cognitiva, pues la duración puede variar con diferentes procesos neuronales (Radach et al, 1999; Godijn and Theeuwes, 2002).

3.3. Electrocardiografía

La actividad rítmica asociada a las contracciones del músculo cardíaco o miocardio es la responsable de la difusión sanguínea que conlleva el transporte de oxígeno y nutrientes a todas las células del organismo, captación y eliminación del CO_2 asociado a los procesos respiratorios celulares, distribución de hormonas, regulación de la temperatura corporal, etc. Ésta se adapta a las necesidades de organismo, variando según los requerimientos energéticos durante una actividad deportiva, en función de la temperatura ambiente, ciclo de vigilia/sueño, etc., viéndose afectado también por aspectos psicológicos como son ansiedad, estrés, ira, etc.

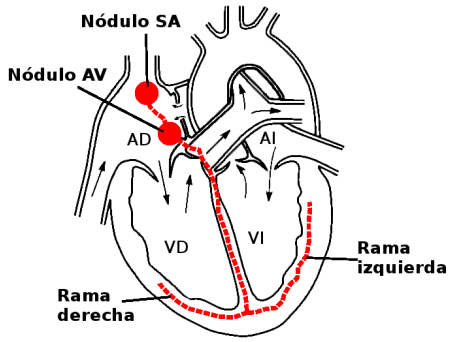

Figura 3.9: Esquema del corazón[2](Nódulo SA: nódulo sinusal; Nódulo AV: nódulo ariculoventricular; AD: aurícula derecha; AI: aurícula izquierda; VD: ventrículo derecho; VI: ventrículo izquierdo).

El corazón está constituido por dos cavidades superiores llamadas aurículas, y dos inferiores denominadas ventrículos (figura 3.9). La aurícula derecha recibe la sangre desoxigenada y la transfiere al ventrículo derecho para que éste la impulse hacia los pulmones, donde se producirá la expulsión del CO_2 y captación de O_2. La aurícula izquierda recibirá la sangre oxigenada de los pulmones y la emitirá al ventrículo izquierdo para que seguidamente fluya al resto del organismo. El proceso de contracción y relajación de las diferentes cavidades que permite la emisión y recepción de sangre se denomina sístole y diástole. Éste se realiza de manera coordinada,

[2]La imagen es una modificación de otra con licencia copyleft. La original: "Atrial septal defect-null" por Manco Capac - Trabajo propio. Licencia bajo CC BY-SA 3.0 a través de Wikimedia Commons.

de forma que, en un primer estado, la sístole auricular conlleva la diástole ventricular, y posteriormente se llevará a cabo la sístole ventricular, que supone la diástole auricular.

El responsable de este patrón de contracciones es el tejido nodal (figura 3.9), cuyas células poseen la capacidad de generar potenciales de acción de forma autónoma, sin la intervención de ninguna neurona. Este proceso es posible gracias a que la despolarización de una célula es capaz de despolizar las células vecinas. La contracción se inicia en el nódulo sinusal (NSA), situado sobre la aurícula derecha, y se desplaza por las células auriculares del miocardio produciendo la sístole auricular. La propagación continúa hasta el nódulo ariculoventricular (NAV) donde se divide en dos ramas, provocando que los ventrículos se contraigan de forma sincronizada.

El comportamiento del tejido nodal puede verse modificado debido al SNS y el SNPS, lo que se denomina control eferente. El primero puede provocar un incremento en la frecuencia cardíaca (taquicardia) debido a la activación sináptica de la inervación del NSA y áreas ventriculares, o a causa de la segregación de adrenalina. El segundo inerva principalmente zonas próximas al NSA y al NAV, con escasa inervación ventricular. Su acción sobre el NSA provoca bradicardia, esto es, una ralentización o irregularidad en el ritmo cardíaco, mientras que el efecto sobre el NAV produce una disminución en la velocidad de propagación del potencial de acción.

El control neuronal que influye sobre la actividad del miocardio recibe información de otros elementos que conforma una retroalimentación aferente. Así, la variación de la presión sanguínea provoca que el sistema nervioso modifique la actividad cardíaca, disminuyéndola o incrementándola en función de si ésta se incrementa o disminuye en exceso. Otro elemento influyente es el nivel de CO_2 y O_2, de forma que un incremento del CO_2 o la disminución de O_2 en sangre produce bradicardia y aumento de la presión sanguínea. Por último, la expansión y contracción del tórax producidas por la actividad respiratoria puede causar arritmias, de manera que la tasa cardíaca aumenta en la inspiración y disminuye con la exhalación.

3.3.1. Registro de ECG

La electrocardiografía es una técnica no invasiva que registra la actividad eléctrica del corazón, permitiendo estudiar y detectar diversas patologías. En los datos resultantes puede diferenciarse hasta 6 ondas diferentes principalmente, que pueden proporcionan información relevante de diferentes anomalías. Éstas son, según su aparición temporal en los datos: onda P, Q, R, S, T y U (figura 3.10). De todas ellas, las ondas Q, R y S forman el complejo más importante, debido a que facilita la localización de las otras componentes, además de informar de comportamientos anómalos del corazón, como contracción ventricular/auricular prematura, taquicardia supraventricular, latidos ectópicos, etc.

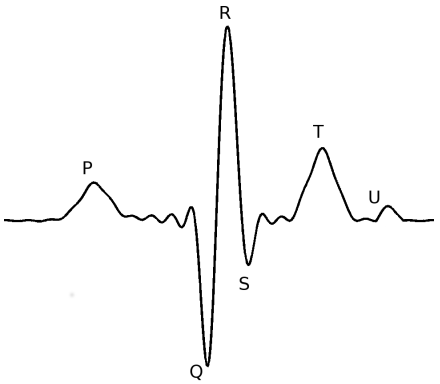

Figura 3.10: Electrocardiograma.

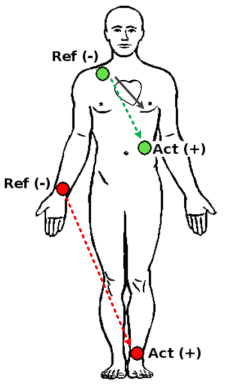

Figura 3.11: Ejemplo de dos montajes para captar la señal de ECG.

El registro de los datos ECG suele realizarse mediante mediciones bipolares sobre el tronco o las extremidades, situando los electrodos en zonas libres de musculatura para minimizar la interferencia de EMG (figura 3.11). Sobre el tronco, uno de los esquemas más comunes es fijar los electrodos a la clavícula derecha y la zona de las costillas flotantes en la parte izquierda del torso. Esta configuración permite detectar diferentes anomalías cardíacas, y su uso es recomendable cuando el sujeto tiene que realizar algún tipo de actividad que implique movimientos en las extremidades. Respecto al montaje sobre las extremidades, existen tres tipos diferentes: tipo *I*, los electrodos se fijan sobre ambas muñecas, tipo *II*, los electrodos se emplazan sobre la muñeca derecha y el tobillo izquierdo, y tipo *III*, los electrodos se sitúan sobre las extremidades izquierdas, muñeca y tobillo. Estos montajes suelen ser más cómodos, aunque pueden limitar la movilidad del sujeto y son más sensibles a artefactos derivados de las contracciones musculares.

3.3.2. Características del ECG

A continuación se procede a describir la información que ofrece cada una de las ondas que componen el ECG, la relación de éstas con diferentes comportamientos anómalos y patologías, y las variaciones que se producen en estos datos ante cambios emocionales en los individuos.

Características generales

Las diferentes ondas que conforma los datos de ECG están relacionadas con las diferentes etapas de polarización/despolarización del corazón, y a raíz de las cuales se pueden detectar diferentes patologías (Sörnmo et al, 2014):

1. *Onda P*: relacionada con sístole auricular causada por la despolarización de sus fibras musculares. Su amplitud no suele exceder los 300μV

con una duración inferior a 120ms, y su frecuencia se sitúa por debajo de los 10Hz. Esta onda ha sido relacionada con arritmias auriculares. La ausencia de esta onda puede deberse a una contracción ventricular ectópica que ocurre antes de que el nodo NSA comience su acción, lo que causa una despolarización simultánea de aurículas y ventrículos. De esta forma, ésta puede ser usada para predecir fibrilaciones de origen auricular (Kurisu et al, 2014; Guidera and Steinberg, 1993).

2. *Complejo QRS*: refleja la despolarización ventricular que produce su sístole cuya duración oscila entre 70 y 110ms en condiciones normales, llegando hasta los 250ms en caso de latidos ectópicos. La amplitud de este complejo llega a alcanzar los 2-3mV, siendo la mayor que acontece en las ondas que componen el ECG, y su rango de frecuencia se sitúa mayoritariamente entre 8 y 20Hz (Benitez et al, 2000). Su morfología general está compuesta por tres elementos (puede variar según el esquema de registro usado): dos desviaciones convexas situadas en los límites del complejo llamadas ondas Q y S, y una desviación cóncava llamada onda R. Cambios en el complejo QRS han sido asociados con latidos ectópicos prematuros de origen ventricular o supravetricular (próximos a la aurícula o al NAV), bloqueos en la conducción del potencial de acción hacia el ventrículo derecho o izquierdo, necrosis del tejido cardíaco, infarto de miocardio, fibrilaciones, etc. (Surawicz et al, 1997; Birnbaum et al, 2014; Ozkan et al, 2014; Pellicori et al, 2015). Por otro lado, el complejo QRS enmascara la repolarización que tiene lugar durante la diástole auricular debido a la diferencia de potencia.

3. *Onda T*: asociada a la repolarización de las fibras musculares de los ventrículos durante la diástole. En condiciones normales, ésta muestra una suave curva redondeada de forma cóncava cuya duración aproximada es de 300ms y su frequencia es inferior a 10Hz. Ésta ha sido asociada a arritmia, isquemia e infarto de miocardio (Järvenpää et al, 2007; Korhonen et al, 2009)

4. *Onda U*: es una pequeña desviación que sigue a la onda T y la cual no siempre está presente. Ésta se ha relacionado con la repolarización de los ventrículos, aunque su origen ha sido objeto de debate desde comienzo del siglo XX. Un reciente estudio concluye que las ondas T y U forman un continuo, resultante del proceso de repolarización ventricular (Ritsema Van Eck et al, 2005). La aparición de la onda U parece estar condicionada a pequeños cambios de voltaje al final de los potenciales de acción que se propagan y a la posición de electrodo respecto al miocardio. Esta onda ha sido relacionada con la repolarización anormal y el infarto de miocardio (Duke, 1975; Tamura et al, 1997; Wang et al, 2013).

Características psicofisilógicas

Los cambios del sistema cardíaco asociados a reacciones ante estímulos internos o externos pueden variar en función de que éstos sean interpretados como perjudiciales o beneficiosos (Lacey, 1967). Un estímulo interpretado como potencialmente peligroso produce una reacción de *lucha o huida* (Cannon, 1929) que provoca un aumento de la tasa cardíaca (Stemmler, 1989; Levenson, 1992), mientras que cuando se percibe como beneficioso puede desembocar en bradicardia para facilitar la atención a un determinado evento (Obrist, 1976; Turpin, 1986; Vila and Fernández, 1989). Estas modificaciones del comportamiento del músculo cardíaco están relacionadas con la influencia ejercida por el SNA (Saul, 1990; Saul et al, 1990; Rajendra Acharya et al, 2006). Un incremento en la actividad del SNS o disminución el SNPS se traduce en una aceleración de la actividad cardíaca, y a la inversa, una disminución en la tasa de latidos del corazón es consecuencia de una baja o alta actividad del SNS o SNPS.

Entre las diferentes características que se pueden extraer de la señal ECG, destaca el análisis de la variabilidad del ritmo cardíaco (en inglés HRV, heart rate variability) que permite extraer información sobre el balance entre el SNS y el SNPS (Akselrod et al, 1981; Pomeranz et al, 1985; Saul, 1990; Saul et al, 1990). Éste se basa en mediar las fluctuaciones que acontecen en los periodos de tiempo que transcurren entre dos ondas R consecutivas, lo que se denomina intervalo RR, y su valor de media para un adulto en reposo es de unos 860ms, equivalente a unos 70 latidos por minutos. La imprecisión en la localización de los complejos QRS puede afectar sustancialmente el resultado del análisis de los datos (Electrophysiology, 1996), por lo que se recomienda la aplicación de un procesamiento adicional que excluya de los segmentos RR aquellos valores atípicos, como por ejemplo desechar los que superen 1.5 veces el valor del rango intercuartílico o seleccionar aquéllos que no excedan el 20% del valor del intervalo previo.

El análisis de la HRV se puede acometer desde la perspectiva temporal y/o frecuencial (Electrophysiology, 1996; Sörnmo et al, 2014) y los cuales están resumidos en las tablas 3.1 y 3.2. En el primer grupo, los parámetros más comunes son: desviación estandar de los segmentos RR (SDNN), raíz cuadrada del valor medio de las diferencias sucesivas al cuadrado de los segmentos RR adyacentes (RMSSD), porcentaje de segmentos RR consecutivos que difieren más de 50ms entre sí (pNN50), y ancho de la base del triángulo con error mínimo respecto al histograma de los segmentos RR y cuyo máximo coincide con el del histograma (TINN). El otro grupo de parámetros está basado en el cálculo de la densidad de espectro de potencia (PDS) de los segmentos RR. Éste se divide en cuatro segmentos y se calcula la influencia de cada uno en el PDS: frecuencias ultra bajas con rango de 0 a 0.003Hz (ULF), frecuencias muy bajas con rango de 0.003 a 0.04Hz (VLF), frecuencias bajas con rango de 0.04 a 0.15Hz (LF), frecuencias altas

con rango de 0.15 a 4Hz (HF), y razón entre LF y HF (LF/HF). Además de los parámetros descritos, otros que se pueden encontrar en la literatura son la entropía de los segmentos RR que permite cuantificar la variabilidad de los datos, los centroides de las bandas de frecuencias, la mediana de los segmentos RR, etcétera (Babloyantz and Destexhe, 1988; Howorka et al, 2010; Amirian et al, 2014).

La actividad del SNS ha sido asociada con la banda LF, observándose un mayor valor durante el día y un incremento durante tareas mentales y actividades físicas, mientras que el SNPS se ha relacionado con el rango de frecuencia de la banda HF, advirtiéndose un aumento a causa del control respiratorio y durante la noche (Malliani et al, 1991). Asimismo, la relación entre ambas bandas medida mediante el cociente LF/HF refleja el balance entre ambos sistemas (Malliani, 1994).

Los parámetros temporales se ven afectados por la actividad general del SNA, por lo que son útiles para detectar anomalías en él, sin embargo no permiten cuantificar la actividad específica del SNS y el SNPS (Kleiger et al, 1992; Pumprla et al, 2002). Así, se ha observado una disminución en la HRV a causa de una atenuación en la actividad del SNPS (Ewing et al, 1984), sin embargo las variaciones a causa de la actividad del SNS son más complejas de relacionar debido a la influencia existente de algunos neurotransmisores o la respiración, entre otros (Greenwood et al, 1997).

Los parámetros frecuenciales son preferibles respecto a los temporales cuando se tratan con datos de corta duración (inferiores a 10 minutos) al ser más sencilla su interpretación en términos de regulación fisiológica, limitando la posible aplicación de los segundos a registros de larga duración (al menos 18 horas) (Electrophysiology, 1996). Por otro lado, los parámetros frecuenciales requieren de un tiempo mínimo de datos para poder enfrentar con cierta garantía el análisis de éstos. Las bandas HF y LF precisan de un mínimo de 1 y 2 minutos respectivamente, mientras que VLF y ULF deben ser evitadas cuando los registros son inferiores a 5 minutos debido a que no existe una relación bien definida para ambas bandas y la actividad cardíaca (Electrophysiology, 1996).

Tabla 3.1: Parámetros temporales de ECG

Abreviatura	Definición	Ecuación
SDNN	Desviación estandar de los segmentos RR.	$\overline{RR} = \frac{1}{N}\sum_{i=1}^{N} RR_i$ $SDNN = \sqrt{\frac{1}{N}\sum_{i=1}^{N}(RR_i - \overline{RR})^2}$
RMSSD	Raíz cuadrada del valor medio de las diferencias sucesivas al cuadrado de los segmentos RR adyacentes.	$RMSSD = \sqrt{\frac{1}{N-1}\sum_{i=2}^{N}(RR_i - RR_{i-1})^2}$
pNN50	Porcentaje de segmentos RR consecutivos que difieren más de 50ms entre sí.	$pNN50 = \frac{100}{N-1}\sum_{i=2}^{N} u(\lvert RR_i - RR_{i-1}\rvert - 50ms)$ donde "u"es la función escalón unitario o de Heaviside.
TINN	Ancho de la base del triángulo con error mínimo respecto al histograma de los segmentos RR y cuyo máximo coincide con el del histograma.	
Mrr	Mediana de los segmentos RR.	$Mrr = RR_{N/2}$ donde $RR_i < RR_{i+1}$
Secg	Entropía de los segmentos RR.	$Secg = -\sum_i (p_{RR_i} \cdot log_2(p_{RR_i}))$ p_{RR_i} es la probabilidad del segmento RR_i.

Tabla 3.2: Parámetros frecuenciales de ECG

Abreviatura	Definición	Ecuación
ULF	Banda de frecuencias ultra bajas con rango de 0 a 0.003Hz.	$E_{ecg} = \sum PSD^2$ $ULF = 2 \cdot \frac{\sum_{f=0Hz}^{0,003Hz} PDS_f}{E_{ecg}}$
VLF	Banda de frecuencias muy bajas con rango de 0.003 a 0.04Hz.	$VLF = 2 \cdot \frac{\sum_{f=0,003Hz}^{0,04Hz} PDS_f}{E_{ecg}}$
LF	Banda de frecuencias bajas con rango de 0.04 a 0.15Hz.	$LF = 2 \cdot \frac{\sum_{f=0,04Hz}^{0,15Hz} PDS_f}{E_{ecg}}$
HF	Banda de frecuencias altas con rango de 0.15 a 4Hz.	$HF = 2 \cdot \frac{\sum_{f=0,15Hz}^{4Hz} PDS_f}{E_{ecg}}$
LF/HF	Razón entre LF y HF.	
fVLF	Frecuencia centroide de la banda VLF.	$fVLF = \frac{\sum_{f=0,003Hz}^{0,04Hz} PDS_f \cdot f}{\sum_{f=0,003Hz}^{0,04Hz} PSD_f}$
fLF	Frecuencia centroide de la banda LF.	$fLF = \frac{\sum_{f=0,04Hz}^{0,15Hz} PDS_f \cdot f}{\sum_{f=0,04Hz}^{0,15Hz} PSD_f}$
fHF	Frecuencia centroide de la banda HF.	$fHF = \frac{\sum_{f=0,15Hz}^{4Hz} PDS_f \cdot f}{\sum_{f=0,15Hz}^{4Hz} PSD_f}$

Capítulo 4

Resultados

Establecido el marco de desarrollo del presente trabajo de investigación y las bases fisiológicas de las bioseñales que son objeto de estudio, se procede a presentar los artículos que componen esta tesis, con un resumen y aplicaciones en las que pueden tener utilidad.

4.1. Electrooculografía

Dada la capacidad de ser controlada a voluntad, esta señal puede ser aplicada tanto en interfaces HCI como en PC.

4.1.1. Procesamiento

El procesamiento de la señal de EOG debe hacer frente a diversos problemas para conseguir unos resultados satisfactorios: ruido, derivas, pestañeos y sobredisparos (Merino et al, 2010b). Uno de los procedimientos más comunes usados para eliminarlos es el filtro de mediana (Juhola, 1991; Neejärvi et al, 1993; Martinez et al, 2008; Krupiński and Mazurek, 2009a,b, 2010; Bulling et al, 2008, 2009, 2011), sin embargo su eficacia depende mucho del número de muestras que se tome.

Los pestañeos y sobredisparos están caracterizados por una curva en forma de campana, que para los primeros será cóncava, mientras que para los segundos podrá ser cóncava o convexa dependiendo de si la dirección de la sacada que lo precede es ascendente o descendente (figura 4.1). En base a esta característica, se ha desarrollado uno de los algoritmos presentados en esta tesis: Merino et al (2015a) (sección 4.1.3), el cual se identificará como EFS (en inglés, envelope filter sequence), tanto para su versión offline como para su variante online, y cuyo núcleo es un proceso de filtrado basado en la envolvente inferior de los datos.

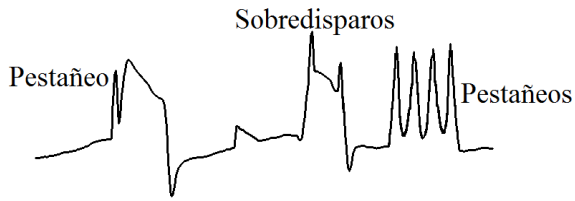

Figura 4.1: Señal EOG. Sacadas, pestañeos y sobredisparos.

Este filtro de envolvente (FE) lleva a cabo los siguientes pasos:

1. Calcular el promedio de dos envolventes inferiores. La primera se extrae directamente de los datos de entrada, mientras que la segunda se obtiene a partir de la primera envolvente.

2. El resultado del paso anterior se restará a los datos de entrada, y se volverá a aplicar el paso 1 sobre esta diferencia.

3. La salida del filtro será la suma de los promedios obtenidos en los pasos 1 y 2.

Definido el FE, el algoritmo EFS sigue los siguientes pasos (figura 4.2):

1. Generar un ruido blanco y añadirlo a la señal. El objetivo es crear pequeñas oscilaciones que mejoren el ajuste de la envolvente a los datos de EOG.

2. Emplear un filtrado de media para eliminar los "dientes de sierra" situados en la cima de los pestañeos y sobredisparos.

3. Aplicar el filtro de envolvente descrito anteriormente e invertir su salida. Con esto se eliminan los pestañeos y los sobredisparos cóncavos.

4. Sobre el resultado del paso anterior, repetir los pasos desde el 1 al 3 para eliminar los sobredisparos convexos.

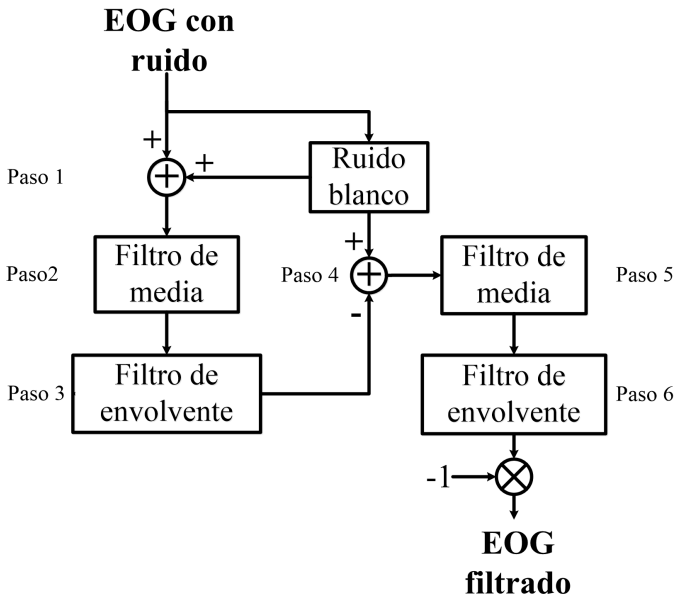

Figura 4.2: Algoritmo EFS: filtrado de pestañeos y sobredisparos.

Para medir la eficacia del procesamiento se ha desarrollado un modelo de la señal EOG que se detalla en el artículo Merino et al (2015a), el cual permite comparar el resultado del filtro con la salida ideal, pudiéndose cuantificar con precisión la cantidad de ruido eliminado. A su vez, el comportamiento ante datos reales se analiza con 7 señales de EOG. Se ha evaluado la reducción de la amplitud del pestañeo, el efecto de pendientes descendentes durante las fijaciones, la capacidad de eliminación de ruido y la preservación de la forma de onda en 3 casos diferentes: movimientos oculares de ida y vuelta desde la posición central del globo ocular (señal pseudorectangular), movimientos durante la lectura de un texto (señal en forma de escalera), y movimientos naturales (aleatorios).

Los resultados de esta técnica se han comparado con un filtro de mediana de 300ms de anchura y están resumidos en la tabla 4.1. La reducción de la amplitud de los pestañeos es siempre mayor al 97.5% en EFS, mientras que para la mediana, ésta cae rápidamente hasta el 40% conforme la duración de los pestañeos aumenta. Asimismo, la preservación de la forma de onda es siempre mejor para el filtro de mediana, tanto para desplazamientos oculares de ida y vuelta, de lectura y naturales. Por último, el efecto de pendientes descendente en los periodos de fijación es menor en EFS, consiguiendo una robustez al ruido que se sitúa entre 10 y 14dB frente al rango del filtro de mediana que va desde los 7 a los 9dB. Para más detalles, consultar el artículo Merino et al (2015a) en la sección 4.1.3.

Tabla 4.1: Resumen de la eficiencia de los filtros EFS y mediana para el modelo de EOG.

Prueba	EFS	Mediana
Pestañeo	(99-97.5) %	(91-40) %
Ida-Vuelta	(70-97) %	>99.9 %
Lectura	(98.2-99.7) %	>99.9 %
Naturales	(73-97) %	(96-99.95) %
Fijación	(14.18-10.08)dB	(9.02-7.40)dB

Por otro lado, los datos reales arrojan resultados similares (figura 4.3), de manera que la capacidad de reducir la amplitud de los pestañeos y los sobredisparos es hasta un 54% superior para EFS respecto a los datos de la mediana, tanto para la versión offline como para su implementación en tiempo real, mientras que la mediana conserva mejor las pendientes de las sacadas.

4.1.2. Análisis y aplicaciones

Definido el procesamiento de los datos EOG, el siguiente paso es detectar los movimientos oculares y/o parpadeos en los sistemas de control, o extraer las características relevantes que permiten determinar el estado emocional del sujeto en las interfaces PC.

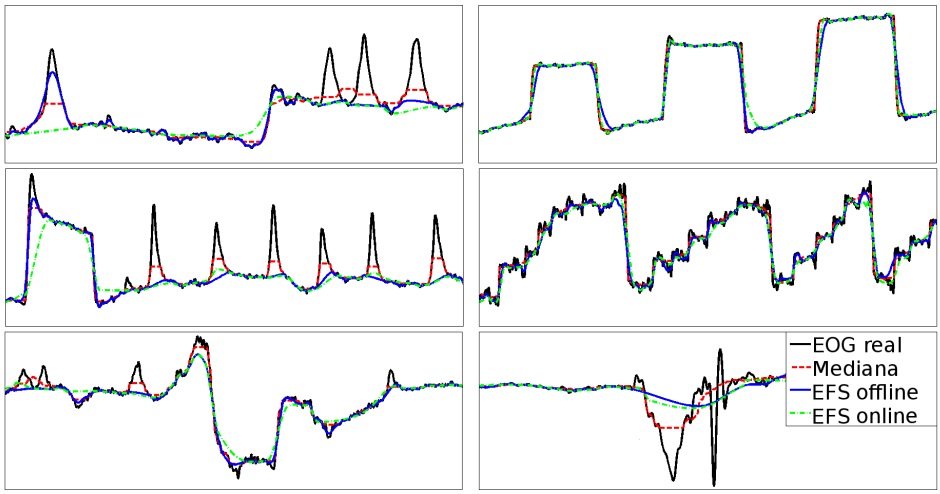

Figura 4.3: Resultados del procesamiento de datos EOG reales.

La sacada es la principal fuente de información sobre el movimiento ocular en HCI (Barea et al, 2000; Yathunanthan et al, 2008; Bulling et al, 2008, 2009, 2011; Merino et al, 2010a,b), y la velocidad de la misma ha sido relacionada con la actividad del sistema nervioso central (Galley, 1989; Findlay and Walker, 1999), siendo indicativo de somnolencia (App and Debus, 1998; Harrison and Horne, 2000; Sallinen et al, 2004; Gould et al, 2009; Fabbri et al, 2010; Russo et al, 2003). En base a las características descritas previamente (sección 3.2), de las que se pueden destacar el hecho de la lineal para movimientos de ±30° (Singh and Singh, 2012) y su duración de hasta 100ms para desplazamientos de 20° (Duchowski, 2007), se puede considerar la ecuación 4.1, usada en Merino et al (2010b), donde se obtiene la diferencia entre muestras separadas 60ms con el objetivo de destacar la sacada y así poder calcular la dirección del movimiento y su duración.

$$EOG'(i) = EOG(i) - EOG(i - 60ms) \tag{4.1}$$

Por otro lado, el parpadeo es otro elemento útil tanto como evento discreto en interfaces de control, así como indicador de concentración y somnolencia (Iwanaga et al, 2000; Galley et al, 2004; Schleicher et al, 2008; Ashtiani and Mackenzie, 2010; MacKenzie and Ashtiani, 2011). Mediante la diferencia de los datos de EOG y la salida del procesamiento EFS se obtiene una señal que contiene tanto pestañeos como sobredisparos, siendo necesario un procesamiento adicional que permita quedarnos únicamente con los parpadeos.

Como se dijo al comienzo de este documento, los trabajos aquí expuestos son la continuación de investigaciones previas en las que se validó esta señal como interfaz HCI controlando un teclado virtual. Los detalles se muestran

en los artículos Merino et al (2010a) y Merino et al (2010b) (anexos A y B). Ambos trabajos junto al desarrollado en Merino et al (2012) (sección 4.2.4) refuerzan la utilidad de esta señal como sistema de control.

4.1.3 Publicación 1

Merino *et al. BioMed Eng OnLine (2015) 14:48*
DOI 10.1186/s12938-015-0046-0

BioMedical Engineering OnLine

RESEARCH Open Access

Envelope filter sequence to delete blinks and overshoots

Manuel Merino*, Isabel María Gómez and Alberto J Molina

*Correspondence:
manmermon@dte.us.es
Department of Electronic Technology, University of Seville, Avd. Reina Mercedes s/n, 41012 Seville, Spain

Abstract

Background: Eye movements have been used in control interfaces and as indicators of somnolence, workload and concentration. Different techniques can be used to detect them: we focus on the electrooculogram (EOG) in which two kinds of interference occur: blinks and overshoots. While they both draw bell-shaped waveforms, blinks are caused by the eyelid, whereas overshoots occur due to target localization error and are placed on saccade. They need to be extracted from the EOG to increase processing effectiveness.

Methods: This paper describes off- and online processing implementations based on lower envelope for removing bell-shaped noise; they are compared with a 300-ms-median filter. Techniques were analyzed using two kinds of EOG data: those modeled from our own design, and real signals. Using a model signal allowed to compare filtered outputs with ideal data, so that it was possible to quantify processing precision to remove noise caused by blinks, overshoots, and general interferences. We analyzed the ability to delete blinks and overshoots, and waveform preservation.

Results: Our technique had a high capacity for reducing interference amplitudes (>97%), even exceeding median filter (MF) results. However, the MF obtained better waveform preservation, with a smaller dependence on fixation width.

Conclusions: The proposed technique is better at deleting blinks and overshoots than the MF in model and real EOG signals.

Keywords: Biosignal processing, EOG signal, Envelope filter, Blink, Overshoot

Background

The eye's goal is to project reflected light from an object onto ocular fovea. Eye movements can be grouped into slow and quick [1]. The former make it possible to maintain either a projected image of non-static objects or a projected image when the head is turned (velocity <30°/s), while quick movements prevent an image from being lost as it is projected on the same place in the retina (microsaccadic—steps <0.25°/s), and if there is a quick change of point of view (saccadic—variations <700°/s). The eyelids are the other important element of the human visual system. They moisten, clean and protect eyes from external physical agents. Their movements are called blinks.

Eye and blink movements are used in studies on somnolence, workload, or concentration. Different studies have related eye movements to central nervous system activity [2]

and somnolence [3, 4]. In turn, blink rate has been reported as an indicator of sleeplessness and attention/concentration, whereby sleep deprivation raises its frequency and duration, while an increase in attention levels produces a decrease in blinking [5, 6]. Some control interfaces have been based on them: for example, activity recognition or handling a computer through events. Classifying activities are based on pattern detection, as in reading which involves small eye movements from the beginning of a text line and a big shift at the end [7]. Event activities are mainly based on go-and-back movement (GBM) from eyeball center to an extreme: for example, a virtual keyboard [8], a mouse pointer [9], or a wheelchair [10].

Ocular activity can be recorded using several techniques, such as infrared light [11], video camera [12], or electrooculography (EOG), which is our focus. EOG is a well-known eye-tracker technique which measures the electric potential difference between cornea and retina (± 1 mV [13]—depending on several factors such as light level [14]) and is recorded when ocular movements occur. It measures electrical activity with Ag/AgCl electrodes placed around the eyes. The most common electrode layout is shown in Figure 1. Two electrodes for each horizontal or vertical direction are employed, providing bipolar data. A monocular configuration is utilized in vertical eye movements, and a binocular setting is used in horizontal shiftings [1]. EOG amplitudes range from 5 to 20 μV/°, so that $\pm 30°$ ocular movements [15] are quasi linear, and essential frequency components range from 0 to 30 Hz [16]. The duration of a saccade depends on the angle of eye movement, with the most common being under 20°, and lasting from 10 to 100 ms [12]. The time between two consecutive saccades is termed fixation and the average value lies between 100 and 200 ms [17].

The eye-tracker system using an EOG faces a series of problems: noise, drift, blinks and overshoots [18]. This paper focuses on the last two. The blinking signal is a bell-shaped noise which overlaps on the electrical activity of eyes, while overshoots are similar to blinking impulses located in the saccadic area and they occur due to target localization error corrected by a secondary saccadic eye movement [19, 20] (Figure 2). Blinks are caused by eyelid movements, while overshoots happen mainly with fast, high amplitude, eye movements. The blink rate of a relaxed individual is between 12 and 19 blinks per minute [21], with an average duration of 100 up to 400 ms [22].

The median filter (MF) is one of the most commonly used techniques for deleting these noises because the saccadic-edge slopes are preserved and noise is attenuated

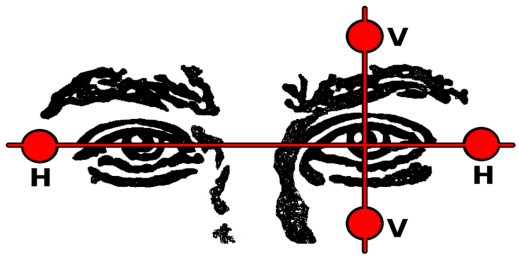

Figure 1 EOG electrode layout. Electrodes H and V record horizontal and vertical eye movements.

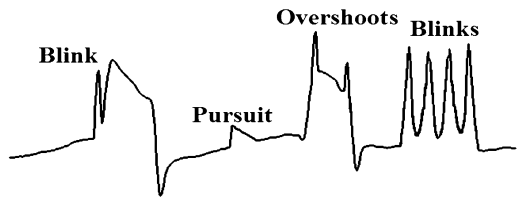

Figure 2 EOG signal. Saccades, blinks, overshoots and pursuit movements.

when the duration is at its most buffered [23]. This can be used in online and/or offline processings because it is based on split windows. Two other algorithms based on MF are FIR median hybrid filters (FMH) and weighted FMH filters (WFMH) [24]. The former applies the MF to the output of an FIR filter, whereas in the latter, the MF is obtained for each output of an FIR filter multiplied by a constant. Two versions of WFMH are interesting: center weighted FMH filter (CWFMH) and subfilter weighted FMH filter (SWFMH) [24]. CWFMH leaves all FIR outputs intact, apart from the middle element which is multiplied by a constant. The edges and sinusoidal signals are preserved. SWFMH multiplies the extremes and the central elements remain intact. High frequency noise is removed and the edges are maintained. All these filters were analyzed in Martinez et al. [25]. FMH and WFMH results are not better than MF, while SWFMH produces non-meaningful differences in detection rate in relation to MF. In addition, a serial sequence of MF may improve the results of a single MF [26, 27]. However, a sequence or a single MF encounters several problems for deleting noise [28]. A blink in the saccade vicinity causes the edge slope to be smoothed, whereas a sequence of consecutive blinks produces a squared pulse similar to eye movement (Figure 2). In contrast, small steps are caused by smooth pursuit movements and a big MF mask size delays the saccadic edges.

In this paper, we propose an algorithm for removing overshoots and blinks. The methodology is detailed in the next section, with a description of the proposed filter, and procedures to evaluate processing effectiveness. We then go on to analyze and discuss processing outputs.

Methods

This section goes into the details of the online and offline versions of the proposed algorithm for processing EOG data (first subsection), and the tests performed to determine effectiveness (second subsection). We performed the tests with our own seven acquired EOG signals to evaluate in real data and simulated EOG signals to measure and verify different processing features. We developed this model because we were unable to find EOG databases with specialist annotations of saccade movements, blinks and overshoots ("Appendices 1, 2"). By using the model we were able to evaluate processing precision versus inserted noise level from blinks, overshoots, and general interferences, and to compare filtered outputs with ideal data. Version 8.0.0.783 of Matlab was utilized to develop and simulate the processings and to analyze their results.

EOG filter

This section describes the process for deleting blinks and overshoots in the EOG signal. The algorithm is based on obtaining envelopes to signals as occurs in empirical mode decomposition technique [29]; a similar process was used to detect QRS waveforms in electrocardiogram signals [30], to filter peak and spike noise in EEG signals [31], to study foot muscle coordination from EMG data [32], and to obtain power dependencies in neuroimaging data [33]. The next two subsections explain the process for obtaining lower envelope and how it is used to filter; the last two add detail to the proposed technique.

Lower envelope

Essentially, the algorithm finds a set of envelopes of the EOG signal (Figure 3a) by following two steps.

Step 1: Find all local minimums from data.

Step 2: Generate a new signal based on the cubic Hermite interpolant that crosses each extreme and passes by the first and final value of the input data.

This interpolation provides a piecewise cubic function based on values at neighboring grid points using third-degree polynomials with Hermite form, so that a smooth approximation of the EOG signal is obtained.

Envelope filter

Let *D* be the input data of size n. Let *F* be a zero vector, also of size n, where the filtered data are stored.

Step 1: Let *E1* be the first lower envelope obtained from *D* by applying the procedure described in previous subsection.

Step 2: Let *E2* be the second lower envelope from applying the procedure to E1 (step 1).

Step 3: Add the average of *E1* and *E2* to *F* (1).

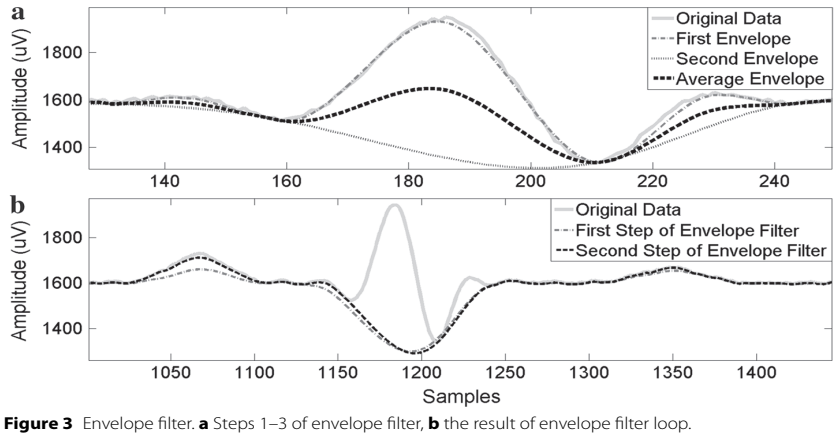

Figure 3 Envelope filter. **a** Steps 1–3 of envelope filter, **b** the result of envelope filter loop.

$$F = F + \frac{E1 + E2}{2} \tag{1}$$

Step 4: Assign to D the difference between data and the previously filtered data ($D = D - F$). The next iteration is performed on this new D.

Step 5: Repeat steps 1–4 twice in total.

The algorithm obtains two lower envelopes (steps 1 and 2). The first of them extracted directly from data and the second based on the first extracted envelope. The first envelope cannot filter blinks or overshoots with a sawtooth-shaped top. For this reason, a second envelope is obtained from the first (Figure 3a). The latter decreases saccade edge slopes excessively. To reduce this negative effect of the second envelope, the average between both envelopes is calculated. Although the blinks and overshoots with sway-shaped tops are not totally filtered, their amplitudes are reduced (Figure 3b). Furthermore, a second iteration causes the output fixations to be closer to input-data fixations.

EOG filter: envelope filter sequence (EFS)

The procedure to filter blinks and overshoots from EOG, which is shown in Figure 4, is as follows.

Step 1: Generate white noise and add to EOG input. This white-noise signal is known as EFS-WN. It is obtained using (2) where wn and E_{wn} are an initial white-noise signal and its energy, E_s is the energy of input data without DC component and SNR is the signal–noise rate measured in decibels of EFS-WN in relation to input data.

$$EFS\text{-}WN = wn \cdot \sqrt{\frac{E_s}{E_{wn} \cdot 10^{\frac{SNR}{10}}}} \tag{2}$$

Step 2: Apply a mean filter.

Step 3: Employ the envelope filter from the output of step 2.

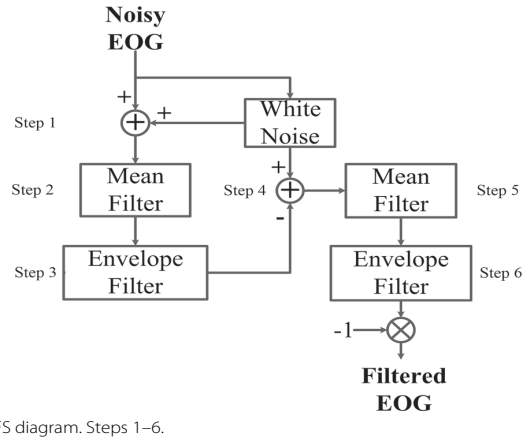

Figure 4 Offline EFS diagram. Steps 1–6.

Step 4: Add the EFS-WN obtained in step 1 to the inverted output of the envelope filter.

Step 5: Apply a mean filter.

Step 6: Employ the envelope filter from the output of step 5. The output must be inverted to keep the original eye-movement directions.

The resulting algorithm is referred to as EFS, and applies two envelope filters (steps 3 and 6). The first deletes concave variations (blinks and top overshoots), whereas the second removes convex curves (down overshoots). EFS-WN is added to cause oscillations in the data (steps 1 and 4). The envelopes are more similar to original data when small variations happen, therefore EFS-WN amplitude has to be small. The output of step 3 is inverted to delete down overshoots correctly (step 4). The mean filters are used to delete small sway-shapes on the top of blinks and overshoots (steps 2 and 5). Thus, sawtooth shapes are generated through the EFS-WN and mean filters. The output of the algorithm must be inverted to maintain initial ocular-movement direction.

Envelope filter sequence supposes that blinks have concave shapes (Figure 2). For this reason, lower envelope is its core. Nevertheless, there are schemes where blink form is convex. In such cases, the input data must be inverted before applying this processing.

EFS: online version

Some systems, for example control interfaces, require real-time processing to achieve their goals. An online version is described in this subsection and Figure 5.

Step 1: Three persistent FIFO (First In, First Out) buffers must be established: input-data buffer (IB), white-noise buffer (WNB), and another containing the final fragment of EFS output (OB). The aim of the EFS is to filter blinks and overshoots, so IB length must be wide enough to contain at least one blink. This buffer acts as a sliding window with overlapping. The aim of the overlap is to prevent that part of output becoming deformed because blink waveform is not stored completely in IB. WNB contains the white noise of overlapped data from the previous window. This stops local minimums from this fragment changing in the next execution, and output showing gaps. Finally, output derivability is a desired feature, thus OB is used as a link between iterations and envelopes must cross for their data.

Step 2: When IB is full, calculate EFS-WN from EOG input, join with WNB, and add to IB.

Step 3: Apply a mean filter.

Step 4: Employ the envelope filter, so that each envelope beginning must cross for OB. Two considerations have to be taken into account. First, step 2 of the "Lower envelope"

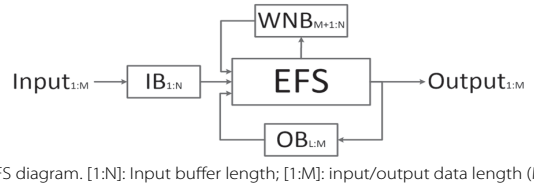

Figure 5 Online EFS diagram. [1:N]: Input buffer length; [1:M]: input/output data length (M < N); [M + 1:N]: overlapping width; [L:M]: fragment size of filtered data (L ≤ M).

changes slightly. It says that the interpolation must cross the first sample of the input signal, but now, this is replaced by OB. Second, the envelope filter makes two interactions, and OB is used in the first. In the second, OB is replaced by a new zero vector.

Step 5: Add EFS-WN to the inverted output of step 4.

Step 6: Apply a mean filter.

Step 7: Repeat step 4. Invert its output.

Step 8: Store the overlapping segment of EFS-WN in WNB and the final fragment of output in OB.

Step 9: Returned filtered data are not overlapped. Bell-shaped partial waveforms stored in IB may reduce the effectiveness of filtering. To prevent this effect, processing output discards the overlapped buffer segment.

Procedure

Nine tests were conducted. The first three determined the EFS parameters for offline and online versions. The other tests compared filtering results of EFS and MF. According to [25], MF length was set to 300 ms. The first eight tests used 100 signals from the model described in "Appendix 1". Henceforth, the model name is EOG system generator (EOG-SG). The main features of these signals are explained in this subsection. However, more details are given in "Appendix 2". The ninth test compared MF and both versions of EFS from real EOG signals. All tests applied a 30-Hz-lowpass filter [16].

Envelope filter sequence parameters were established in Tests 1 and 2: they were EFS-WN amplitude and mean-filter length. EFS parameters were calculated versus sampling rate. In both tests, one of the EFS parameters was set and the other changed. Test 1 obtained EFS-WN amplitude by increasing *SNR* by 1 dB from 1 to 60 dB in (2) for the same input data. Energy of the input signal was used as E_s, and mean-filter length was set at 31.25 ms. With the best EFS-WN amplitudes set in Test 1, mean-filter length was modified from 2 to 100 samples. The best values of EFS parameters were obtained through correlation coefficients (CC) based on Agrawal and Gupta [34] whose expression was (3), where L was the number of samples, EM was the ideal signal without overshoots and blinks obtained from (17) in "Appendix 1", and NI was the non-ideal signal, so that it could have been filter output or input data. In this case, NI was the output data. This feature measured the similarity between signals and its value ranged between 0 and 1. The selected EFS parameters had a CC value over 0.97.

$$CC = \frac{\left(\sum_{i=1}^{L} EM_i \cdot NI_i\right)}{\left(\sum_{i=1}^{L} (EM_i)^2\right) \cdot \left(\sum_{i=1}^{L} (NI_i)^2\right)} \tag{3}$$

Test 3 determined the lengths of three buffers and the overlapping area of the online version of EFS. The values of parameters obtained in Tests 1 and 2 were set. Buffer lengths were modified in each iteration, such that IB increased by 0.1 s in each iteration from 0.6 up to 1 s; overlapping area and WNB width changed from 0.1 to 0.4 s, increasing 0.1 s (WNB depends on overlapping); and OB was modified between 0.05, 0.10 and 0.15 s. The CC and root mean square error (RMSE) (4) were obtained in each case.

$$RMSE = \sqrt{\frac{\sum_{i=1}^{L} (EM_i - NI_i)^2}{L}} \tag{4}$$

Tests 1–3 used EOG-SG signals with 100 GBMs, blinks and overshoots. Different features of the model were set randomly. The range of eye movement oscillated between −40° and +40°, with horizontal fixations whose time was established between 0.6 and 1.5 s. Blink width varied between 0.3 and 0.55 s with a frequency of 19 blinks per minute. They happened in periods between GBMs which this time was set between 3 and 5 s. In addition, sampling rates in Tests 1 and 2 were {128, 256, 360, 512, 1,200, 2,400} Hz, while Test 3 used 128 Hz, because it was considered that the results of the first two tests were similar for all sampling rates.

With EFS parameters set, Tests 4–8 analyzed the ability of MF and EFS filters to delete blinks and overshoots and waveform preservation for a 128 Hz sampling rate. This value was selected to reduce model and analysis computing time.

Test 4 measured the level of bell-shaped removal through blink signals without saccadic movements. Blink durations were increased 0.1 s in each iteration from an initial interval of [0.1, 0.2] s up to [0.4, 0.5] s. Blink frequency varied randomly between 12 and 22 blinks per minute. Besides CC and RMSE from filter output, we calculated the percentage decrease of blink amplitudes and percentage of processed blinks whose output amplitudes remained higher than the 25% raw blink amplitude. Tests 5–7 studied waveform preservation of both filters versus fixation time without blinks and overshoots. The duration varied randomly from an initial interval between 0.3 and 0.4 s up to fixations between 1.4 and 1.5 s. The interval width was increased by 0.1 s in each new signal. Test 5 focused on signals with 1,000 GBMs; Test 6 used 125 stair-shaped waveforms in each signal to simulate reading activity; and Test 7 analyzed signals with 1,000 consecutive random saccadic movements to imitate natural eye movements. In Test 6, the ocular shiftings in a stair waveform moved from the start point of −15° up to the final position of +15° where the number of saccades oscillated randomly between 6 and 10. Tests 5 and 7 used saccades whose values were between −40° and +40°. In these tests, the CC and RMSE were calculated from filtered data. Test 8 analyzed the effect of fixation slopes in 1,000 GBMs signals with overshoots and blinks, as defined for Tests 1–3, but with a sampling rate of only 128 Hz. The difference with respect to these tests was the fixation slope, that is, the variation of amplitude between two consecutive saccades (“Appendix 1”—second subsection). This dropped during fixation time, with the decrease ranging from 5% in each iteration from an initial interval [0, 5]% up to [35, 40]%. Note that variation in the fixation slopes made it difficult to restore their horizontal-shaped waveforms. Hence, this test established the signal with variations in the fixation slope as the ideal signal, as defined in (17). This test calculated the following features: CC, RMSE, SNR, saccadic slope variations (SSV) and the number of non-filtered overshoots from the filtered signal. They were obtained for input and output signals. SNR was obtained by (5) where *NI* could be the input signal or the output data; thus, it measured how they were affected by noise. SSV was calculated by (6) where *P* was the number of saccades, *S*(*i*) was the set of samples of the saccade slope, and *FO* was filter output.

$$SNR = 10 \log_{10} \left(\frac{\sum_{i=1}^{L} (EM_i)^2}{\sum_{i=1}^{L} (EM_i - NI_i)^2} \right) \tag{5}$$

$$SSV = \frac{100}{P} \cdot \sum_{i=1}^{P} \left(1 - \frac{\sum_{j=1}^{S(i)} \left(FO_j - FO_{j-1} \right)}{\sum_{j=1}^{S(i)} \left(EM_j - EM_{j-1} \right)} \right) \quad (6)$$

The ethics committee of the University of Seville accepted Test 9 with real data from individuals. This one was performed with 55 min of real EOG data from seven signals from three subjects: eye movements were recorded while the individual watched a film (natural eye movement), read a book (stair-waveform), did GBM, and watched dark screen for null activity (blinkings). Only the vertical channel was obtained for natural movements, whereas horizontal and vertical shiftings were recorded for other signals. They were recorded using the bioamplifier model gtec gUSBamp, and version 2.0 of the BCI2000 software [35]. Their features are summarized in Table 1. Sampling rate was 1,200 Hz for natural movement, and 256 Hz for the others. Notch to remove power line interference and 30 Hz lowpass filters were applied to all of them [16]. The reason for these sampling rates was that the data we used were recorded before the EFS technique and this paper's tests were developed. Data were filtered through MF and offline and online versions of EFS. Data were then split to select only intervals of blinks, saccades and overshoots. Segments of raw data and processing outputs were normalized between 0 and 1. Normalization values of raw data were applied to filtered signals. The extracted features were: mean of SSV for saccade slopes; mean of overshoot amplitude reduction; and summation of blink area reduction.

Outlier values of all measured features were avoided using the interquartile-range method (7), where *f* were values of the feature used, and *Q1* and *Q3* were quartiles 1 and 3 respectively.

$$f \in [Q1 - 1.5(Q3 - Q1), \quad Q3 + 1.5(Q3 - Q1)] \quad (7)$$

Results

The analysis of results of Tests 1 and 2 provides EFS parameters for its offline version. They are summarized in Table 2 and Figure 6. The selected intervals have a CC over 0.97. The SNR of EFS-WN and mean-filter length increased with sampling rate. These SNR values translated into smaller EFS-WN amplitudes, because more noise data were recorded. Furthermore, when mean-filter length time was calculated, it appeared as more stable.

Test-3 results provided buffer lengths for the EFS online version (Figure 7). There was practically no change in error in relation to OB. The smallest length was selected (0.05 s). In addition, an overlapping area of 0.2 s produced the best results for all cases. Finally, output data were more similar to the ideal signal when IB width enlarged, as more signal

Table 1 Real EOG signal features

Signal	Time (min)	Sampling rate (Hz)	Blinks		Saccades			Overshoots	
			Number	Width (ms)	Number	Fixation width (ms)	Slope width (ms)	Number	Width (ms)
Blinks	8	256	132	479 ± 8	0	0	0	0	0
GBM	4	256	19	496 ± 22	73	1,637 ± 42	155 ± 8	25	154 ± 10
Natural	21	1,200	103	268 ± 13	278	2,365 ± 165	156 ± 6	49	113 ± 6
Reading	22	256	28	287 ± 12	1,612	301 ± 4	44 ± 0.48	16	116 ± 11

Real EOG features. Mean and standard error are shown for blink, saccade, and overshoot times for each real signal.

Table 2 Best values of EFS parameters

Sampling rate (Hz)	Test 1		Test 2	
	SNR (dB)	Best value (dB)	Mean-filter length (ms)	Best value (ms)
128	[22, 52]	32	[15.63, 187.5]	31.25
256	[27, 58]	36	[7.81, 250.00]	35.16
360	[30, 60]	40	[8.33, 250.00]	36.11
512	[33, 60]	41	[9.77, 193.36]	37.11
1,200	[40, 60]	50	[8.330, 82.50]	26.67
2,400	[46, 60]	56	[8.330, 41.25]	25.00

Best values of EFS parameters versus sampling rate. CC values are 0.97 higher in each interval of the table.

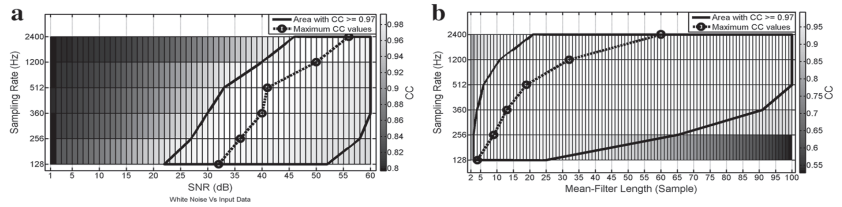

Figure 6 Results of Tests 1 and 2. **a** Best amplitudes of FS-WN; **b** best lengths of mean filter.

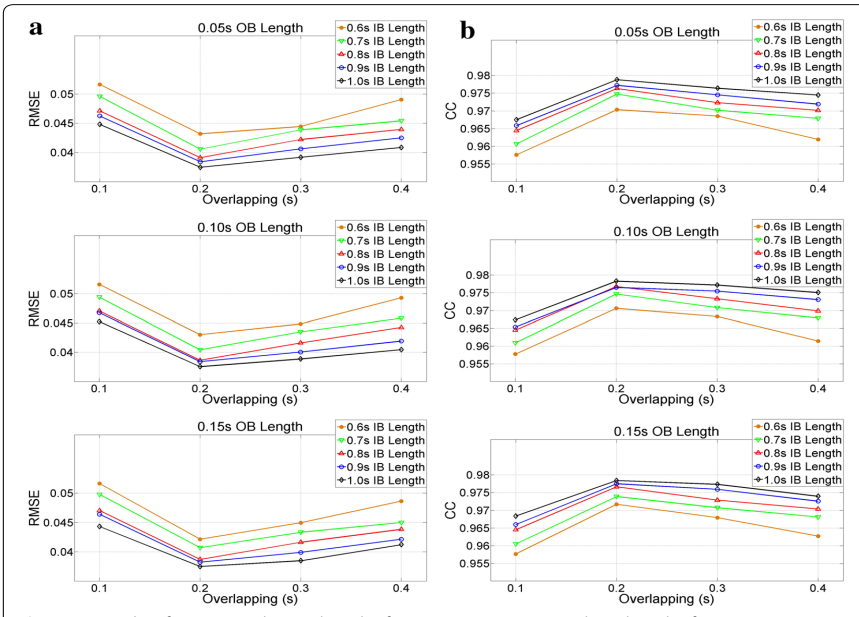

Figure 7 Results of Test 3. Matching IB length of {0.6, 0.7, 0.8, 0.9, 1.0} s with OB length of {0.05, 0.10, 0.15} s with overlapping of {0.1, 0.2, 0.3, 0.4} s. **a** Root mean square error; **b** cross correlation.

information was stored. However, a greater length produced an increased delay in real time systems. Thus, an IB of 0.7 s was selected, because this length obtained a CC over 0.97. The online EFS parameters, that is, EFS-WN amplitude and mean-filter length, were equal to the offline version, because we supposed that each segment of signal had an SNR value similar to the total signal. In contrast, Test 3 CC results were similar to Tests 1 and 2, thus the results of Tests 4–8 can be extrapolated to the online version.

Test-4 results are shown in Figure 8. The median filter's ability to remove bell-shaped interference decreased with blink duration, while it remained constant with the EFS filter (the error was between 6 and 15 times smaller). In this way, blink amplitude was reduced from 99 to 97.5% with the EFS algorithm in all cases, whereas MF effectiveness fell abruptly from 91 to 40% as bell-shaped width increased. In addition, the number of blinks whose amplitude exceeded 25% of the original value increased as the duration increased, such that it was only 4.6% for EFS processing in the worst case, and always far below the MF.

Waveform preservation test results (Tests 5–7) are summarized in Figures 9, 10 and 11. RSME shows that MF fitted better than EFS in all cases. These differences decreased as fixation duration increased. Both processings had a much larger error with random ocular movements versus other cases, while the reading activity produced the best error

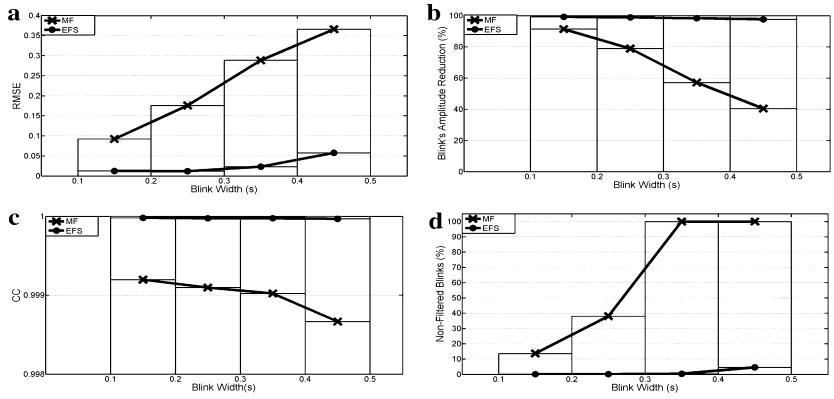

Figure 8 Blink removal. **a** Root mean square error; **b** percentage decrease of blink amplitudes; **c** cross correlation; **d** percentage of blinks whose amplitudes after filtered processing exceeded 25% of original amplitudes.

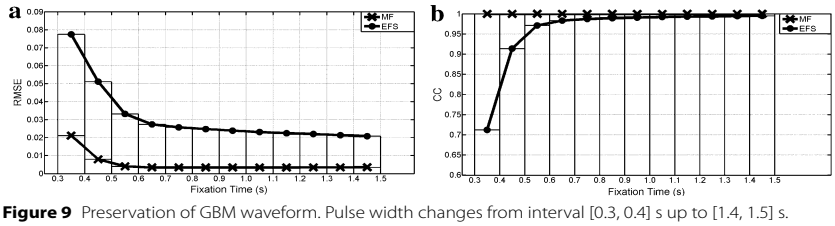

Figure 9 Preservation of GBM waveform. Pulse width changes from interval [0.3, 0.4] s up to [1.4, 1.5] s. **a** Root mean square error; **b** cross correlation.

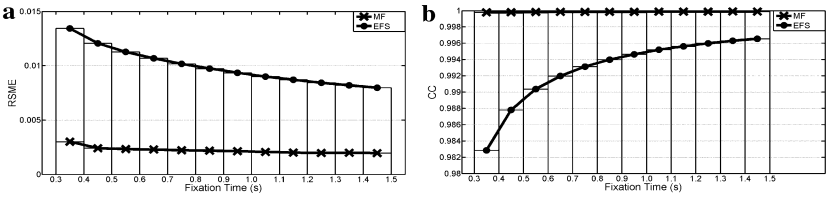

Figure 10 Preservation of stair waveform (reading activity). Step width changes from interval [0.3, 0.4] s up to [1.4, 1.5] s. **a** Root mean square error; **b** cross correlation.

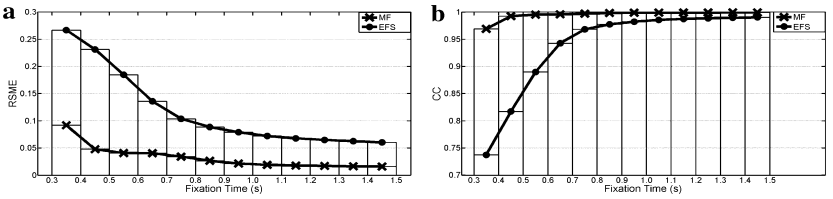

Figure 11 Preservation of random waveform. Step widths change from interval [0.3, 0.4] s up to [1.4, 1.5] s. **a** Root mean square error; **b** cross correlation.

values. EFS showed CC values over 0.97 when fixation widths were higher than 0.5 and 0.7 s for GBM and random ocular movements, whereas its smallest value was 0.98 for reading the EOG signal. Meanwhile, the MF had no fixation problems, with the output signal being almost equal to the input signal (CC > 0.99), when input was free of blinks and overshoots.

Results of Test 8 are summarized in Table 3 and Figure 12. SNR shows that the capacity to obtain the ideal signal with MF and EFS decreased with the fixation slope. EFS processing was more effective at restoring the ideal signal as shown in all table features. However, the fixation-slope effect produced smaller variations of SNR, CC and RSME in MF.

The best values of SNR, CC and RMSE were reached when fixation slopes were between 0 and 5%. EFS processing obtained a good SNR value for all cases (>10 dB), CC increased about 22% and RMSE dropped to 76% in relation to input data, whereas the MF SNR value was below 10 dB, CC increased around 17% and RMSE dropped to 72%.

While saccade slopes in all cases remained virtually unaltered in MF, in EFS, they dropped to 50%. Both techniques filter all overshoots completely (100% deleted).

Finally, Figure 13 shows the features measured in Test 9 for real EOG signals, with a visual analysis in Figure 14. EFS parameters were set from Table 2 for sampling rates of 256 and 1,200 Hz. However, online EFS-WN SNR was set to 27 and 30 dB for better results. A 300 ms MF was much less capable of deleting blinks, with the decreased area being 53.96 and 55.61% lower than the offline and online EFS versions (Figure 13a). Blink interference in horizontal movements was also 39.58 and 42.45% lower. However, non totally-filtered blinks retained a greater amplitude with EFS (Figure 14, markers *). When there was a short time between two blinks,

Table 3 Fixation slope effect

	Fixation slope (%)							
	[0, 5]	[5, 10]	[10, 15]	[15, 20]	[20, 25]	[25, 30]	[30, 35]	[35, 40]
Input								
SNR (dB)	1.754 ± 0.014	1.509 ± 0.015	1.330 ± 0.014	1.079 ± 0.014	0.887 ± 0.013	0.664 ± 0.016	0.41 ± 0.011	0.181 ± 0.014
CC	0.805 ± 4e−4	0.798 ± 5e−4	0.793 ± 5e−4	0.785 ± 5e−4	0.779 ± 4e−4	0.771 ± 6e−4	0.763 ± 3e−4	0.755 ± 5e−4
RMSE	0.145 ± 1e−4	0.146 ± 1e−4	0.145 ± 1e−4	0.145 ± 8e−5	0.146 ± 1e−4	0.146 ± 1e−4	0.146 ± 1e−4	0.146 ± 1e−4
EFS								
SNR (dB)	14.188 ± 0.021	13.742 ± 0.022	13.216 ± 0.021	12.640 ± 0.023	12.017 ± 0.025	11.380 ± 0.028	10.750 ± 0.026	10.080 ± 0.025
CC	0.982 ± 8e−5	0.980 ± 11e−4	0.978 ± 12e−5	0.974 ± 15e−5	0.970 ± 20e−5	0.965 ± 25e−5	0.959 ± 30e−5	0.952 ± 33e−5
RMSE	0.035 ± 1e−4	0.036 ± 1e−4	0.037 ± 1e−4	0.038 ± 1e−4	0.40 ± 1e−4	0.042 ± 1e−4	0.044 ± 1e−4	0.047 ± 1e−4
SSV (%)	50.02 ± 0.026	50.17 ± 0.026	50.28 ± 0.026	50.28 ± 0.027	50.22 ± 0.027	50.21 ± 0.029	50.09 ± 0.030	50.09 ± 0.031
MF								
SNR (dB)	9.020 ± 0.019	8.768 ± 0.020	8.597 ± 0.019	8.335 ± 0.019	8.147 ± 0.015	7.914 ± 0.021	7.650 ± 0.017	7.407 ± 0.020
CC	0.944 ± 22e−5	0.941 ± 25e−5	0.939 ± 25e−5	0.936 ± 25e−5	0.933 ± 21e−5	0.930 ± 31e−5	0.926 ± 24e−5	0.922 ± 32e−5
RMSE	0.041 ± 9e−5	0.041 ± 8e−5	0.041 ± 8e−5	0.042 ± 7e−5	0.042 ± 7e−5	0.042 ± 8e−4	0.042 ± 8e−5	0.042 ± 8e−5
SSV (%)	1.27 ± 5e−3	1.305 ± 6e−3	1.376 ± 6e−3	1.456 ± 6e−3	1.484 ± 6e−3	1.617 ± 7e−3	1.803 ± 7e−3	1.971 ± 8e−3

Analysis of fixation slope effects (mean ± standard error). SNR, CC and RMSE were calculated using the ideal signal as reference.

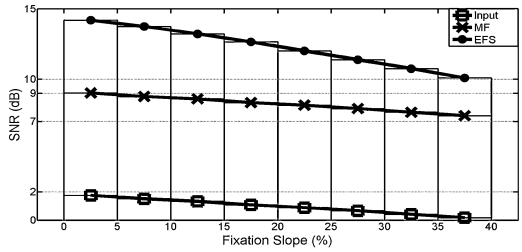

Figure 12 Fixation slope effects. Variation of SNR of input data, MF and EFS outputs. Slope changes from interval [0, 5]% up to [35, 40]%.

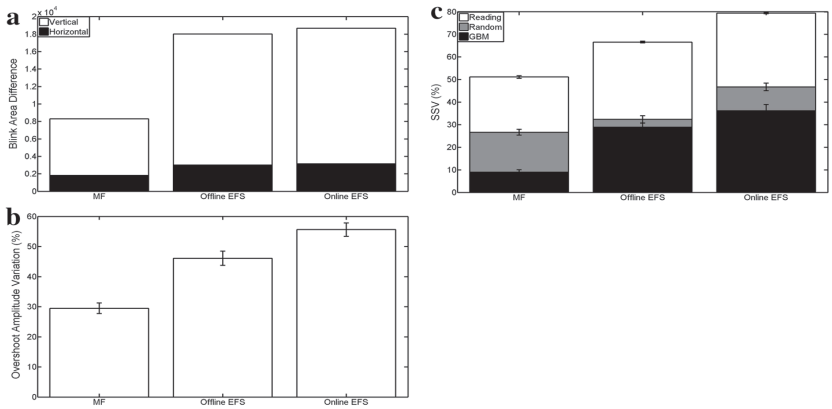

Figure 13 Result of real EOG processing. Results of MF, offline and online EFS. **a** Summation of blink area reduction; **b** overshoot amplitude variation; **c** saccade slope preservation for reading, natural and go-back eye movements.

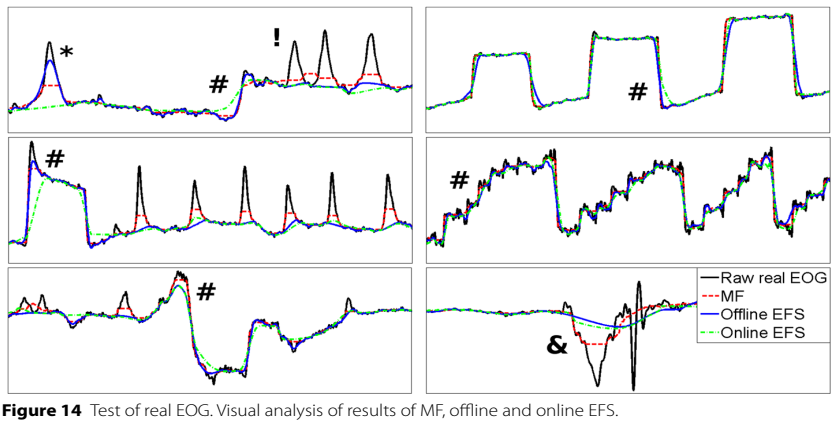

Figure 14 Test of real EOG. Visual analysis of results of MF, offline and online EFS.

MF generated an artificial pulse between them (Figure 14, marker !), and this never occurred with EFS. Overshoot amplitudes only dropped around 30% for MF (Figure 13b), while EFS versions obtained better results (46 and 55%). However, saccadic slopes were better in MF (Figures 13c, 14, markers #). For reading activity, MF preserved 49% of slopes, whereas EFS retained 34 and 20% for offline and online versions. All processings retained better for other signals: 74, 68 and 54% of natural-movement slopes were conserved, and 91, 72 and 64% of GBM slopes were preserved. Finally, spike perturbations were filtered in both cases (Figure 14, marker &), but EFS reduced them to a greater extent.

Discussion

Bell-shaped waveforms, such as blinks and overshoots, are unwanted elements in some control interfaces or activity classifiers [7–10, 18], because they reduce their effectiveness. The offline and online versions of the technique proposed in this paper achieved high and stable levels of elimination with low response delays (EFS-WN, mean filter, finding local minimums and interpolation are linear operations), with their amplitudes decreasing by more than 97%, which was far better than the 300 ms-length MF. This fact was confirmed with real EOG data. Thus, control systems, like the complex state machine developed in Merino et al. [18], could clearly be simplified by using EFS preprocessing. In turn, the ability of EFS to detect bell-shaped waveforms could be used to send commands when a voluntary blink happens.

Some systems are based on GBM eye movements as commands, whereas others use a saccade-movement sequence to determine which activity has occurred. In these systems, EFS processing may not be useful with short fixations, and a fixation-time threshold is required to achieve a satisfactory level of waveform preservation, for example GBM must exceed 0.5 s. The reason for this is that there are few or no local minimums with small fixations. The envelope filter uses these minimums to delete bell-shaped interferences and to be closer to input data through an average from two envelopes. Too few minimums may mean that the average is not similar to input fixation, because the first lower envelope may be free of local minimums, and the second is obtained from those values. Hence, the distance between the envelopes may be considerable. This may be made worse if an input fixation interval does not have local minimums. In this case, there is no similarity between the two envelopes.

Envelope filter sequence requires small oscillations of input data to reach a high level of similarity with ideal EOG signals. The objective of EFS-WN is to increase the number of local minimums. However, blinks and overshoots are not removed when the top or its peaks are sawtooth shaped. For this reason, to reduce sway form, a mean filter is applied after adding EFS-WN. High EFS-WN amplitudes may introduce large swayings on bell-shaped peaks, rendering the mean filter ineffective, and a long mean filter may excessively reduce the number of local minimums. Thus, EFS-WN for the offline EFS version is set at a low value (32 dB) for 128 Hz, and this decreases with a larger sampling rate, because more oscillations (noise) are recorded and EFS-WN may be smaller, or even unnecessary. For the online version, EFS-WN amplitudes are greater (27 versus 36 dB for 256 Hz for offline) due to lower window energy. Meanwhile, the mean filter

smoothes out data and deletes the sawtooth top of blinks and overshoots. Therefore its length, between 25 and 32 ms, is more constant and independent of the sampling rate.

Applying a highpass filter to the EOG signal causes the fixation slopes to drop (Table 3). This may mask a subset of small variations inserted by EFS-WN. Few local minimums are found and envelopes may not be close enough to fixation periods, thereby reducing similarity, as shown in Test 5. Increasing these slopes causes SNR input to drop. Nevertheless, this fact is inverted with the filtered processings, with a good SNR level and high similarity being reached. Thus, EFS should be applied before the highpass filter to avoid this fixation-slope effect.

An important difference with the techniques based on MF is that a shifting window is not required, so EFS may be applied to all input data. The effectiveness of MF depends directly on window length. A low value may not totally remove blinks or overshoots, while a large width may modify saccadic positions. However, MF is relatively robust to sawtooth-shaped tops, waveform preservation is high (higher than EFS), and it obtains a good SNR value for decreasing fixation slopes (lower than EFS). However, it has difficulty deleting blink places in the saccade neighborhood and consecutive blinks. EFS versions remove the problems of neighborhood and sequence, fixation period error is reduced, and saccade positions are maintained. Furthermore, real data confirm that MF retains a better saccade slope. This fact may be very important for an activity classifier, but it may have less impact in control systems.

Conclusion

The EFS algorithm for filtering EOG data has demonstrated that it is highly capable of removing bell-shaped waveform noise without changing saccade positions: blink amplitudes decreased by 97%, and only 5% of them maintained a value over 25% of the initial value, and overshoots were considerably reduced. However, saccadic slopes were smoothed and we found a limit of fixation duration. In contrast, MF was less capable of reducing amplitudes of this kind of interference, but was better at maintaining slopes, with a smaller dependence on fixation width being obtained.

The paper described an online implementation of EFS with a similar level of effectiveness to the offline version. Hence, the EFS algorithm can be used by a control interface based on EOG signals to manage devices such as PCs, activity classifiers, and/or affective computing systems.

Appendix 1: EOG system generator

A model of the EOG signal is described in this appendix. This one can measure and verify different EOG features. This model was developed because we were unable to find databases with specialist annotations of saccade movements, blinks and overshoots. The model allows us to evaluate processing precision versus inserted noise level from blinks, overshoots, and general interferences, and compare filtered outputs with ideal data.

An EOG signal may be split into (8)

$$EOG(t) = EM(t) + O(t) + B(t) + n(t) \tag{8}$$

where EM(t) is the ideal signal consisting of eye movements, O(t) contains overshoots, B(t) are blinks, and n(t) is additive noise (Figure 15). These functions are described in

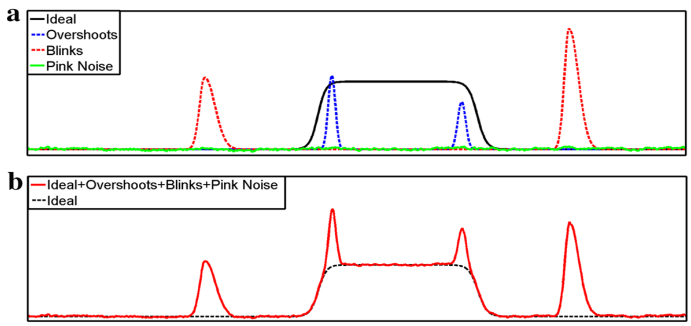

Figure 15 Model EOG signal from EOG-SG. **a** Individual elements; **b** joining of all components.

the following subsections. The model of saccades and fixations is explained in first three subsections, it is generalized in the fourth subsection, where EM(t) is obtained. Overshoot and blink models are described in last two subsections.

Saccades model

Saccade movements cause a rapid signal variation, whereas fixations maintain the electric level from saccades [1, 17]. They can both be modeled with a sigmoid function (9). This is defined for all real numbers, its rank is (0, 1), with two horizontal asymptotes in 0 and 1 (Figure 16). Parameter a shifts it along the abscissa axis, while parameter b contracts/dilates it, so that the slope changes with this value.

$$S(x) = \frac{1}{1+e^{-x}} \xrightarrow{x=\frac{t-a}{b}} S\left(\frac{t-a}{b}\right) = \frac{1}{1+e^{-\frac{t-a}{b}}} \tag{9}$$

The main variations of the sigmoid function are found in the interval $[a - b\ln(1/0.1-1),\quad a - b\ln(1/0.9-1)]$, where it ranges from 0.1 up to 0.9, which is 80% of its slope. Parameter b controls the interval amplitude, so it can be used as a model of saccadic shiftings. Thus, supposing the linear relation between eye-movement angles

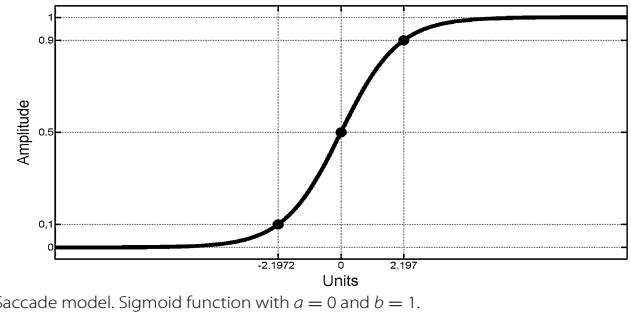

Figure 16 Saccade model. Sigmoid function with $a = 0$ and $b = 1$.

and saccade time widths, with the average time of EOG-saccades slope known as 100 ms for a 20° movement [12], then b is defined as (10)

$$b(A,\rho) = A\rho\left(\frac{0.9}{2\pi\ \ln(9)}\right) \tag{10}$$

where $0 \leq A < \pi$ is movement angle in radians, $0 < \rho < +\infty$ is a random factor of variability of saccades (RFVS) to involve variations in the slopes.

Fixations model

Ocular position is maintained after each saccadic movement [17]. This is termed fixation. Under ideal conditions, the electrical level reached is upheld and only changes when a new saccade occurs. In contrast, applying a high pass filter to the EOG signal is a normal action because this shows a DC level. This filter causes the fixation slope to decrease, because the signal is constant in them. So, Eq. (11) models this behavior, where δ and γ are start time and duration of decrease, and m is decreased level, whose value is between 0 and 1. Note, 98% of the slope is in interval [0, 1] when $\delta = 0$ and $\gamma = 1$.

$$D(m,t,\delta,\gamma) = 1 - mS\left(\ln(99)\cdot\left(\frac{2(t-\delta)}{\gamma} - 1\right)\right) \tag{11}$$

A high pass filter could be used instead of (11), but fixation slope control is lost. So, (11) through parameter m handles this EOG feature better.

Saccade-fixation model

A fixation always happens after a saccade [1, 17]. So, this relation is drawn in Figure 17 and is defined in Eq. (12)

$$SF(t,a,b,m,\delta,\gamma) = S\left(\frac{t-a}{b}\right)\cdot D(m,t,\delta,\gamma) \tag{12}$$

where

$$\delta = a - b\ln\left(\frac{1}{0.99} - 1\right) > a - b\ln\left(\frac{1}{0.9} - 1\right) \tag{13}$$

is the start time of the decreased fixation slope and is located after the saccade and coincides with the time instant when (9) is 0.99. Furthermore, the fixation slope time

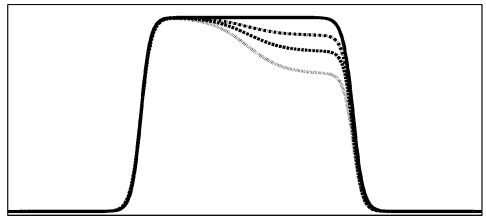

Figure 17 Different fixation slopes. Model EOG signal with four different fixation slopes.

depends on when the next saccade occurs. If a_2 and b_2 are the next saccade localization and its slope, then fixation width is defined as

$$\gamma = a_2 - b_2 \ln\left(\frac{1}{0.01} - 1\right) - \delta \tag{14}$$

such that the end of fixation coincides with the time instant when (9) is 0.01 for the next saccade (Figure 17).

Saccade sequences

Eyes are constantly in movement, so it is possible to establish a movement sequence as a set of saccades and fixations whose initial and final positions are the center of the eyeball. A sequence of saccades is established as a family of curves in (15), returning to the center position as (16)

$$\begin{aligned} SS(t, A, a, \rho, m, \delta, \gamma) = \sum_{j=1}^{L} (\tan(A_j) - \tan(A_{j-1})) \cdot \\ SF(t, a_j, b(|A_j - A_{j-1}|, \rho_j), m_j, \delta_j, \gamma_j) \end{aligned} \tag{15}$$

$$RCP(t, \alpha, \theta) = 1 - S\left(\frac{t - \alpha}{\theta}\right) \tag{16}$$

where $L > 0$ is the number of saccades of a sequence, A, a, ρ, m, δ, and γ are vectors whose components mean: A_j is movement angle in radians where $\pi/2 > A_j > -\pi/2$ and $A_0 = 0, b(|A_j - A_{j-1}|, \rho_j)$ determine saccadic slope, ρ_j is RFVS, a_j is the start time instant of a saccadic movement where $a_{j+1} > a_j > 0$, m_j is decreased fixation slope, δ_j is the start time of decreased slope, γ_j is the duration; α and θ are real scalars which set the position of the returned saccade to the center localization of the eyeball and its slope. In (15) a tangent function was used because $\pm 30°$ ocular movements are quasi linear [15].

Finally, EM(t) is obtained from a saccade sequence (15) and one single returned movement (16). Its expression is in (17)

$$EM(t) = \sum_{i=1}^{K} RCP(t, \alpha_i, b(|A_{i,L(i)}|, \tau_i) \cdot SS(t, A_i, a_i, \rho_i, m_i, \delta_i, \gamma_i) \tag{17}$$

where $K > 0$ is the number of ocular movement sequences, $L(i) > 0$ is the number of saccades of sequence i, A_i, a_i, ρ_i, m_i, δ_i, and γ_i are vectors of sequence i that were described in (15) and (16), $A_{i,L(i)}$ is the last component of vector A_i, $\alpha_i > a_{i,L(i)}$ is the localization of the returned saccade to the eyeball center and is larger than the last saccade component of vector a_i, and τ_i is RFVS of this back eye movement.

Sequence of overshoots

Overshoots can be defined as a Gauss function (18). This is an even-symmetry function, whose maximum value is 1; μ and σ shift and contract/dilate it. Of its area, 99.99% is in the interval $[\mu - 4\sigma, \mu + 4\sigma]$, where its width is controlled through parameter σ. Thus, overshoot widths can be defined in this interval.

$$G(t,\mu,\sigma) = e^{-0.5\cdot\left(\frac{t-\mu}{\sigma}\right)^2} \tag{18}$$

A target localization error causes overshoots in the EOG signal, so they overlap with saccades [19, 20]. An overshoot sequence is defined in (19)

$$O(t) = \sum_{i=1}^{K}\sum_{j=1}^{L(i)} C_{i,j}\cdot G\left(t,\mu_{i,j},\sigma_{i,j}\right) \tag{19}$$

where $C_{i,j}$ is the amplitude of overshoot, $\sigma_{i,j}$ is overshoot width (20), and, $\mu_{i,j}$ is the time localization of the overshoot that must be equal to (21); $b(|A_{i,j}-A_{i,j-1}|,\ \rho_{i,j})$ was defined in (10) and $\theta_{i,j}$ can be $a_{i,j}$ if it is on saccade sequence or α_i if it is on returned saccade to center localization of the eyeball (17), and *sign*() is the sign function. In this way, overshoots range from 0.5 up to 0.999 in (9).

$$\sigma_{i,j} = \ln(999)\cdot\frac{b\left(\left|A_{i,j}-A_{i,j-1}\right|,\rho_{i,j}\right)}{8} \tag{20}$$

$$\mu_{i,j} = \theta_{i,j} - 0.5\cdot sign\left(\frac{\partial EM(\theta_{i,j})}{\partial t}\right)\cdot b\left(\left|A_{i,j}-A_{i,j-1}\right|,\rho_{i,j}\right)\cdot\ln\left(\frac{1}{0.999}-1\right) \tag{21}$$

Sequence of blinks

A blink has a higher slope before its peak than afterwards. So, this can be formed as (22).

$\beta(t)$ is a piecewise function based on two Gauss functions, where one is double dilated in relation to the other. It is known that about 99% of the area of (18) is in the interval $[p-3h, p+3h]$. Thus, the interval $[p-3h, p+6h]$ contains 99% of $\beta(t)$ area.

$$\beta(t,p,h) = \begin{cases} G(t,p,h) & t \le 0 \\ G(t,p,2h) & t > 0 \end{cases} \tag{22}$$

Equation (23) defines the blink signal where R is the number of blinks, V_j is the amplitude of one blink, h_j determines blink width, and p_j is the localization of the blink peak where $p_{j+1} \ge p_j + 6h_j$.

$$B(t) = \sum_{j=1}^{R} V_j\cdot\beta\left(t,p_j,h_j\right) \tag{23}$$

Additive noise

Bioamplifiers are not perfect systems, and their outputs show interference from pink noise due to surface electrodes [36]. Therefore, we added this kind of noise, $n(t)$, of 27 dB in relation to (17). This gave outputs which were more like real EOG signals from bioamplifiers.

Appendix 2: Test settings

The model of "Appendix 1" was used in this paper's tests, and its main parameters are summarized in Table 4.

Three implicit concepts of EOG-SG must be described before explaining the signal generated in each test. The first is the time between sequences (TbS) in (17). This

Table 4 Test settings: main EOG-SG parameters

Pars.	Tests 1–3	Test 4	Test 5	Test 6	Test 7	Test 8
K	100	0	1,000	125	1	1,000
L	1	0	1	[6, 10]	1,000	1
A (º)	±40	0	±40	±15	±40	±40
ρ	[0.9, 1.1]	0	[0.9, 1.1]	[0.9, 1.1]	[0.9, 1.1]	[0.9, 1.1]
m	0	0	0	0	0	[0, 0.05] −[0.35, 0.40]
TSS (s)	[0.6, 1.5]	0	[0.3, 0.4] −[1.4, 1.5]	[0.3, 0.4] −[1.4, 1.5]	[0.3, 0.4] −[1.4, 1.5]	[0.6, 1.5]
9h (s)	[0.3, 0.55]	[0.1, 0.2] −[0.4, 0.5]	0	0	0	[0.3, 0.55]

Settings of tests. Square brackets mean random variations. Meaning of acronyms in the order of appearance.

K number of saccade sequences, *L* number of saccadic movements per sequence, *A* eye movement angle, ρ random factor of variability of saccade, *m* fixation slope, *TSS* time between two successive saccades, *9h* blink width, º degree, *s* second.

is defined as the period from the final saccadic movement (α_i) of sequence i in (16) up to the first saccade $a_{i+1,1}$ of the next sequence $i + 1$ in (15). Another concept is the rate of blinks in a minute (BM), which establishes a limit for the number of blinks. Therefore, this affects blink localizations (p_j) in (23). However, if their positions are between sequences of saccade-fixation movements (17), as defined in (24), then blinks and ocular movements do not overlap. The last concept is when an overshoot happens. With these concepts defined, their values were set: TbS changed between 3 and 5 s for all tests (25); blinks happened between the sequence of ocular movements (24) and a frequency of 19 BM for Tests 1–3 and 5, between 12 and 22 BM for Test 4 and 0 BM in the others [21]; overshoots were generated when an eye shift exceeded +25° in absolute value from previous eye position in Tests 1–3 and 5. The others tests were without overshoots.

$$a_{i+1,1} > p_j > \alpha_i \tag{24}$$

$$a_{i+1,1} - \alpha_i \in [3, 5] \tag{25}$$

The same setting was established for Tests 1–3, where parameters of proposal technique were obtained. They defined 100 sequences (K) of GBMs whose amplitudes (A) changed randomly between ±40°. This kind of movement occurs when the length of vector A is 1 in (17), that is, L is 1 in (15). The time between two successive saccades (TSS), that is, GBM width, was set between 0.6 and 1.5 s (26) with horizontal slope ($m = 0$) in (11). In contrast, blink width ($9h$) in (23) oscillated between 0.3 and 0.55 s [22].

$$a_{i,n+1} - a_{i,n} \in [0.6, 1.5] \tag{26}$$

Test 4 analyzed the ability to delete blinks. For this reason, the signals obtained were without saccade sequences ($K = 0$ and $L = 0$). Their widths were increased 0.1 s from an initial interval [0.1, 0.2] up to [0.4, 0.5] s.

Waveform preservation was analyzed in Tests 5–7. For this reason, the signals were free of blinks and overshoots. The distance between saccades changed 0.1 s in each iteration, [17], from an initial random value of [0.3, 0.4] up to [1.4, 1.5] s. The width limit of GBMs was studied in Test 5. 1,000 of them were generated with amplitudes between

±40°. Test 6 used signals with 125 sequences [7]. The total rank of eye movement was set in the interval [−15°, +15°]. The first saccade moved from the center position (0°) up to −15°, and the last shifted from +15° to center position (0°). Thus, the amplitude of stair-shaped waveforms was 30°. The number of saccades between them oscillated between 6 and 10. Test 7 was based on 1,000 random ocular movements ($L = 1{,}000$) with an amplitude between ±40° in a single sequence ($K = 1$), so that one saccade compared to the previous one could reach 80° of the distance.

The configuration of Test 8 was practically identical to Tests 1–3, but with 1,000 GBMs and non-horizontal fixation slopes, so they decreased 5% in each iteration, from [0, 5]% up to [35, 40]% of the slope.

Finally, the parameter of RFVS (ρ) in (10) was set between [0.9, 1.1] for all tests, so that the variability of the saccade slope was 20%.

Abbreviations

EOG: electrooculogram; GBM: go-and-back movement; MF: median filter; FMH: FIR median hybrid filter; WFMH: weighted FIR median hybrid filter; CWFMH: center weighted FIR median hybrid filter; SWFMH: subfilter weighted FIR median hybrid filter; EFS: envelope filter sequence; EFS-WN: white noise signal generated by step 1 of EFS algorithm; SNR: signal–noise rate; FIFO: First In, First Out; IB: input-data buffer of online EFS; WNB: white-noise buffer of online EFS; OB: output buffer with the final fragment of online EFS output; CC: correlation coefficient; RMSE: root mean square error; EOG-SG: EOG system generation; SSV: saccadic slope variation; RFVS: random factor of variability of saccades; TbS: time between sequences; BM: blink in a minute; TSS: time between two successive saccades.

Authors' contributions

MM conceived the idea, designed the algorithm and EOG model, collected the data, and drafted the manuscript. All authors analyzed and interpreted data, and participated in writing up and revising the manuscript. All authors read and approved the final manuscript.

Compliance with ethical guidelines

Competing interests

The authors declare that they have no competing interests.

Received: 21 January 2015 Accepted: 1 May 2015
Published online: 30 May 2015

References

1. Carretié Arangüe L, Iglesia Dorado J, editors. Psicofisiología. Fundamentos metodológicos. Pirámide; 2000. ISBN: 84-368-0877-0.
2. Galley N. Saccadic eye movement velocity as an indicator of (de)activation. A review and some speculation. Int J Psychophysiol. 1989;3:229–44.
3. App E, Debus G. Saccadic velocity and activation: development of a diagnostic tool for assessing energy regulation. Ergonomics. 1998;41(5):689–97.
4. Fabbri M, Pizza F, Mogosso E, Ursino M, Contardi S, Cirignotta F, et al. Automatic slow eye movement (SEM) detection of sleep onset in patients with obstructive sleep apnea syndrome (OSAS): comparison between multiple sleep latency test (MSLT) and maintenance of wakefulness test (MWT). Sleep Med. 2010;11:253–7.
5. Iwanaga K, Saito S, Shimomura Y, Harada H, Katsuura T. The effect of mental loads on muscle tension, blood pressure and blink rate. J Physiol Anthropol Appl Hum Sci. 2000;19(3):135–41.
6. Galley N, Schleicher R, Galley L. Blink parameter as indicators of driver's sleepiness—possibilities and limitations. In: Gale A, editor. Vision in vehicles X. Amsterdam: Elsevier; 2003.
7. Bulling A, Ward JA, Gellersen H, Tröster G. Eye movement analysis for activity recognition using electrooculography. IEEE Trans Pattern Anal Mach Intell. 2011;33(4):741–53.
8. Dhillon HS, Singla R, Rekhi NS, Jha R. EOG and EMG based virtual keyboard: a brain–computer interface. In: 2nd IEEE international conference on computer science and information technology, 2009 (ICCSIT 2009). 2009.
9. Estrany B, Fuster P, Garcia A, Luo Y. EOG signal processing, and analysis for controlling computer by eye movements. PETRA'09. 2009.
10. Yathunanthan S, Chandrasena LUR, Umakanthan A, Vasuki V, Munasinghe SR. Controlling a wheelchair by use of EOG signal. In: 4th international conference on information and automation for sustainability, 2008 (ICIAFS 2008). 2008.
11. Rivera O, Molina A, Gómez I, Merino M. A flexible, open, multimodal system of computer control based on infrared light. Int J Latest Trend Comput. 2011;2(4):498–507.
12. Duchowski A. Eye tracking methodology: theory and practice. Secaucus: Springer; 2007.

13. Schgöl A, Keinrath C, Zimmermann D, Scherer R, Leeb R, Pfurtscheller G. A fully automated correction method of EOG artifacts in EEG recordings. Clin Neurophysiol. 2007;118:98–104. doi:10.1016/j.clinph.2006.09.003.
14. Denney D, Denney C. The eye blink electro-oculogram. Br J Opththalomol. 1984;68:225–8.
15. Barea R, Boquete L, Mazo M, Lopez E, Bergasa LM. EOG guidance of wheelchair using neural networks. In: Proceedings of 15th international conference on patter recognition, vol. 4. 2000. p. 668–671.
16. Brown M, Marmor M, Vaegan EZ, Brigell M, Bach M. ISCEV standard for clinical electro-oculography (EOG). Doc Ophthamol. 2006;113(3):205–12.
17. Manor BR, Gordon E. Defining the temporal threshold for ocular fixation in free-viewing visuocognitive tasks. J Neurosci Methods. 2003;128(1–2):85–93.
18. Merino M, Rivera O, Gómez I, Molina A, Dorronzoro E. A method of EOG signal processing to detect the direction of eye movements. In: Proceedings of the 1st international conference on sensor device technologies and applications. 2010. p. 100–105.
19. Weber RB, Daroff RB. The metrics of horizontal saccadic eye movements in normal humans. Vis Res. 1971;11:921–8.
20. Bahill AT, Clark MR, Stark L. Dynamic overshoot in saccadic eye movements is caused by neurological control signal reversals. Exp Neurol. 1975;48:107–22.
21. Karson CN, Berman KF, Donnelly EF, Mendelson WB, Kleinman JE, Wyatt RJ. Speaking, thinking, and blinking. Psychiatry Res. 1981;5(3):243–6.
22. Schiffman HR. Sensation and perception: an integrated approach. 5th ed. New York: John Wiley; 2001.
23. Juhola M. Median filtering is appropriate to signals of saccadic eye movements. Comput Biol Med. 1991;21(1/2):43–9.
24. Neejärvi J, Värri A, Fotopoulos S, Neuvo Y. Weighted FMH filters. Signal Process. 1993;31:181–90.
25. Martínez M, Soria E, Magdalena R, Serrano AJ, Martín JD, Vila J. Comparative study of several FIR median hybrid filters for blink noise removal in electrooculograms. WSEAS Trans Signal Process. 2008;4:53–9.
26. Krupinski R, Mazurek P. Estimation of eye blinking using biopotentials measurements for computer animation applications. In: International conference on computer vision and graphics (ICCVG 2008), vol. 5337. LNCS; 2008. p. 302–310.
27. Krupinski R, Mazurek P. Median filter optimization for electrooculography and blinking signal separation using synthetic model. In: 14th international conference on methods and models in automation and robotics (MMAR'09), vol. 14(part 1). 2009. p. 326–331.
28. Krupinski R, Mazurek P. Towards to real-time system with optimization based approach for EOG and blinking signals separation for human computer interaction (ICCHP 2010), part I, vol. 6179. LNCS; 2010. p. 154–161.
29. Huang NE, Shen Z, Long SR, Wu MC, Shih HH, Zheng Q, et al. The empirical mode decomposition and the Hilbert spectrum for nonlinear and non-stationary time series analysis. Proc R Soc Lond A Math Phys Eng Sci. 1971;1998(454):903–95.
30. Merino M, Gomez IM, Molina AJ. Envelopment filter and K-mean for the detection of QRS waveforms in electrocardiogram. Med Eng Phys. 2015;37(6):605–9. doi:10.1016/j.medengphy.2015.03.019.
31. Umberto M, Clariá F, Vallverdú M, Caminal P. Filtering and thresholding the analytic signal envelope in order to improve peak and spike noise reduction in EEG signals. Med Eng Phys. 2014;36:547–53.
32. Zelik KE, La Scaleia V, Ivanenko YP, Lacquaniti F. Coordination of intrinsic and extrinsic foot muscles during walking. Eur J Appl Physiol. 2015;115:691–701.
33. Dähne S, Nikulin VV, Ramírez D, Schreier PJ, Müller KR, Haufe S. Finding brain oscillations with power dependencies in neuroimaging data. NeuroImage. 2014;96:334–48.
34. Agrawal S, Gupta A. Fractal and EMD based removal of baseline wander and powerline interference from ECG signals. Comput Biol Med. 2013;43:1889–99.
35. Schalk G, McFarland DJ, Hinterberger T, Birbaumer N, Wolpaw JR. BCI2000: a general-purpose brain–computer interface (BCI) system. IEEE Trans Biomed Eng. 2004;51(6):1034–43.
36. Huigen E, Peper A, Grimbergen CA. Investigation into the origin of the noise of surface electrodes. Med Biol Eng Comput. 2002;40:332–8.

4.2. Electrocardiografía

Dada la imposibilidad de que el sujeto pueda modificar el comportamiento de manera voluntaria, esta señal se ve limitada a interfaces PC.

4.2.1. Procesamiento

La detección del complejo QRS ha sido objeto de multitud de estudios que han logrado una eficacia superior al 90%, en algunos casos incluso mayor al 99% (Nygårds and Sörnmo, 1983; Song-kai et al, 1988; Mehta et al, 2010; Pan and Tompkins, 1985; Wang et al, 2011; Bustamante et al, 2013; Pal and Mitra, 2012; Manikandan and Soman, 2012; Madeiro et al, 2012; Chikh et al, 2012; Dohare et al, 2014; Ye et al, 2012; Köhler et al, 2002; Agrawal and Gupta, 2013; Das and Ari, 2013; Yan and Lu, 2014). En todas ellas, se pueden diferenciar dos fases diferentes: preprocesamiento y clasificación. La primera tiene como objetivo destacar el complejo QRS respecto a las otras ondas, mientras que la segunda toma dicho resultado y determina dónde se han producido dichos complejos. Estos algoritmos, para llevar a cabo su cometido, requieren de la especificación de varios parámetros, como umbrales de decisión fijos o adaptativos, anchura de ventana de integración, o de un proceso de entrenamiento previo del clasificador, etc.

Para superar estas desventajas, en esta tesis se ha desarrollado una nueva técnica libre de parámetros y sin necesidad de realizar un proceso de aprendizaje supervisado previo: Merino et al (2015b), detallado en la sección 4.2.3. Los bioamplificadores son sistemas enfocados a la captación de una o varias bioseñales. Los datos registrados presentan interferencias de diversa índole, como la red eléctrica (50Hz en la Unión Europea), ruido rosa causado por los electrodos de superficies (Huigen et al, 2002), interferencias de otras bioseñales, etc. Aprovechando las oscilaciones generadas por el ruido, se ha desarrollado un algoritmo, así como una versión en tiempo real del mismo, para detectar los complejos QRS basado en el FE descrito en la sección 4.1.1 y el clasificador no supervisado K-means. Este procedimiento se identificará como SFE+K (secuencia de filtro de envolvente y K-means).

El algoritmo, que se muestra en la figura 4.4, consiste en:

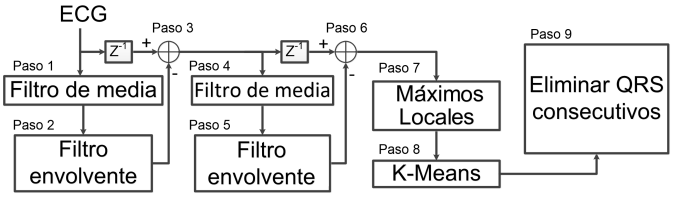

Figura 4.4: Diagrama del algoritmo SFE+K para detectar complejos QRS.

1. Aplicar un filtrado de media para eliminar las cimas en forma de "dientes de sierra" de los complejos QRS.

2. Emplear el FE descrito en la sección 4.1.1.

3. Restar la salida del paso anterior con los datos de ECG. Con esto se consigue destacar el complejo QRS y eliminar casi en su totalidad las otras ondas de la señal (figura 4.5.a).

4. Repetir los pasos 1 y 2 sobre el resultado del paso 3.

5. Con los datos de salida del paso anterior, localizar todos los máximos locales de la señal y aplicar el clasificador K-means de dos grupos: QRS y no-QRS (figura 4.5.b).

6. Finalmente, eliminar los QRS consecutivos, esto es, los puntos etiquetados como QRS entre los cuales no hay ningún valor no-QRS. El resultado será un vector con la localización de los complejos QRS de la señal ECG.

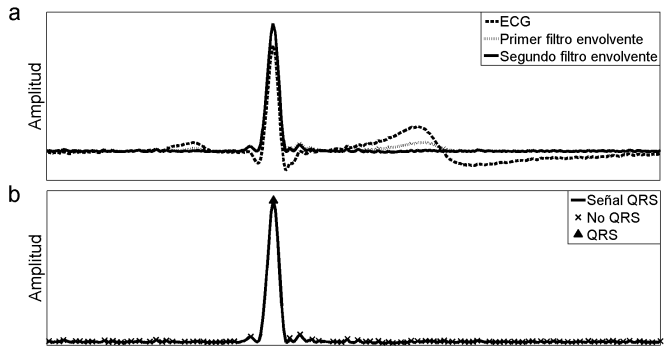

Figura 4.5: Resultado del algoritmo: a) salida del proceso de filtrado, b) clasificación de datos con K-means.

La eficacia de la técnica se midió con 22 horas y 11 minutos de señales obtenidas de cinco bases de datos de Physionet (PDB) (Goldberger et al, 2000). Tres de ellas contienen algún tipo de patología, mientras que los datos de las otras dos muestran latidos normales. Para ello, se cuantificó el número de QRS correctos generados por el algoritmo (verdaderos positivos - VP), el número de falsos QRS (falsos positivos - FP), el número de QRS no detectados (falsos negativos - FN), y se calculó la sensibilidad (Se), definida como la capacidad de detectar los complejos (ecuación 4.2), la predicción positiva (P+), definida como la fiabilidad de las salidas del procesamiento de ser complejos QRS reales (ecuación 4.3), y precisión (Pre), definida como la eficacia del algoritmo (ecuación 4.4). El resultado del procesamiento está resumido en la tabla 4.2. En ella se muestra que ambas versiones de SFE+K

obtienen unos resultados superiores al 99.75% tanto para Se, P+ y Pre, con el 99.97% y 93.31% de los complejos QRS normales y anormales detectados, y con errores que no sobrepasan el 0.95%.

$$Se = 100 \cdot \frac{VP}{VP + FN} \tag{4.2}$$

$$P+ = 100 \cdot \frac{VP}{VP + FP} \tag{4.3}$$

$$Pre = 100 \cdot \frac{VP}{VP + FP + FN} \tag{4.4}$$

Tabla 4.2: Resumen de la eficiencia del algoritmo SFE+K.

			Algoritmo	
		Physionet	**Offline**	**Online**
	No. QRS	87639	87699	87740
Verdaderos Positivos	**QRS normales**	86922	86899	86908
	QRS anormales	717	669	670
Falsos Positivos	**Morfológicos**		97	104
	Ruido		34	58
Eficacia (%)	**Sensibilidad**		99.92	99.93
	Predicción positiva		99.85	99.81
	Precisión		99.77	99.75

4.2.2. Análisis y aplicaciones

El análisis y selección de características es un elemento esencial en PC, junto con el contexto de la acción. Por ello, como parte de esta tesis, se han estudiado las variaciones de éstas en dos situaciones diferentes y sus resultados están recogidos en las secciónes 4.2.4 y 4.2.5. En la primera, se analizaron los parámetros durante la escritura de un texto usando un teclado virtual controlado por eventos mediante las bioseñales EMG y ECG (Merino et al, 2012), estudiando si el efecto de la interfaz, mientras que en la segunda se midió la influencia de situaciones de estrés causados por tareas de aritmética y de memoria con limitación de tiempo (Monge et al, 2014).

En el primero de ellos, se obtuvo que las características que mostraron cambios significativos durante la actividad fueron SDNN, RMSSD, pNN50 y las bandas de frecuencias ULF, VLF, LF, HF y LF/HF, y no se observó un efecto significativo sobre las señales a causa de la interfaz usada. En el segundo artículo se concluyó que los parámetros que mejor marcan situaciones de estrés son Mrr, pNN50 y HF. Ambos trabajos emplearon el algoritmo descrito en Pan and Tompkins (1985).

4.2.3 Publicación 2

Extensión de los resultados

Adicionalmente a los resultados arrojados por el artículo presentado anteriormente, se realizó diversos análisis que no se pudieron incorporar debido a las limitaciones impuestas por la revista. Así, se estudió de forma empírica la carga computacional del algoritmo en su versión offline, la desviación en la localización del pico máximo de la onda R y el efecto del ancho del buffer sobre la versión en tiempo real.

El análisis temporal se realizó sobre segmentos incrementales de cada señal de PDB. Cada nuevo segmento duplicaba la longitud del anterior e incluía al previo. Se obtuvieron 45 segmentos por cada señal donde el incremento del último fue del 4500% respecto a la longitud del primero, y abarcaba la totalidad de la duración de los datos. Por cada uno de ellos, se calculó el incremento temporal respecto al primer segmento (el de menor tamaño). El resultado está recogido en la figura 4.6. Se puede observar que la tendencia mostrada es lineal.

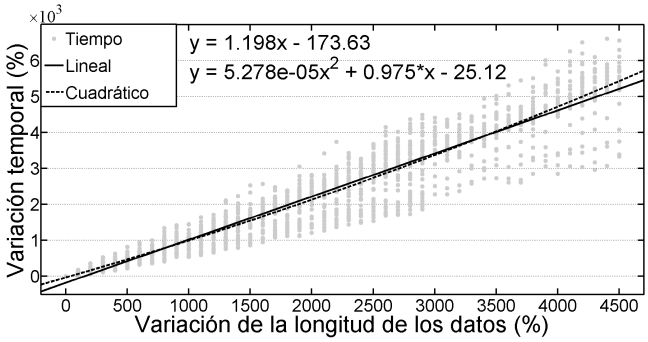

Figura 4.6: Coste computacional. La línea continua corresponde a la recta de regresión lineal, mientras que la punteada a un ajuste cuadrático.

La detección del pico máximo de la onda R puede influir notablemente a la hora de analizar las variaciones de la actividad cardíaca, especialmente a los parámetros de HRV. Por ello, se calcularon las desviaciones más comunes que se dan en la localización del QRS dado por SFE+K. El resultado está recogido en la figura 4.7. El intervalo ±8ms contiene el 99.89% de los datos del histograma para la versión offline, y entre el 99.53% y el 99.87% para el procesamiento online y diferentes longitudes de buffer. Además, se destaca que el valor modal de las desviaciones es 0 en ambas versiones, con una frecuencia 10 veces superior al inmediatamente siguiente, correspondiendo éste al 77.92% de los complejos QRS para la implementación offline, y al rango que va desde el 77.23% hasta el 79.22% para la versión en tiempo real. De esta manera, se puede concluir que la precisión del algoritmo en la localización del pico máximo de la onda R es muy alta.

En base a las posiciones temporales de los complejos QRS y las distancias RR proporcionadas por SFE+K y los expertos de PDB, se obtienen

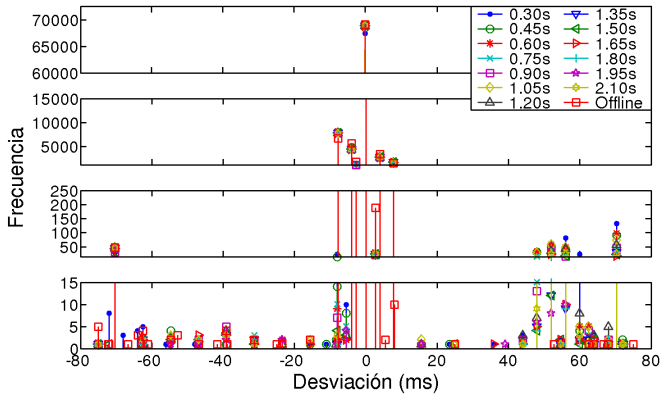

Figura 4.7: Histograma de la desviación en la localización del pico máximo de la onda R para la versiones offline y en tiempo real con longitud de buffer desde 0.3 a 2.1s.

las matrices mostradas en la ecuación 4.5, donde l_i es la localización del complejo QRS i-ésimo, RR_i es la distancia de éste al complejo previo y los superíndices indican el origen (SFE+K o Physionet). Definidas estas matrices, se llevo a cabo el análisis del efecto de la longitud del buffer mediante el cálculo del error cuadrático medio (ECM) y la correlación cruzada (CC). Este análisis no obtiene unos valores precisos de Se, P+ y Pre, pero permite valorar el efecto del buffer sobre los resultados.

$$MRR^{SFE+K} = \begin{pmatrix} l_i^{SFE+K} & RR_i^{SFE+K} \\ l_{i+1}^{SFE+K} & RR_{i+1}^{SFE+K} \\ \dots & \\ l_{i+N}^{SFE+K} & RR_{i+N}^{SFE+K} \end{pmatrix} MRR^{PDB} = \begin{pmatrix} l_i^{PDB} & RR_i^{PDB} \\ l_{i+1}^{PDB} & RR_{i+1}^{PDB} \\ \dots & \\ l_{i+N}^{PDB} & RR_{i+N}^{PDB} \end{pmatrix} \quad (4.5)$$

El análisis se llevo a cabo variando el buffer desde un valor inicial de 0.3s hasta los 2.1s, incrementándolo en 150ms en cada iteración. La posible discordancia entre las localizaciones de los expertos y las obtenidas por la técnica SFE+K, esto es, $l_i^{SFE+K} \neq l_i^{PDB}$, hace necesario interpolar linealmente puntos de forma que ambas matrices tengan las mismas posiciones temporales (ecuación 4.6; figura 4.8). En la figura 4.9 se resume el resultado obtenido. Se puede apreciar que la diferencia entre los datos obtenidos por SFE+K y las anotaciones de los expertos difieren muy poco para las distintas longitudes del buffer, lo que afianza los resultados obtenidos en el artículo Merino et al (2015b) (sección 4.1.3). Asimismo, se observa una leve mejoría en el rendimiento cuando la dimensión del buffer supera los 1.05s de longitud. De esta manera, se puede concluir que la técnica es suficientemente robusta a la hora de detectar complejos QRS y permite su uso en los casos en los que la velocidad en la detección sea un elemento crítico.

$$MRR^{SFE+K}_{intrpl} = \begin{pmatrix} l^{SFE+K}_{i} & RR^{SFE+K}_{i} \\ l^{PDB}_{i} & RR^{SFE+K}_{i_{intrpl}} \\ l^{SFE+K}_{i+1} & RR^{SFE+K}_{i+1} \\ l^{PDB}_{i+1} & RR^{SFE+K}_{i+1_{intrpl}} \\ \dots & \\ l^{SFE+K}_{i+N} & RR^{SFE+K}_{i+N} \\ l^{PDB}_{i+N} & RR^{SFE+K}_{i+M_{intrpl}} \end{pmatrix} \quad MRR^{PDB}_{intrpl} = \begin{pmatrix} l^{SFE+K}_{i} & RR^{PDB}_{i_{intrpl}} \\ l^{PDB}_{i} & RR^{PDB}_{i} \\ l^{SFE+K}_{i+1} & RR^{PDB}_{i+1_{intrpl}} \\ l^{PDB}_{i+1} & RR^{PDB}_{i+1} \\ \dots & \\ l^{SFE+K}_{i+N} & RR^{PDB}_{i+N_{intrpl}} \\ l^{PDB}_{i+N} & RR^{PDB}_{i+N} \end{pmatrix} \tag{4.6}$$

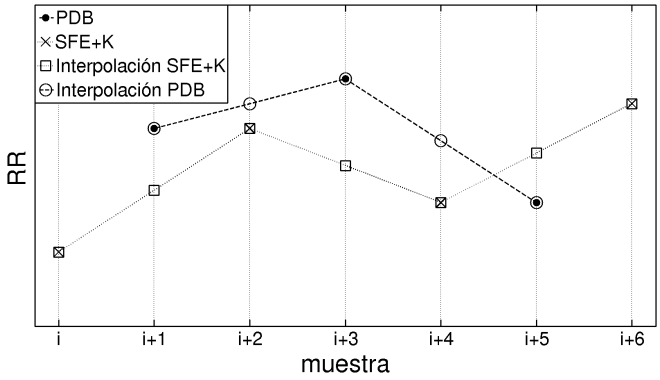

Figura 4.8: Interpolación de valores RR.

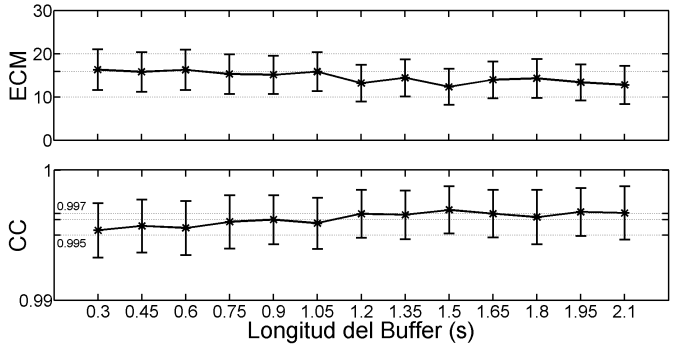

Figura 4.9: Efecto de la longitud del buffer sobre los resultados de la versión en tiempo real.

4.2.4 Publicación 3

Assessment of Biosignals for Managing a Virtual Keyboard

Manuel Merino[1], Isabel Gómez[1], Alberto J. Molina[1], and Kevin Guzman[2]

[1] Electronic Technology Department, University of Seville
Avd. Reina Mercedes s/n, 41012, Seville, Spain
manmermon@dte.us.es
{igomez,almolina}@us.es
http://matrix.dte.us.es/grupotais/
[2] Guadaltel S.A. Pastor y Landero, 19, 41001, Seville, Spain
kevinguzman@guadaltel.es

Abstract. In this paper we propose an assessment of biosignals for handling an application based on virtual keyboard and automatic scanning. The aim of this work is to measure the effect of using such application, through different interfaces based on electromyography and electrooculography, on cardiac and electrodermal activities. Five people without disabilities have been tested. Each subject wrote twice the same text using an electromyography interface in first test and electrooculography in the second one. Each test was divided into four parts: instruction, initial relax, writing and final relax. The results of the tests show important differences in the electrocardiogram and electrodermal activity among the parts of tests.

Keywords: affective interfaces, biosignals, control system, disability.

1 Introduction

According to the Eurostat [1], the total population in Europe was 362 million in 1996 which 14.8% of the population between 6 and 64 years old have physical, psychological or sensory disabilities. Therefore, assistive and adapted systems have to be developed. The aim of these ones is to help users in their diary tasks, letting them to live in a more comfortable way.

Focus on software, in general, it can be claimed that these applications have a high degree of flexibility and customizable, but their throughput strongly depends on the adapted device or interface the user needs to interact with it. The aforementioned throughput might also be dramatically reduced for people who suffer from severe disability. Another lack of these software programs is that they cannot be automatically adapted when they are running and self-adjusting to user requirements.

The goal of developing a method for matching parameters that could be modified in an adaptative row-column scanning to each individual user is discussed in [2], but, in that paper contextual information of the application is considered instead of physiological signals. Nowadays there are several researches focus on in incorporate the

K. Miesenberger et al. (Eds.): ICCHP 2012, Part II, LNCS 7383, pp. 331–337, 2012.

feature of self-adaptation in different systems or applications. So, based on this concept there are papers whose aim is modify the environment to adapt to the user needs/preferences (Ambient Intelligence) or use biosignals to adjust an application automatically (Physiological Computation [3]).

This paper describes how the use of virtual keyboard (VK) affects different physiological signals and how these ones could be used to incorporate automatic adaptation of functioning parameters in this VK application.

2 Related Work

Disable people need interfaces to be adapted to their physical and cognitive skills. Whatever the user's type of disability, the interface needs to detect user's will in order to select the highlighted row or column on the virtual keyboard. In most cases, user is able to move some muscles and press a special switch, or control a mouse pointer on computer screen through an accelerometer [4]. But sometimes user's ability is constrained to move the eyes; therefore an eye-tracker is required. Electric biosignals can be used instead of those systems. For instance, an electromyography (EMG) system can record muscle activity and substitute the switch, and also electrodes placed around the eyes can be used to detect gaze [5, 6]. Moreover, interfaces based on Brain Computer Interface (BCI) don't require user movements [7] because this one is based on electroencephalogram (EEG).

Biosignals can be also used as a source of information when user emotional state must be determined. Electrodermal activity (EDA) [8] and electrocardiogram (ECG) are two of the biosignals most used in this area. EDA has been used in several researches about stress and cognitive load [8-10]. It has been shown EDA is a good method to detect different emotional states. A typical experiment to measure the stress [9] is to make a subject calculate several arithmetic operations of different level of difficult in 4 minutes and 3 phases. From phase to phase the level of stress goes up by increasing the operation difficulty. Significance changes in EDA among phases have been reported, such that the cognitive load was evaluated correctly in 82.8% of studied cases.

It has also reported in several papers that the cardiac activity is also affected by the kind of task. In [10] the authors have used biosignals as objective indicators of state of users, where EDA, ECG, EMG and breath frequency were recorded while the subjects played a game.

3 Methodology

3.1 Application

The tests were developed using a customizable VK [6] shown in figure 1. Among other things the VK allows: keys personalization, using different control interfaces based on events and generating a list of predicted words. An extended VK distributed

by rows of six characters each is selected. High frequency characters in Spanish language are placed on first rows. A row/column scanning method was used to select a letter or a word on a prediction list. The minimum number of selected characters used to turn on prediction engine was set to 3. The scan time or dwell time was established in 1.6s for EMG control interface and 1.8s for EOG control interface based on 0.65 rule [11].

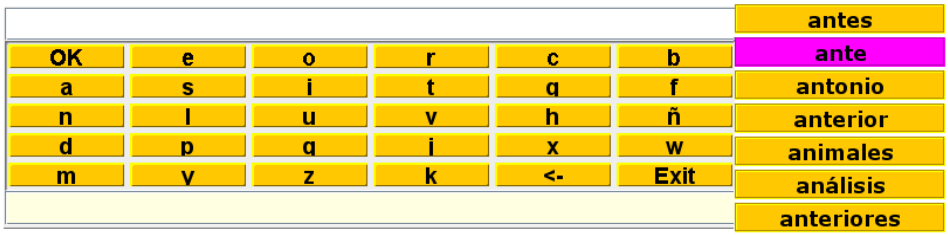

Fig. 1. Extended Letter VK

3.2 Signal Acquisition

Three different biosignals were simultaneously recorded during the tests. One of them was used to manage a VK application (EMG or EOG), and the others were registered to determine the stress/fatigue of the user induced by the control interface (ECG, EDA) [8-10].

The assembly used to record the different biosignal is shown in the figure 2. A monopolar assembly was employed to record the ECG signal (figure 2.a). The EDA assembly was placed on the wrist (figure 2.b) [12]. Three electrodes on the arm were used for the EMG signal (figure 2.c). Finally, to pick EOG signal up two electrodes by direction (figure 2.d) where placed around the eye [13] and the ground and reference sensors were placed respectively in the right and left ears.

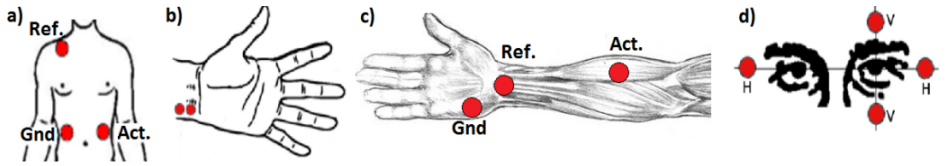

Fig. 2. Electrode positions. a) ECG. b) EDA. c) EMG. d) EOG.

Ag/AgCl electrodes with self-adhesive/conductive gel were used to record the biosignals. Two bioamplifiers were employed: g.USBamp and g.MOBILab of gTec. The first of them registered the control biosignals with a sample frequency of 512Hz for EMG and 128Hz for EOG. A notch filter in (48, 52)Hz was implemented to eliminate the power electric noisy, and a bandpass filter in (5, 200)Hz for EMG and (0.1, 30)Hz for EOG. Also, the version 2.0 of the BCI2000 software was employed [7] to send the event to the VK through a socket. The other bioamplifier recorded the ECG signal with a frequency of 256Hz, a notch filter in (48, 52)Hz and a bandpass filter in (0.5, 100)Hz.

The EDA signal employed a different system: QSensor [12]. This one is a wearable system that wears in the wrist and uses Ag/AgCl electrodes. Different sample frequency can be employed and the data are stored in the internal memory. 32Hz of sample frequency was setting.

The version 7.6.0.324 of Matlab application was utilized to offline analysis of the recorded data.

3.3 Procedure

Trials are focused on text input function of the VK. EMG and EOG signal are considered like control interfaces. Five users without disabilities between 26 and 45 years old participated in these trials (mean 31.2, sd. 7.79); only one of them had used the application before.

The temporal line of the experiment is splitted into four parts:

1. Task explanation and electrode setting. Users are instructed about the task they are going to do. Then electrodes to record EDA, ECG, EOG and EMG signal are placed.
2. Ten minutes of relax. During this time user is reading a magazine.
3. Main activity. Users input a predefined text using virtual keyboard. Command to control the application is based on biosignals. Duration of the trial is user dependent, this is, there is no time to finish it.
4. Rest time. 10 minutes to recover, reading a magazine.

The main task consists in writing a text of 43 words (209 characters). The application is operated by a single event which, in turn, is generated in two different ways: Muscle activity by EMG signal processing or Horizontal Eye Movement by EOG analysis. A wrong character had to be corrected. However, the mistakes made by selecting an incorrect word from the prediction list had to be ignored, so the user had to write the next word.

The ECG and EDA signals are recorded in all phases, excluding phase 1 where the users are instructed. By measuring these signals, it is possible to acquire objective information about the user emotional state. Two State-Trait Anxiety Inventory (STAI) questionnaires were also provided to subjects. They filled them in at the beginning of the relax phases (phases 2 and 4). So, a subjective measure of stress is also achieved.

4 Work and Results

Different parameters of affective signals have been researched. The heart rate variability (HRV) has been the main extracted feature from ECG. Each HRV vector element shows the time between two neighbor heartbeats. The extracted data are classified in two groups: information based on temporal analysis or based on frequency analysis. The standard deviation of beat-to-beat or NN intervals (SDNN), the square root of the mean squared difference of successive NN intervals (RMSSD), the proportion of NN intervals that differ by more than 50 ms (pNN50), the width of the

minimum square difference triangular interpolation of the highest peak of the histogram of all NN intervals (TINN), and the entropy of HRV are the parameters of the first group. The other group is based on calculate the power spectrum density (PSD) of the HRV. The PSD is divided in 4 parts: frequency from DC to 0.003Hz (Ultra Low Frequency - ULF), from 0.003 to 0.04Hz (Very Low Frequency - VLF), from 0.04 to 0.15Hz (Low Frequency) and from 0.15 to 4Hz (High Frequency - HF). One additional parameter is the ratio between HF and LF (HF/LF). The influence of each band about the PSD was calculated as the sum of PSD of the band divided by overall PSD sum. In all parameters, a slide window of 5 minutes of width with a shift of 1 heartbeat was applied.

Five parameters were extracted from EDA signal: tendency, average amplitude, mean of derivative, average increase in periods of rising, and time ratio increase. A slide window of 5 minutes of width with a shift of 1 sample was applied.

The extracted information was analyzed through an analysis of variance (ANOVA) for each single subject with a threshold of 1% (alpha parameter - $p < 0.01$). Four analyses for each subject were realized: relax phase 1 vs. main task, main task vs. relax phase 2, relax phase 1 vs. relax phase 2, and relax phase 1 vs. main task vs. relax phase 2. Difference between using EMG or EOG interfaces was the goal of the next ANOVA analysis: relax phase 1 of EMG control vs. relax phase 1 of EOG, main task of EMG vs. main task of EOG, and relax phase 2 of EMG vs. relax phase 2 of EOG. The expected results were the relax phases weren't affected ($p > 0.01$) and the main activities showed significative difference between EMG and EOG ($p < 0.01$). However, the ANOVA results of majorities of subjects in relax phases showed an important influence of unknown variable ($p < 0.01$). So, variations in ECG and EDA signals due to doing main task with EMG or EOG interfaces are not conclude, in despite of the expected results for main tasks were obtained.

Table 1. STAI test results for control interfaces

Phase	User 1		User 2		User 3		User 4		User 5	
	EMG	EOG	EMG	EOG	EMG	EOG	EMG	EOG	EMG	EOG
Relax 1	40	46	43	38	43	47	52	50	43	44
Relax 2	44	45	44	35	41	36	46	45	38	37

The EMG and EOG control interfaces showed the kind of phase affects directly all EDA parameters ($p < 0.00045$). Also, SDNN, RMSSD, pNN50 ($p < 0.0007$) and the bands ULF and VLF ($p < 0.0085$) of ECG parameters showed significative changes when using the EMG interface, while SDNN, pNN50 ($p < 0.0004$) and all frequency bands ($p = 0$) were affected for EOG control . On the other hand, the table 1 with the STAI result showed that the different phases affected to stress state of the subjects, such that the subjective stress level of two of them was higher in the end of the main task than in the begging of test for EMG. The others were a stress level higher in the begging of the test than in the end of main task. Also, the variance (var.) of the modulus of the difference between phases in STAI test was bigger in EOG (var. 8) than EMG (var. 3.44).

5 Conclusion and Planned Lines of Research

This paper presents how the biosignals can be used to manage an application from two points of view: the voluntary control actions and self-adaptation based on the measure of emotion. EMG and EOG are used to control and EDA and ECG to measure emotion.

To sum up, it have done EMG and EOG test and it has been determined by ANOVA analysis what are the parameters of EDA and ECG signals that are affected in different phases of trial. Significant changes were observed in these parameters. So, important differences were found between relax phases and main task. However, it was not possible determinate ECG and EDA changes between EMG or EOG interface, because an unknown variable affected the relaxed periods.

In the future, the aim will be develop an intelligent agent to incorporate to the VK application. This one will adapt automatically the software depending on emotional state of the user to do easier the use of system. So, it is necessary to determine exactly what the causes are which produce the changes in the biosignals, tired or stressed, and how these states affect to the measured parameters.

Acknowledgements. This project has been carried out within the framework of a research program: (p08-TIC-3631) – Multimodal Wireless interface funded by the Regional Government of Andalusia.

References

1. Eurostat. Heath Statistics. Luxembrourg: Office for Official Publications of the European communuties (2002), http://epp.eurostat.ec.europa.eu ISBN: 92-894-3730-8 (retrieved on January 2012)
2. Simpson, R.C., Koester, H.H.: Adaptive One-Switch Row-Column Scanning. IEEE Transactions on Rehabilitation Engineering 7(4), 464–473 (1999)
3. Fairclough, S.H.: Fundamentals of Physiological Computing. Interacting with computers 21(1-2), 133–145 (2009)
4. Gómez, I., Anaya, P., Cabrera, R., Molina, A.J., Rivera, O., Merino, M.: Augmented and Alternative Communication System Based on Dasher Application and an Accelerometer. In: Miesenberger, K., Klaus, J., Zagler, W., Karshmer, A. (eds.) ICCHP 2010. LNCS, vol. 6180, pp. 98–103. Springer, Heidelberg (2010)
5. Dhillon, H.S., Singla, R., Rekhi, N.S., Rameshwar, J.: EOG and EMG Based Virtual Keyboard: A Brain-Computer Interface. In: 2nd IEEE International Conference on Computer Science and Information Technology (2009)
6. Merino, M., Gómez, I., Rivera, O., Molina, A.J.: Customizable Software Interface for Monitoring Applications. In: Miesenberger, K., Klaus, J., Zagler, W., Karshmer, A. (eds.) ICCHP 2010, Part I. LNCS, vol. 6179, pp. 147–153. Springer, Heidelberg (2010)
7. Schalk, G., McFarland, D.J., Hinterberger, T., Birbaumer, N., Wolpaw, J.R.: BCI 2000: A General-Purpose Brain-Computer Interface (BCI) System. IEEE Transactions on Biomedical Engineering 51(6), 1034–1043 (2004)
8. Boucsein, W.: Electrodermal Activity, 1st edn. Springer (1992)

9. Setz, C., Arnrich, B., Schumm, J., La Marca, R.: Discriminating Stress from Cognitive Load Using a Wareable EDA Device. IEEE Transactions on Information Technology in Biomedicine 14(2), 410–417 (2010)
10. Mandryk, R.L., Inkpen, K.M., Calvert, T.W.: Using Psychophysiological Technique to Measure User Experience with Entertainment Technologies. Behavior & Information Technology 25(2), 141–158 (2006)
11. Simpson, R., Koester, H.H., Lopresti, E.F.: Selecting an appropriate scan rate: the rule. 65. Assistive Technology 19(2), 51–58 (2007)
12. Poh, M.-Z., Swenson, N.C., Picard, R.W.: A Wearable Sensor for Unobtrusive, Long-Term Assessment of Electrodermal Activity. IEEE Transactions on Biomedical Engineering 57(5), 1243–1251
13. Merino, M., Rivera, O., Gómez, I., Molina, A., Dorronzoro, E.: A Method of EOG Signal Processing to Detect the Direction of Eye Movements. In: SensorDevices 2010, pp. 100–105 (2010)

4.2.5 Publicación 4

Experimental and Clinical Cardiology

Stress and heart rate: significant parameters and their variations

Article Type: original article

Manuel Merino, Isabel Gómez*, Alberto Molina

Electronic Technology Department, Universidad de Sevilla, Spain
*Corresponding author: Isabel Gómez, Electronic Technology Department, ETS Ingeniería Informática, Avd. Reina Mercedes s/n, 41012. Tel: +34-954552787; E-mail: igomez@us.es.

Abstract The aim of this paper is to identify heart rate parameters with higher significant values when a set of people are performing a task under stress condition. In order to accomplish this, one computer application with arithmetic and memory activities which lets drive the subjects to different stages of activity and stress has been designed. Tests are formed by initial and final rest periods and three task phases with incremental stressful level. Electrocardiogram is measured in each state and parameters are extracted from it. A statistical study using analysis of variance (ANOVA) is done to see which ones are the most significant. It is concluded that the median of RR segments is the parameter to best determine the state of stress.

Keywords: Electrocardiogram, Heart Rate, Stress, Physiological Computing.

1. Introduction

Nowadays, interaction with most computing systems does not take into account the state of the users operating them, responding identically to different users or their emotional state. Overcoming this obstacle is the goal of Affective Computing (AC) that has been a promising research field since the end of the last century. AC can be defined as using emotional and contextual information of the user, such as facial expression [1], nonverbal features of speech [2], etc., to modify the behavior of an application [3-6]. A subfield in AC is Physiological Computing (PC) based on data from the human body and how it changes to "provide one means of monitoring, quantifying and representing the context of the user to the system in order to enable proactive and implicit adaptation in real-time" [7].

This intelligent technology can be used in many different fields to improve the adaptive capability of a system [8]. PC has been researched as an assistive system for reducing the frustration, arousal states, mental block and workload, for example, in driving [9-12] and regulating a notifications system [13]. It has also been applied to maintain the level of challenge and prevent boredom in computer games [14,15]. In addition, reinforcing positive emotional states or reducing negative emotion is another domain of research of PC; for example, changing music according to the mood of the subject [16] or speeding up the recovery from stress [17] by using biofeedback technique. The main idea in all these systems is to determine the subject's emotional state. Some research has concentrated on identifying these states as anger, happiness, disgust, surprise, sadness and fear [18] or a subset of these [19-24], while others have focused on arousal, stress, workload and/or cognitive-mental load [25-32]. They have tried to establish the effect of various psychological states with diverse physiological elements (many-to-many relationship), to determine how several emotional states affect a unique body measure (one-to-many relationship), or gauge the influence of a psychological state on different physiological data (many-to-one relationship) [33,34]. Thus, when designing an AC system one has to determine how the task modifies body parameters.

This paper attempts to establish a one-to-one relationship focus on heart activity and stress state. An individual feels different situations and levels of psychological pressure in the course of a day. Stress, defined as the organism's psychosomatic response to external influences identified as dangerous, threatening or unpleasant, causing a fight-escape reaction [35], has been identified as the second cause of occupational health problems by the European Foundation for the Improvement of Living and Working Conditions [36]. The most common causes of stress are situations that evoke a negative memory of previous stressful situations. There is a large interest in knowing how stress can be efficiently detected by measuring heart rate variability and/or other additional information such the one collected by filling in a diary [37] or a questionnaire [38]. Putting together all these informations might improve efficiency of a stress classifier. Nevertheless, physiological measurements by themselves, like HRV, usually outperforms diaries [38]. In [37] the diary method improves physiological data, but in that case just one subject took part in the study. Measuring HRV can be accomplished by detecting QRS complex in a conventional ECG or by analyzing the signal from finger plethysmography [39].

This work is framed inside a project whose main goal is the adaptation of an application (game, etc.) to prevent or mitigate stressful situations detected in the user by electrocardiogram measurements. To achieve this goal, on one hand we want to study how this heart rate signal changes under stressful situations and select a subset of parameters extracted from it that allow us to identify such situations in a reliable way. On the other hand, to mitigate stress or induce stress recovery, the environment has to react in some way. Some ideas have been pointed out in different works. One of them is based on reproducing sounds of nature in a virtual reality forest [40]. In the next section, we describe the experimental protocol (Section 2). Sections 3, 4 and 5 present the experimental results, discussions and conclusions.

2. Methodology

2.1 Procedure

The experimentation took place in a room with artificial lighting which was kept at a comfortable temperature. Subjects were seated on a padded chair placed 50 cm away from a 17" monitor with a resolution of 1280x1024 pixels and 32 bits of color. Each subject was asked to attend two 22-minute sessions with one week elapsing between each session. Subjects were randomly grouped into two subsets. Subset 1 performed the arithmetic task in the first week and the memory task in the second, while subset 2 performed the tasks the other way round.

Similar to other experiments conducted to analyze stress [30,41], each session consisted of 5 parts: the initial and final rest periods of 5 minutes and three 4-min phases (Figure 1) in which the task had to be completed. Subjects became accustomed to the task in the first phase, and the level of difficulty and stress were increased in the following phases. Phase 3 should have the greatest level of stress.

Two questionnaires based on the standard State-Trait Anxiety Inventory (STAI) were filled in at the beginning of each relaxation phase [42], where the subject relaxed reading a magazine. The range of results of testing was between 0 and 60 with the minimum and maximum values indicating total stress/anxiety and complete relaxation.

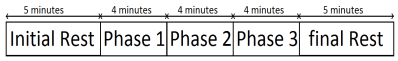

Figure 1.Timing of trials.

A Java application was developed to implement the different tasks the subjects had to carry out. The application contains two activities (memory and arithmetic) with different difficulty levels (Figure 2. The application screen has four areas: time bar, performance bar with two indicators (correct answers and comparison to population), answer panel that shows 1 out of 3 messages (correct/non-correct/time out) and a task panel showing the activity.

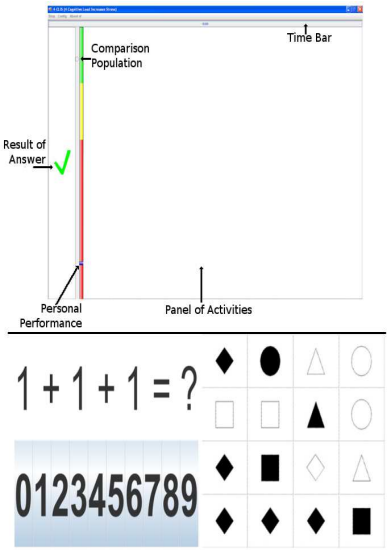

Figure 2. On the top: the Main Application Window, showing the panel for memory and arithmetic activities. In the down-left, the arithmetic panel and on the down-right, the memory panel.

The arithmetic task is based on the Montreal Imaging Stress Task (MIST) [26] where the subjects perform basic math

operations (add, subtract, multiplication) whose results are always in the range between 0-9.

The memory activity consists of a matrix where each cell contains a black or white geometric figure (circle, square, triangle, diamond). The individual must memorize the geometric figure, its color and position and then fill in an empty 2x3 matrix [25].

A timer is incorporated to limit the answer periods and set a timeout interval for all phases. The timeout decreases by 10% after 3 consecutive correct answers and increases by 10% when the subject accumulates 3 incorrect responses or/and exhausted timers. The purpose of the timer is to prevent success in the task and to increase stress. Timing in the memory task is greater than in the arithmetic task to allow subjects to finish it properly.

The answer panel shows the result of the subject's (correct or incorrect) answer or a timer timeout. A personal score increases by one unit after a correct answer, otherwise it decreases by two.

The performance bar only compares the correct answers with 1.5 times the average of results for other subjects. For the first subject we used data obtained from application testing. A red color (0-60%) shows bad performances, yellow (60-80%) mediocre and green (>80%) very good performances.

Finally, the population mark, on the left of the screen, shows 90% of the average for all individuals who have taken the test since it was first implemented.

In Phase 1, or accommodation period, the subjects grew accustomed to the task. This phase is free of pressure and the performance bar is not shown. The average of the results for the population was calculated with the correct answers for this period (the subjects were not aware of this) to determine the population comparison indicator (Figure 1).

In Phase 2, each subject was asked to try and exceed the population result indicator, being told that otherwise the data could not be used to compute the average for other individuals. The mental stress and arousal were therefore higher in this phase.

In Phase 3, the researcher introduced stressors by telling the subject that the data from the last phase was useless because he/she had not achieved the goal, unlike the rest of the subjects who had passed the phase correctly. Even more stress was added by asking questions such as "Did you sleep well?", "Do you have personal problems?", etc. and making comments such as "You've got it wrong", "You must concentrate", "Time's running out".

2.2 Subjects

The trials were conducted with 13 healthy subjects aged between 26-56 (mean 37.86; sd 9.93), two of them were women and eleven men. All of them are voluntary and they work in our same site.Twelve subjects completed the arithmetic task, while eleven performed the memory task. We should also mention that the ethics committee of the University of Seville approved this research.

2.3 Equipment

The biosignal was recorded using bioamplifier model gtec gUSBamp, and version 2.0 of the BCI2000 software [43]. The sample rate of the bioamplifier was set at 256 Hz, with a notch filter (48, 52)Hz to delete electrical power signals. A bandpass filter of 0.5, 100 Hz was applied.

Auto-adhesive Ag/AgCl Electrodes with conductive gel were used.

The offline data analysis was done with version 7.6.0.324 of Matlab.

2.4 Data Acquisition

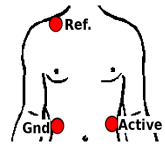

Figure 3. Electrode assembly.

The Electrocardiogram (ECG) signal was recorded using monopolar assembly. The reference was set on the right clavicle whereas the ground electrode was fixed below the right floating rib and the active sensor was placed below the left floating rib (Figure 3).

2.5 Parameters extracted from ECG

In this section we will explain how ECG was processed and what features were extracted from it. Also, the outlier values were avoided in our analysis using the interquartile-range method, that is, the values out of [Q1 - 1.5(Q3 - Q1), Q3 + 1.5(Q3 - Q1)] were eliminated, where Q1 and Q3 are the lower and upper quartiles respectively.

The RR segments are obtained from the ECG signal through the Pan-Tompkins algorithm [44]. Different parameters are extracted from HR and they may be classified in two groups: information based on temporal analysis and that based on frequency analysis [45]. The more common calculated parameters of the first group are the standard deviation of RR intervals (SDNN), the square root of the mean squared difference of successive RR segments (RMSSD), the

proportion of RR intervals that differ by more than 50ms (pNN50), the width of the minimum square difference triangular interpolation of the highest peak of the histogram of all RR intervals (TINN). The other group is based on calculating the power spectrum density (PSD) of the HR. Normally, the PSD is divided in 4 parts: frequency from DC to 0.003Hz (Ultra Low Frequency - ULF), from 0.003 to 0.04Hz (Very Low Frequency - VLF), from 0.04 to 0.15Hz (Low Frequency) and from 0.15 to 4Hz (High Frequency - HF). One additional parameter is the ratio between LF and HF (LF/HF). The influence of each band on the PSD is calculated as the sum of the PSD of the band divided by the sum of all PSD. The SDNN, RMSSD and TINN are used to determine the variability over a short time period to obtain the influence of Parasympathetic Nervous System (PSNS). Important information about quick random changes of heartbeat is extracted from pNN50. The frequency bands can inform about different pathologies, such as the thermoregulatory system (ULF band), blood pressure (LF) and breath (HF). Also, the HF band is connected with the parasympathetic system, whereas the sympathetic system is linked with LF. Thus, the LF/HF ratio is associated with the Autonomic Nervous System (ANS), so that an increase in sympathetic activity causes its value to rise, while an increase in parasympathetic activity causes its value to fall.

Additionally, we obtained the main frequencies of each band (fmVLF, fmLF, fmHF), by applying equation (1), main frequency (fm) is calculated as the average weighted spectral frequencies with energy spectrum density (ESD).

$$fmb = \left(\sum_i f(i) \cdot ESD(i)\right) \Big/ \sum_i ESD(i) \quad \text{(Eq. 1)}$$

The median of RR segments (Mrr), was obtained too. This measure is based in the histogram too, it is simple but not as common as the other measures based in HR.

3. Results

We are not just interested in discovering how the different features change through the phases for a specific subject, but also in choosing the best features for detecting the onset of a stressful situation for a population as a whole. After obtaining the features for the set of subjects in each phase we studied the ANOVA test for the variations of such features through the different phases in order to select the ones with statistical significance. The variations between phases were obtained by applying the equation (2), where ΔJ^{i}_{ref} is the variation of the parameter *J* in the phase *i* with phase *ref* as refline; ΔJ^{i} and ΔJ^{ref} are the values of the parameter *J* in the phase *i* and *ref* where $i \neq ref$.

$$\Delta J^{i}_{ref} = 100 \cdot \left(\left(J^{i} / J^{ref} \right) - 1 \right) \quad i \neq ref \quad \text{(Eq. 2)}$$

The expected behavior for the change from the initial-rest period to the first task phase is a change resulting from a higher-induced stress level, since the subject passes from an initial relaxed state to a mental-activity period and because the individual does not know how the task and the control of the application work. Thus, the stress level is confirmed if these variations occur in the other activity phases compared to the initial rest time. So, a significant difference between task phases and rest periods is the a priori expected behavior (PEB), making it possible to distinguish between the activity and relaxed states. This is the goal of the first analysis (A1). The parameters which do not show those changes must be rejected as correct indicators of stress level, even if one of the phases has a significant change.

Passing from one phase to the next means an increase in what a subject is required to do in an activity. In fact, from rest to the performance period (or viceversa) means moving from relaxed (or arousal) to arousal (or relaxed) state, because the individual goes from reading a magazine to answering different mental operations without having the pressure of an aim. In addition, the second activity phase raises the stress level, in that the subject must achieve a target, and the third phase increases the arousal state because the subject did not succeed in the previous phase. This is the focus in the second analysis (A2). The desired behavior is a significant change from one phase to the next, with the stress level being higher in an activity phase and lower in the relaxed periods.

The arousal of the first activity phase is the induced initial stress level. Taking this phase as baseline, the expected behavior of the parameters is a significant variation from their values in rest periods. Also, the other activity phases must maintain or increase stress levels. Thus, we expect results to include significant changes for the start and finish relaxed phases, and significant variations or not depending on whether stress levels are similar or vary. Therefore, the target of the third analysis (A3) is to distinguish between the stress level and arousal produced by the task.

The three analyses mentioned above were carried out using a one-way analysis (ANOVA). The A1 analysis was performed using the initial rest phase as reference, so that the changes due to the task could be observed. The A2 analysis compared one phase to the previous phase (ref line). This showed the differences between phases, and made it possible to determine whether there was an incremental stress effect. The A3 analysis was done with the first activity phase as refline. The first performance period was used because the subject grew accustomed to the task without

pressure. Using this phase as triger line made it possible to calculate the variations caused by the stress level.

Outliers were dismissed beforehand because the ANOVA is very sensitive to them, although we did not find more than 3 outliers in the worst case.

3.1 Test STAI

As we mentioned earlier, the subjects were given two stress tests during the initial and final rest phases for arithmetic and memory tasks. The difference between the final and initial STAI scores gave us information about whether or not the task was stressful. Negative differences indicated that the task was stressful, whatever the experimental situation for both tasks. Specifically, in the arithmetic task, the average difference was -7.5 with a standard error of 2.18%, and in the memory task this difference was -5.0 with a standard error of 1.46%. An ANOVA analysis applied to the initial and final STAI tests confirmed that such differences were significant (arithmetic p= 0.004, memory p=0.05)

3.2 Electrocardiogram

Table 1 contains the maximum p-value obtained using A1 analysis for each parameter and task in no significant cases. Exceptions are ΔpNN50 and ΔHF band in the memory task as shown below.

	Arithmetic	Memory
ΔSDNN	0.97	0.78
ΔRMSSD	0.25	0.13
ΔTINN	0.88	0.67
ΔVLF	0.39	0.51
ΔLF	0.65	0.91
ΔLF/HF	0.81	0.21
ΔfmVLF	0.51	0.93
ΔfmLF	0.69	0.71
ΔfmHF	0.79	0.68

Table 1. Maximum p-value in task phases for A1 analysis.

Although the averages of most parameters applied to subjects were not statistically significant, there were changes in heart rate for all of them. In Figure 4 we can see the histogram in both the two phases of rest and the three of activity for one of the subjects who performed the test. It can be observed that RR intervals changed significantly throughout the experimental task. The maximum for the histogram shifted to the left when the subject went from rest period 1 to phase 1. This implies a reduction in the RR interval or, equivalently, an increase in heart rate. One can also see how, even in the most stressful phase, phase 3, this histogram shifted even further to the left. The final period, rest 2, caused the histogram to shift to the right and go back to the initial position. Hence, a parameter exhibiting the shifting of the histogram through the different phases and showing robustness against outliers is needed. The median of RR segments (Mrr) was not sensitive to outliers and adjusted fairly well to the shifting of the histogram, so this might be a good choice.

A first approximation of the performance of this parameter is shown in Figure 5. The horizontal axis contains all the experimental subjects, with the vertical axis showing the ΔMrr parameter according to the experimental phase. The expected behavior for phase 1 was that the position of the median would decrease from the refline (rest 1) and continue to drop even further as the experimentation moved into phase 2 and 3. This behavior was observed for most subjects in both tasks. Subjects 4, 5, 7, 8 and 10, in the arithmetic task, and 2, 8 and 11, in the memory task, showed a sequential decrease in Mrr values through the phase. In the memory task, subjects 1, 4, 5, 6, 7, 9, and 10, and 2, 9 and 11 in the arithmetic task exhibited a lower value in the third performance than in the second. The final rest period had a higher value in 13 cases (6 arithmetic / 7 memory) than in the initial rest time and in 5 cases they were almost the same.

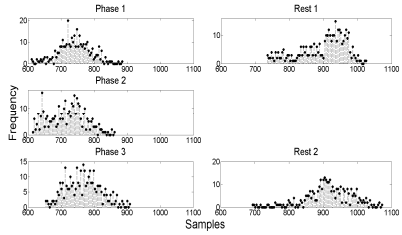

Figure 4. RR interval Histogram for a subject in different phases.

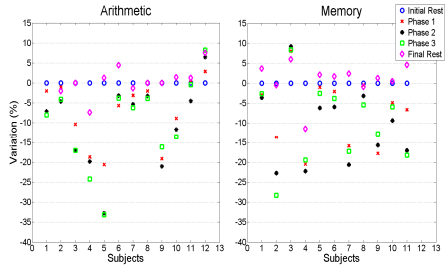

Figure 5. Median variations for subjects.

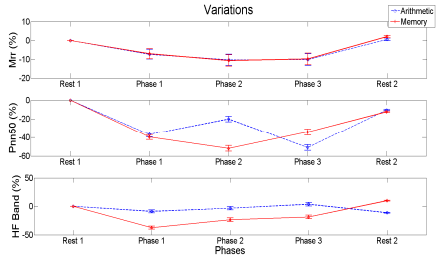

Figure 6. ΔMrr, ΔPnn50 and ΔHF-band averages.

*Las figuras 4, 5 y 6 se muestran con más detalles en la página 92.

Figure 6 shows the ΔMrr averages for all phases and tasks based on analysis A1. One can see that for both tasks its behavior was very similar. For phase 1 ΔMrr fell showing that the RR interval decreased, and for phases 2 and 3, when more stress was applied, the ΔMrr dropped again close to -10% (±3%) but it is not easy to distinguish phase 3 from the previous one. As the task ended and the subject went to the final rest period, the median rose up to the refline. The ANOVA test confirmed what we can see in Figure 6 ΔMrr was very significant for the A1 analysis in which the p-value was lower than 0.01 for all phases and tasks, excluding the final rest period, and the p-value for phase 3 in analysis A2 and A3 was not significant.

The ΔpNN50 did not behave as expected as we can see in Figure 6. In the arithmetic task, this parameter drew a w-shape, going down in phase 1, then up in phase 2, and so on to the end. The ANOVA test (Table 2) showed this feature was not significant in the A1 analysis (p=0.25 in phase 2). This situation was similar for this parameter and the memory task, where the curve it described was not PEB compliant but the A1 ANOVA test was significant (p<0.01 for phases 1-3).

		Phase				
		Rest 1	**Phase1**	**Phase2**	**Phase3**	**Rest 2**
A1	ΔMrr		<0.01a 0.02m	<0.01a <0.01m	<0.01a <0.01m	0.31a <0.01m
	ΔpNN50		<0.01a <0.01m	0.25a <0.01m	<0.01a <0.01m	0.33a 0.14m
	ΔHF		0.52a <0.01m	0.81a 0.05m	0.80a 0.05m	0.79a 0.43m
A2	ΔMrr		<0.01a 0.02m	0.02a 0.02m	0.21a 0.39m	<0.01a <0.01m
	ΔpNN50		<0.01a <0.01m	0.07a <0.01m	0.27a 0.46m	0.05a <0.01m
	ΔHF		0.52a <0.01m	0.73a 0.78m	0.12a 0.12m	0.50a 0.15m
A3	ΔMrr	<0.01a 0.02m		0.02a 0.02m	0.10a 0.30m	<0.01a <0.01m
	ΔpNN50	0.37a 0.04m		0.07a <0.01m	0.15a 0.33m	0.13a <0.01m
	ΔHF	0.54a 0.03m		0.73a 0.78m	0.90a 0.17m	0.87a 0.02m

Table 2. ANOVA Analysis of ECG. a=arithmetic, m=memory.

ΔHF showed PEB in the arithmetic task but not in the memory task. Focusing on the first task, the ANOVA test was not significant either for activity or stress detection. The significance in this feature only appeared as an indicator of activity in the memory task.

4. Discussion

During the development of a stressful activity changes occur in the homeostasis of the human body which can be detected because several regulatory variables modify their resting values. The progressive increase in the level of stressors during the subject's task would determine the dependence of the analyzed variables with the degree of induced stress. The analysis conducted in this study aimed to identify such dependencies and profile a subset of these variables which would be suitable for stress detection in a population. To achieve this goal we have to take into account, on the one hand, that a variable is suitable for detecting stress when it is significant from a statistical point of view. Due to the variability in resting values in a population, the statistical analysis requires, on the other hand, changes in these variables to be processed subject by subject before they can be used in a statistical study, otherwise the results could be irrelevant.

The trials were designed to increase the stress level in each activity phases. However, observing the ANOVA results and parameter's variation charts could be concluded the subjects were less arousal in the third task period, where it had to be the most stressful performance. This fact may be caused by the users tried relax and concentrate because they previously did twice the operations and their nervousness level made that they failed. Furthermore, it should also take into account that the main difference between the third and second phase were the questions of the person driving the experiment. The desired stress increase could not be achieved.

It is important in this study to identify an activity period from a rest phase, differentiate properly an unstressful activity from a stressful one, and check variable dependency on stressor intensity. To achieve these goals, we carried out three types of analysis. In analysis A1, we wanted to calibrate the changes in the set of values of the physiological variables when the task (or stressful task) was performed compared to the rest state and thus determine how the activity and stress affected them. In the second analysis, A2 and A3, we identified stress by erasing the effect the activity had over the analyzed variables.

Finally, to confirm that the proposed tasks were stressful, the STAI test was given to subjects at the beginning and at the end of each trial. The results confirmed that the tasks subjects performed did produce stress.

Most of the typical features widely used in ECGs are not suited to showing clearly the shifts in the RR- histogram even if the outliers are deleted. Their sensitivity to extreme values may be the cause. However, the median of RR segments was less sensitive to outliers and was better for showing the histogram shift between phases.

The value of the median, ΔMrr, in the arithmetic and memory tasks decreased significantly during phases, while it was similar in rest periods. Furthermore, the changes from one phase to the next showed that the stress level was the cause of this variation. The phase 3 showed a behavior

indistinguishable from the others two task periods (analysis A2 and A3 show that), in spite of changes of this feature (Figure 3.2.3) drew similar values of average and standard error respect to phases 1 and 2. This can be due to the fact that the subjects knew the operations and they tried to get relaxed. We conclude that this feature is appropriate for being used as a stress detector.

On the other hand, the ΔpNN50 and ΔHF band only exhibited relevance in the memory task. A low pNN50 meant that the variability of the RR segment was also low, so the PSNS activity was lower and thus subjects were more aroused. The HF band was also linked to PSNS, so low values in this band represented a reduction in activity in PSNS, meaning individuals were more overexcited.

5. Conclusions

The goal of this research was to determine the statistical significance of the effect of stress levels in parameters related with HR and verify the results with a subjective psychological questionnaire. To do this, these biosignals were recorded, processed and analyzed. The STAI test confirmed that the significant parameter changes were caused by increased stress levels during task periods, since the results showed lower values after activity periods than before they had started. Some features extracted from biosignals changed depending on the task and their variations were significant during the arithmetic tasks while others were significant during the memory activity task. A summary of significant parameters is shown in Table 3.

The most interesting parameters were those that made it possible to distinguish activity and stress situations in both memory and arithmetic tasks. This was the case of ΔMrr in ECG.

ΔpNN50 and ΔHF of ECG also showed effects in both tasks but only weakly.

PHYSIOLOGICAL SIGNAL	PARAMETER	ACTIVITY INDICATOR	STRESS INDICATOR
ECG	ΔMrr	both tasks	both tasks
	ΔpNN50	both tasks	both tasks
	ΔHF	both tasks	both task

Table 3. Significant parameters.

In future work, we will analyze stressor effects on others biosignals as a result of the tasks described in this paper, examining the best features for detecting such a situation. When significant physiological variables are detected, they should all be combined into a system capable of deciding about the state of the subject and acting accordingly, so as to lead the subject towards a less stressful state.

6. Acknowledgements

This project has been carried out within the framework of a research program: (p08-TIC-3631) – Multimodal Wireless interface funded by the Regional Government of Andalusia.

7. References

1. Kappas, A. (2010). “Smile when you read this, whether you like it or not: Conceptual challenges to affect detection”. IEEE Trans. Affective Comput. ISBN: 19493045, vol. 1, n. 1, pp. 38-41.

2. Pfister, T., and Robinson, P.. (2011). “Real-Time Recognition of Affective States from Nonverbal Features of Speech and Its Application for Public Speaking Skill Analysis”. IEEE Transactions on Affective Computing, vol. 2, n. 2, pp. 66-78.

3. Picard, R.W., (1997) Affective Computing.

4. El Kaliouby, R., Picard, R., Baron-Cohen, S., eds. Affective computing and autism. ; 2006. Bainbridge W.S. and Roco M.C., eds.; No. 1093.

5. Calvo, R.A., D'Mello, S. (2010). “Affect detection: An interdisciplinary review of models, methods, and their applications”. IEEE Trans Affective Comput. ISBN: 19493045, vol. 1, n. 1, pp. 18-37.

6. Reisenzein, R. (2010). Broadening the scope of affect detection research. IEEE Trans Affective Comput. Vol. 1, n. 1, pp. 42-45.

7. Fairclough, S.H. (2009). “Fundamentals of physiological computing”, Interacting with Computers, vol. 21 , n.1-2, pp. 133-145.

8. Norman, D.A. (2007). “The Design of Future Things”. Basic Books, New York.

9. Nasoz F., Lisetti C.L., and Vasilakos A.V. (2010). “Affectively intelligent and adaptive car interfaces”, Information Sciences, vol. 180, pp. 3817-3836.

10. Wu, D., Courtney, C.G., Lance, B.J., Narayanan, S.S., Dawson, M.E., Oie, K.S., and Parsons, T.D. (2010). “Optimal arousal identification and classification for affective computing using physiological signals: Virtual reality stroop task”. IEEE Trans. Affective Comput.; ISBN: 19493045, vol. 1, n. 2, pp. 109-118.

11. Singh, RR, Conjeti, S, and Banerjee, R. (2011). “An approach for real-time stress-trend detection using physiological signals in wearable computing systems for

automotive drivers". IEEE Conf. Intell. Transport Syst. Proc. ITSC., ISBN: 9781457721984, pp. 1477-1482.

12. Conjeti, S., Singh, RR., and Banerjee, R. (2012). "Bio-inspired wearable computing architecture and physiological signal processing for on-road stress monitoring". Proc - IEEE-EMBS Int. Conf. Biomed. Health Informatics: Global Grand Chall Health Informatics, BHI., ISBN: 9781457721779, pp. 479-482.

13. Chen, D., and Vertegaal, R.. (2004). "Using mental load for managing interruptions in physiologically attentive user interfaces". Extended abstracts of the 2004 Conference on Human Factors in Computing Systems, CHI 2004, Vienna, Austria, April 24 - 29. ACM 2004.

14. Chanel, G., Rebetez, C., Bétrancourt, M., and Pun, T. (2011). "Emotion Assessment From Physiological Signals for Adaptation of Game Difficulty". IEEE Transactions on Systems, Man, and Cybernetics, part a: Systems and Humans, vol. 41, issue: 6, pp. 1052-1063.

15. Giakoumis, D., Tzovaras, D., Moustakas, K., Hassapis, G. (2011). "Automatic recognition of boredom in video games using novel biosignal moment-based features". IEEE Trans Affective Comput. vol. 2, n. 3, pp. 119-133.

16. Janssen, J.H., Van Den Broek, E.L., and Westerink, J.H.D.M. (2012). "Tune i to your emotions: A robust personalized affective music player". User Modelling and User-Adapted Interaction, ISBN: 09241868, vol. 22, n. 3, pp. 255-279.

17. Whited, A., Larkin, K,; Whited,M. (2014). "Effectiveness of emWave biofeedback in improving heart rate variability reactivity to and recovery from stress". Appl. Psychophysiol biofeedback. Springer Science+Business media New York (2014). DOI 10.1007/s10484-014-9243-z

18. Ekman ,P., Friesen, W.V., O'Sullivan, M., Chan, A., Diacoyanni-Tarlatzis, I., Heider, K., Krause, R., LeCompte, W.A., Pitcairn, T., Ricci-Bitti, P.E., Scherer, K., Tomita, M., Tzavaras, A. (1987). "Universals and Cultural Differences in the Judgments of Facial Expressions of Emotion". J.Pers.Soc.Psychol., ISBN: 00223514, vol. 53, n. 4, pp. 712-717.

19. Kim, K. H., Bang, S. W., and Kim, S. R. (2004). "Emotion recognition system using short-term monitoring of physiological signals". Medical & Biological Engineering & Computing, vol. 42, n. 3, pp. 419-427.

20. Soleymani, M., Chanel, G., Kierkels, J. J. M., and Pun, T. (2008). "Affective characterization of movie scenes based on multimedia content analysis and user's physiological emotional responses", 10th IEEE International Symposium on Multimedia, ISM 2008 , art. no. 4741174 , pp. 228-235.

21. Laparra-Hernández, J., Belda-Lois, J. M., Medina, E., Campos, N., and Poveda, R. (2009). "EMG and GSR signals for evaluating user's perception of different types of ceramic flooring". International Journal of Industrial Ergonomics, vol. 39, pp 326-332.

22. Petrantonakis, P.C., Hadjileontiadis, L.J. (2010). "Emotion recognition from brain signals using hybrid adaptive filtering and higher order crossings analysis". IEEE Trans Affective Comput. 2010, vol. 1, n. 2, pp. 81-97.

23. Petrantonakis, P.C., Hadjileontiadis, L.J. (2010). "Emotion recognition from EEG using higher order crossings". IEEE Trans Inf Technol Biomed. 2010, vol. 14, n. 2, pp. 186-197.

24. Petrantonakis, P.C., Hadjileontiadis L.J. (2009). "EEG-based emotion recognition using hybrid filtering and higher order crossings". Proc - Int Conf Affective Comput Intelligent Interact Workshops, ACII. 2009.

25. Iwanaga, K., Saito, S., Shimomura, Y., Harada, H., and Katsuura, T. (2000). "The Effect of Mental Loads on Muscle Tension, Blood Pressure and Blink Rate". Journal of Physiological Anthropology and applied human science, vol. 19, n. 3, pp. 135-141.

26. Dedovic , K., Renwick , R., Mahani , N. K., Engert , V., Lupien , S. J., and Pruessner, J. C. (2005). "The Montreal Imaging Stress Task: using functional imaging to investigate the effects of perceiving and processing psychosocial stress in the human brain". J Psychiatry Neurosci. ISBN: 1488-2434 , vol. 30, n. 5, pp. 319–325.

27. Pfurtscheller, G., Grabner, R. H., Brunner, C. and Neuper, C. (2007). "Phasic heart rate changes during word translation of different difficulties". Psychophysiology. vol.44, pp. 807-813.

28. Shi, Y., Ruiz, N., Taib, R., Choi, E.H.C., and Chen, F. (2007). "Galvanic skin response (GSR) as an index of cognitive load". Conference on Human Factors in Computing Systems - Proceedings, pp. 2651-2656.

29. Luttmann, A., Schmidt, K., and Jäger, M. (2010). "Working conditions, muscular activity and complaints of office workers". International Journal of Industrial Ergonomics, vol. 40, n. 5, pp. 549-559.

30. Setz, C., Arnrich, B., Schumm, J., Marca, R. L., Tröster, G., and Ehlert, U. (2010). "Discriminating Stress From Cognitive Load Using a Wearable EDA Device". IEEE Transactions on

Information Technology in Biomedicine, vol. 14, n. 2, pp. 410-417.

31. Steven, A., Murray, M., Yanagi, C., and Burcu , D. (2010). "The Effects of Acute Stress on Cognitive Performance". Office of Naval Research.

32. Sun, F.-T., Kuo, C., Cheng, H.-T., Buthpitiya, S., and Collins, P.. (2010). "Activity-aware Mental Stress Detection Using Physiological Sensors". Lecture Notes of the Institute for Computer Sciences, Social Informatics and Telecommunications Engineering, vol. 76, pp. 211-230.

33. Cacioppo, J.T., and Tassinary, L.G. (1990). "Inferring psychological significance from physiological signals". American Psychologist, vol. 45, n. 1, pp. 16-28.

34. Cacioppo, J.T., Tassinary, L.G., and Berntson, G.G. (2000). "Handbook of Self-regulation". Psychophysiological science. In: Cacioppo, J.T., Tassinary, L.G., and Berntson, G.G. (Eds.). Cambridge University Press, Cambridge UK, pp. 3-26.

35. Canon, W. (1915). "Bodily Change in Pain, Hunger, Fear and Rage: An Account of Recent Research into the Function of Emotional Excitement". Appleton, New York, NY, US.

36. European Foundation for the Improvement of Living and Working Conditions. (2007). "Work-related stress". (Online). Available: http://www.eurofound.european.eu/ewco/reports/TN0502TR01/TN0502TR01.pdf

37. Muaremi, A., Arnrich, B., Tröster, G. (2013). "Towards measuring stress with smartphones and wearable devices during workday and sleep". BioNanoSci, vol. 3, pp. 172-183. Springer. DOI: 10.1007/s12668-013-0089-2

38. Atz, U. (2013) "Evaluating experience sampling of stress in a signle-subject research design". Pers Ubiquit Comput 17-639-652. Springer. DOI 10.1007/s00779-012-0512-7

39. Minakuchi, E. et al. (2013). "Evaluation of mental stres by physiological indices derived from finger plethysmography". Journal of physiological anthropology.

40. Annerstedt, M., Jönsson, P., Wallergard, M., Johansson, G., Karlson, B., Grahn, P., Hansen, A. M., Währborg, P. (2013). "Inducing physiological stress recovery with sounds of nature in a virtual raeality forest- Results from a pilot study". Physiology & Behavior, vol. 118, pp. 240-250.

41. Campisi, J., Bravo, Y., Cole, J., and Gobeil, K. (2012). "Acute psychosocial stress differentially influences salivary endocrine and immune measures in undergraduate students". Physiology & Behavior, vol. 107, pp. 317-321.

42. Spielberger, C. D., Gorsuch, R. L., Lushene, R., Vagg, P. R., and Jacobs, G. A. (1983). "Manual for the State-Trait Anxiety Inventory". Palo Alto, CA: Consulting Psychologists Press.

43. Schalk , G., McFarland , D. J., Hinterberger , T., Birbaumer, N., and Wolpaw, J. R. (June 2004). "BCI2000: A General-Purpose Brain-Computer Interface (BCI) System". IEEE Transactions on Biomedical Engineering, vol. 51, n. 6, pp. 1034-1043.

44. Pan, J., and Tompkins, W. J. (1985). "A Real-Time QRS Detection Algorithm". IEEE Transactions on Biomedical Engineering, vol. BME-32, n. 3, pp. 230-236.

45. Sörnmo, L., and Laguna, P. (2005). "Bioelectric Signal Processing in Cardiac and Neurological Applications". Elsevier Academic Press.2005.

Figuras 4, 5 y 6 del apartado 4.2.5 (Monge et al, 2014)

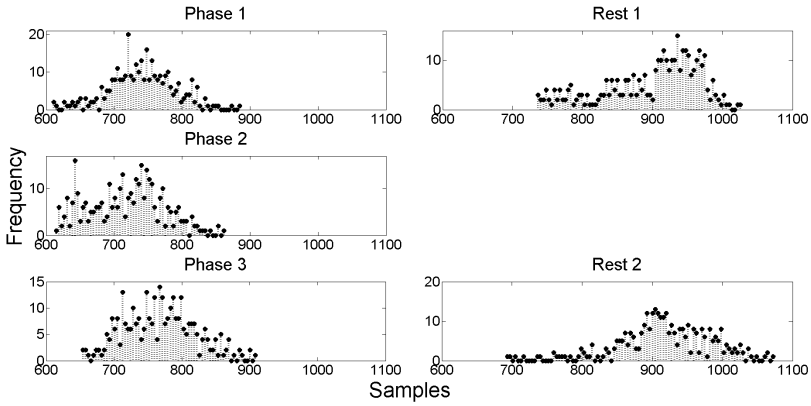

Figure 4. RR interval Histogram for a subject in different phases.

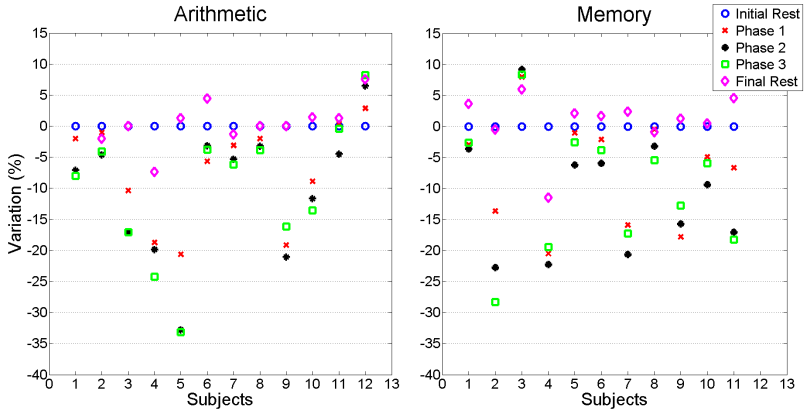

Figure 5. Median variations for subjects.

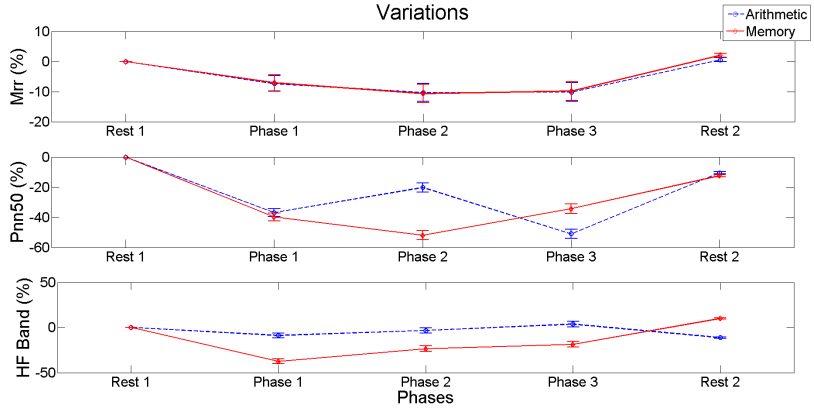

Figure 6. ΔMrr, ΔPnn50 and ΔHF-band averages.

4.3. Electroencefalografía

En las pruebas realizadas en el artículo Monge et al (2014) (sección 4.2.5), además de registrar los datos de ECG, se recolectaron datos de EEG, y se realizó un análisis similar de los mismos. De esta forma, se calcularon la variaciones de 32 características y se analizaron estadísticamente para determinar el efecto que tienen las tareas sobre ellas.

La tarea de aritmética mostró una menor influencia en el número de parámetros que la acción de memorizar en un corto periodo de tiempo. Los cálculos matemáticos muestran un incremento de las características EEG en el lóbulo frontal, principalmente en el hemisferio izquierdo (región lógica). La memoria a corto plazo produce un incremento de la amplitud y dispersión de las bandas θ y α en la zona frontal, y una atenuación de la energía de las bandas en la región parietal. Se observó un comportamiento inverso entre la influencia de las bandas θ y β en el área frontal, con una tendencia en θ hacia las frecuencias de la banda δ.

Se concluye que los electrodos situados sobre el lóbulo frontal, en las posiciones etiquetadas con la letra F, concentran principalmente los parámetros que modificaron sus valores de manera significativa durante la actividad, en relación a los periodos de relajación. Asimismo, aunque el test STAI reflejó un incremento del nivel de estrés, éste no se observó en los datos, pudiendo deberse a un periodo demasiado corto o un posible estado de acomodación.

4.3.1 Publicación 5

EEG Feature Variations under Stress Situations

Manuel Merino[1], Isabel Gómez[1], Alberto J. Molina[1]

***Abstract*— The goal of this study is to identify EEG parameters and electrode positions with the highest significant values to differentiate between tasks and relax periods. Different signals were recorded as 12 subjects are doing arithmetic and memory tasks under stress condition. The test consisted of an initial and final 5-minute relax periods and three 4-minute performance phases with increased stress level. θ and α bands concentrated mainly features whose variation were significant, and F3 and P4 were the best positions to distinguish between performed tasks and arousal level.**

I. Introduction

Nowadays, interaction with most computing systems does not take into account the state of the users operating them, responding identically to different users or their emotional state. Overcoming this obstacle is the goal of Affective Computing (AC) that has been a promising research field since the end of the last century. AC can be defined as using emotional and contextual information of the user, such as facial expression, nonverbal features of speech, etc., to modify the behavior of an application [1]. A subfield in AC is Physiological Computing (PC) based on data from the human body and how it changes to "provide one means of monitoring, quantifying and representing the context of the user to the system in order to enable proactive and implicit adaptation in real-time" [2].

This intelligent technology can be used in many different fields to improve the adaptive capability of a system or reducing negative feelings like stress [3]–[5], such that determining the subject's emotional state is main task. Some research has concentrated on identifying these states as arousal, stress, workload and/or cognitive-mental load [6]–[9]. They have tried to establish the effect of various psychological states with diverse physiological elements (many-to-many relationship), to determine how several emotional states affect a unique body measure (one-to-many relationship), or gauge the influence of a psychological state on different physiological data (many-to-one relationship) [10]. Thus, when designing an AC system one has to determine how the task modifies body parameters.

EEG signal are mainly split in frequency five bands: δ band (<4Hz) associates to deep asleep; θ band (4-8Hz) links with the drowsiness and asleep states; α band (8-14Hz) shows acitivity with awake, relaxed, no-open-eye states, mainly in occipital area; β band (14-30Hz) connects to states of activity, mainly frontal and center area of brain; γ band (>30Hz) is related with information processing. θ and α bands may be used like attention index, workload and level of activity [9], [11]–[13]. Cognitive and workload processes have been associated to large power in the highest segments of the α band (10-12Hz), whereas desynchronization of the lowest segments (8-10Hz) were assigned to level of attention [14]. Also, increasing memory activity have been related with decreasing the powre in θ and α bands [15]. θ power increasing in the middle frontal area was reported during memory and codification periods of new information [16]. δ and β bands decreasing were related with the cognitive aspects of a task [17], and γ band increasing was linked with changes of attention, in special in the parietal cortex [18].

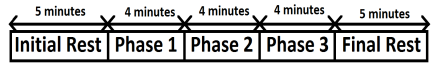

Fig. 1. Trial Timing

This paper attempts to establish a one-to-one relationship focus on EEG signal and stress state, because it has been identified as the second cause of occupational health problems. This work is framed in a study in which we are interested in knowing how EEG features change under stressful situations. This knowledge will allow us to identify the subset of parameters and sensor positions for identifying stress reliable way. In the next section, we describe the experimental protocol (Section 2). Sections 3 and 4 present the experimental results and conclusions.

II. Methology

The experimentation took place in a room with artificial lighting and comfortable temperature. Each subject was asked to attend two 22-minute sessions with one week elapsing between them. Subjects were randomly grouped into two subsets. Subset 1 performed the arithmetic task in the first week and the memory task in the second, while subset 2 performed the tasks in reverse order.

Experiments were based on others conducted to analyze stress [6], [8], [19]. Each session was split in 5 parts: the initial and final rest periods of 5 minutes and three 4-minute phases (Fig. 1) in which the task had to be completed. Subjects became accustomed to the task in the first phase, and the level of difficulty and stress were increased in the following phases. Phase 3 should have the greatest level of stress.

Two questionnaires based on the standard State-Trait Anxiety Inventory (STAI) were filled in at the beginning of each relaxation phase [20], where the subject relaxed reading a

[1]Electronic Technology Department, University of Seville, Avd. Reina Mercedes s/n, 41012, Seville, Spain. manmermon@dte.us.es; {igomez, almolina}@us.es

978-1-4244-9270-1/15/$31.00 ©2015 IEEE

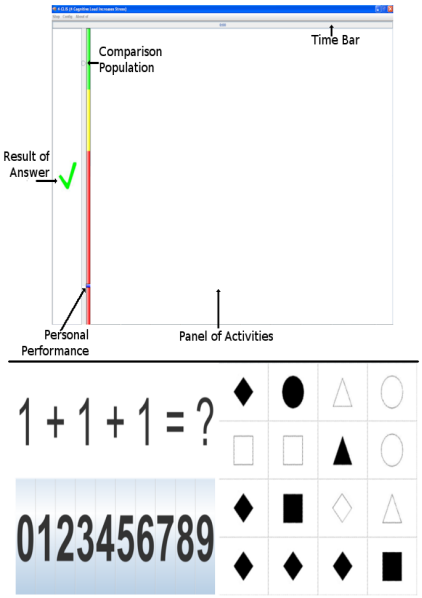

Fig. 2. Trial application. On the top: the Main Application Window showing the panel for memory and arithmetic activities. In the down-left, the arithmetic panel and on the down-right, the memory panel.

magazine. The range of results of testing was between 0 and 60 with the minimum and maximum values indicating total stress/anxiety and complete relaxation.

A Java application was developed to implement the different tasks the subjects had to carry out [19] (Fig. 2). The application screen has four areas: time bar, performance bar with two indicators (comparing user performance with 1.5 times the population result average), answer panel that shows 1 out of 3 messages (correct/non-correct/time out) and a task panel showing the activity. The arithmetic task is based on the Montreal Imaging Stress Task (MIST) [6] where the subjects perform basic math operations (add, subtract, multiplication) whose results are always in the range between 0-9. The memory activity consists of a matrix where each cell contains a black or white geometric figure (circle, square, triangle, diamond). The individual must memorize the geometric figure, its color and position and then fill in an empty 2x3 matrix.

In Phase 1, or accommodation period, the subjects grew accustomed to the task. This phase is free of pressure and the performance bar is not shown. The average of the results for the population was calculated with the correct answers for this period (the subjects were not aware of this) to determine the population comparison indicator.

In Phase 2, each subject was asked to try and exceed the population result indicator, being told that otherwise the data could not be used to compute the average for other individuals. The mental stress and arousal were therefore higher in this phase.

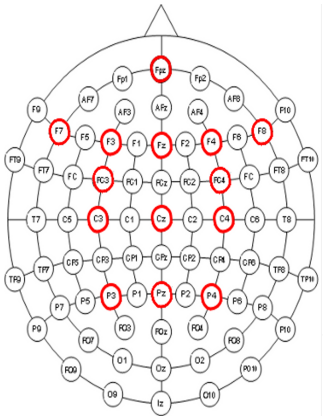

Fig. 3. EEG electrode scheme.

In Phase 3, the researcher introduced stressors by telling the subject that the data from the last phase was useless because he/she had not achieved the goal, unlike the rest of the subjects who had passed the phase correctly. Even more stress was added by asking questions such as"Did you sleep well?", "Do you have personal problems?", etc. and making comments such as "You've got it wrong", "You must concentrate", "Time's running out".

A. Subjects

The trials were conducted with 13 healthy subjects aged between 26-56 (mean 37.86; sd 9.93), two of them were women and eleven men. All of them were voluntary and they work in our same place. Twelve subjects completed the arithmetic task, while eleven performed the memory task. Ethics committee of the University of Seville approved this research.

B. Data Acquisition

The biosignal amplifier was set at 256 Hz, with a Chebyshev notch filter (48, 52)Hz of order 4 to delete electrical power signals. A bandpass filter of (4, 45)Hz and a correlation filter with EOG data as reference signal were applied to remove environment noise, drifts, and EOG interference. Visual inspection was done to delete segments with significant head or body movements interference.

Selected EEG standard positions were: Fpz, F7, F3, Fz, F4, F8, FC3, FC4, C3, Cz, C4, P3, and P4 (Fig. 3), where Fpz was utilized as ground and Cz was used as reference sensor.

The offline data analysis was done with version 7.6.0.324 of Matlab.

C. EEG Parameters

EEG signal was divided in four frequency bands: (4, 8]Hz is θ,(8,14]Hz is α, (14,30]Hz is β, and >30Hz is γ. Thrity two parameters were calculated: band energy (E_θ, E_α, E_β, E_γ), standard deviation of each band (std_θ, std_α,

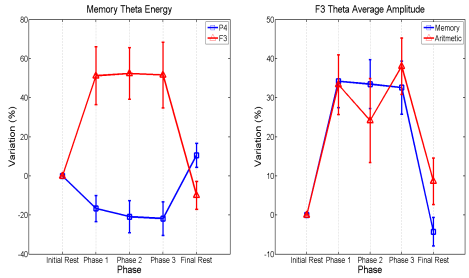

Fig. 4. Feature variations with initial rest as refline. On the left is showed θ energy in F3 and P4 for memory task. On the right is drew θ amplitude mean in F3 for both activities.

std_β, std_γ), spectral amplitude average ($\overline{AS_\theta}$, $\overline{AS_\alpha}$, $\overline{AS_\beta}$, $\overline{AS_\gamma}$), spectral centroid (f_θ, f_α, f_β, f_γ), percentage of each bands in total energy (I_θ, I_α, I_β, I_γ), the logarithm of ratio between E_β and the sum of E_θ and E_α (EEG_ω [5]), and from total EEG signal, in time domain, total energy (E_{EEG}), fractal dimension (FD) using Higuchi method [9], six order AR model coefficients ($AR_j, j \in \mathbb{Z} = \{1,6\}$), and Hjorth's parameters [21], that is, activity (Ac), movility (M) and complexity (COM).

III. Result

We are not just interested in discovering how the different features change through the phases for a specific subject, but also in choosing the best features for detecting the onset of a stressful situation for a population as a whole. After obtaining the features for the set of subjects in each phase we studied the Wilcoxon signed rank test with 0.05 statistical significance for each phase respect using initial rest as refline and for activity phases versus accommodation period (phase 1). ANOVA analysis was rejected because some features did not fulfill the normal-distribution requirements (Shapiro test).

On the other hand, a variation analysis between phases were obtained by applying the equation (1), where $\Delta J^i_{ref}$is the variation of the parameter J in the phase i with phase ref as refline; ΔJ^i and ΔJ^{ref} are the values of the parameter J in the phase i and ref where $i \neq ref$.

$$\Delta J^i_{ref} = 100 \cdot \left(\left(J^i / J^{ref} \right) - 1 \right) \; i \neq ref \tag{1}$$

The expected behavior for the change from the initial-rest period to the first task phase is a change resulting from performance period, since the subject passes from an initial relaxed state to a mental-activity period and because the individual does not know how the task and the control of the application work. So, a significant difference between task phases and rest periods is the a priori expected behavior (PEB), making it possible to distinguish between the activity and relaxed states. Rest periods have to show non-significant differences. This is the goal of the first statistic analysis. The parameters which do not show those changes must be rejected as correct indicators of stress level, even if one of the phases has a significant change. On the other hand, stress level should be confirmed from the second statistic analysis, so that, the stress level is confirmed these variations occur in second and third performance phases compared to first activity phase.

TABLE I

First statistic analysis results (a=PEB in arithmetic task, m=PEB in memory task, ∩=variation in inverted-U shaped, ∪=variation in U shaped).

Feature	F7	F3	Fz	F4	F8	FC3	FC4	C3	C4	P3	P4	Total
Ac											m∪	*1m*
COM		m∩						a∪				*1a* *1m*
EEG_ω		m∩										*1m*
f_θ		m∪	m∪	m∪						m∪	m∪	*5m*
f_α										a∩	a∩	*2a*
I_Θ		m∩	m∩									*2m*
I_α										m∪		*1m*
I_β		m∪	m∪									*2m*
std_θ		m∩	m∩	m∩		m∩						*4m*
std_α		a∩ m∩	a∩									*2a* *1m*
std_β								a∩				*1a*
std_γ								a∩				*1a*
E_θ				m∩							m∪	*2m*
E_β											m∪	*1m*
E_{EEG}						m∪	m∪		m∪		m∪	*4m*
$\overline{AS_\Theta}$		a∩ m∩	a∩ m∩	a∩ m∩	a∩	m∩	a∩					*5a* *4m*
$\overline{AS_\alpha}$		a∩ m∩	a∩									*2a* *1m*
$\overline{AS_\beta}$			a∩									*1a*
$\overline{AS_\gamma}$								a∩				*1a*
Total		*3a* *9m*	*4a* *5m*	*1a* *4m*	*1a*	*3m*	*1a* *1m*	*4a*	*1m*	*1a* *2m*	*1a* *5m*	

A. STAI Test

As we mentioned earlier, the subjects were given two stress tests during the initial and final rest phases for arithmetic and memory tasks. The difference between the final and initial STAI scores gave us information about whether or not the task was stressful. Negative differences indicated that the task was stressful, whatever the experimental situation for both tasks. Specifically, in the arithmetic task, the average difference was -7.5 with a standard error of 2.18%, and in the memory task this difference was -5.0 with a standard error of 1.46%.

B. Electroencephalogram

Table I summarizes first statistic analysis results where PEB was found. EEG positions with more PEB features were F3, Fz and C3 for arithmetic activity, and F3, Fz, and P4 in memory performance. F8, C3 in memory, FC3, C4 in arithmetic, and F7 for both tasks have not shown any PEB features. All arithmetic features showed variations in inverted-U shaped, except COM, while in memory, F3 and P4 showed inverse variations, such that majority of them drew a shape like inverted-U and U respectively. An inverted-U and U shapes mean how are feature changes, so that increasing and decreasing of parameter during performance is inverted-U and U respectively. An example is showed in Fig. 4.

Second statistic analysis showed non-significant changes of all features respect to first activity phase, whereas, in memory, significant variations were obtained in Ac in P4 during second performance, and $\overline{AS_\theta}$ in FC3 and $\overline{AS_\alpha}$ in F3 during third activity phase. Thus, only these parameters could be used as stress index. However, stress-4-minute period may not be enough to achieve stressed EEG data, against used biosignals in others studies, like electrodermal activity or electrocardiogram [8], [19].

θ and α bands causes mainly PEB features in F positions, mainly left area (logical, arithmetic area), such that their values increase with activities what can be observed with spectral amplitude, its dispersion, and influence and frequency centroid of θ [9], [11]–[16]. Cognitive task aspects show inversed behavior of I_θ and I_β, and $\overline{AS_\theta}$ increasing are linked with previous results from [16], [17]. θ frequency centroid shifts towards δ band with activity. This fact may be related with δ power increasing reported in [17]. On the other hand, reports of spectral dispersion were not found.

IV. Conclusion and Future Work

This study is focused on selecting EEG positions and parameters. Activity effects are observed in EEG features, three of them showed stress changes and it is confirm with a questionnaire. However, stressful period should be longer to get more features. θ and α bands congregate the majority of PEB parameters. F3, Fz and F4 electrode positions concentrate mainly these variations, while F7, F8, FC3 and C4 could be rejected as good activity/stress locations. Also, F3 is a common position in both tasks, and P4 is mainly linked with memory performance. Next step is to develop a stress and task classifier based on these results.

References

[1] R. El Kaliouby, R. Picard, and S. Baron-Cohen, "Affective computing and autism," Affiliation: Massachusetts Institute of Technology, Cambridge, MA 02142-1308, United States; Affiliation: University of Cambridge, Cambridge CB3 0FD, United Kingdom; Affiliation: FIEEE, MIT Media Laboratory, E15-448, 20 Ames Street, Cambridge, MA 02142-13, pp. 228–248, 2006.

[2] S. H. Fairclough, "Fundamentals of physiological computing," *Interacting with Computers*, vol. 21, no. 1-2, pp. 133–145, 2009.

[3] F. Nasoz, C. L. Lisetti, and A. V. Vasilakos, "Affectively intelligent and adaptive car interfaces," *Information Sciences*, vol. 180, no. 20, pp. 3817–3836, 2010.

[4] R. R. Singh, S. Conjeti, and R. Banerjee, "An approach for real-time stress-trend detection using physiological signals in wearable computing systems for automotive drivers," in *14th IEEE International Intelligent Transportation Systems Conference, ITSC 2011*. Affiliation: Department of Electrical and Electronics Engineering, Birla Institute of Technology and Science (BITS) Pilani, Rajasthan, 333031, India; Affiliation: Department of Computer Science, Birla Institute of Technology and Science (BITS) Pilani, Raj, 2011, pp. 1477–1482.

[5] G. Chanel, C. Rebetez, M. Bétrancourt, and T. Pun, "Emotion assessment from physiological signals for adaptation of game difficulty," *IEEE Transactions on Systems, Man, and Cybernetics Part A:Systems and Humans*, vol. 41, no. 6, pp. 1052–1063, 2011.

[6] K. Dedovic, R. Renwick, N. K. Mahani, V. Engert, S. J. Lupien, and J. C. Pruessner, "The Montreal Imaging Stress Task: Using functional imaging to investigate the effects of perceiving and processing psychosocial stress in the human brain," *Journal of Psychiatry and Neuroscience*, vol. 30, no. 5, pp. 319–325, 2005.

[7] V. V. Lazarev, "The relationship of theory and methodology in EEG studies of mental activity," *International Journal of Psychophysiology*, vol. 62, no. 3, pp. 384–393, 2006.

[8] C. Setz, B. Arnrich, J. Schumm, R. L. Marca, G. Tr, and U. Ehlert, "Using a Wearable EDA Device," vol. 14, no. 2, pp. 410–417, 2010.

[9] Q. Wang and O. Sourina, "Real-time mental arithmetic task recognition from EEG signals," *IEEE Transactions on Neural Systems and Rehabilitation Engineering*, vol. 21, no. 2, pp. 225–232, 2013.

[10] J. T. Cacioppo and L. G. Tassinary, "Inferring psychological significance from physiological signals." *The American psychologist*, vol. 45, no. 1, pp. 16–28, 1990.

[11] Y. Maki, G. Sano, Y. Kobashi, T. Nakamura, M. Kanoh, and K. Yamada, "Estimating subjective assessments using a simple biosignal sensor," *Proceedings - 13th ACIS International Conference on Software Engineering, Artificial Intelligence, Networking, and Parallel/Distributed Computing, SNPD 2012*, pp. 325–330, 2012.

[12] M. Azarnoosh, A. Motie Nasrabadi, M. R. Mohammadi, and M. Firoozabadi, "Investigation of mental fatigue through EEG signal processing based on nonlinear analysis: Symbolic dynamics," *Chaos, Solitons & Fractals*, vol. 44, no. 12, pp. 1054–1062, 2011.

[13] E. Wascher, B. Rasch, J. Sänger, S. Hoffmann, D. Schneider, G. Rinkenauer, H. Heuer, and I. Gutberlet, "Frontal theta activity reflects distinct aspects of mental fatigue," *Biological Psychology*, vol. 96, no. 1, pp. 57–65, 2014.

[14] W. Klimesch, "EEG alpha and theta oscillations reflect cognitive and memory performance: a review and analysis." *Brain research. Brain research reviews*, vol. 29, no. 2-3, pp. 169–195, 1999.

[15] A. Gevins, M. E. Smith, L. McEvoy, and D. Yu, "High-resolution EEG mapping of cortical activation related to working memory: Effects of task difficulty, type of processing, and practice," *Cerebral Cortex*, vol. 7, no. 4, pp. 374–385, 1997.

[16] A. Gevins, M. E. Smith, H. Leong, L. McEvoy, S. Whitfield, R. Du, and G. Rush, "Monitoring working memory load during computer-based tasks with EEG pattern recognition methods." *Human factors*, vol. 40, no. 1, pp. 79–91, 1998.

[17] T. Fernández, T. Harmony, M. Rodríguez, J. Bernal, J. Silva, A. Reyes, and E. Marosi, "EEG activation patterns during the performance of tasks involving different components of mental calculation." *Electroencephalography and clinical neurophysiology*, vol. 94, no. 3, pp. 175–182, 1995.

[18] T. Gruber, M. M. Müller, A. Keil, and T. Elbert, "Selective visual-spatial attention alters induced gamma band responses in the human EEG," *Clinical Neurophysiology*, vol. 110, no. 12, pp. 2074–2085, 1999.

[19] M. M. Monge, I. Gomez, and A. Molina, "Stress and heart rate : significant parameters and their variations Article Type : original article," *Exp Clin Cardiol*, vol. 20, no. 8, pp. 3509–3517, 2014.

[20] C. D. Spielberger, R. L. Gorsuch, P. R. Lushene, P. R. Vagg, and A. G. Jacobs, *Manual for the State-Trait Anxiety Inventory (Form Y)*, 1983.

[21] B. Hjorth, "EEG analysis based on time domain properties," pp. 306–310, 1970.

Capítulo 5

Resumen, conclusiones y líneas futuras

Las interfaces HCI y PC basadas en bioseñales constan de 3 fases: la captación de los datos, procesamiento y actuación sobre el sistema. El trabajo de esta tesis está centrado en el bloque de procesamiento de la información registrada por los electrodos.

La naturaleza heterogénea de las bioseñales implica diferentes técnicas de captación y procesamiento para destacar y detectar aquellos elementos que son útiles para el objetivo que se busca. Para interfaces HCI, las señales deben se susceptibles de ser modificadas según la voluntad del individuo, destacando los transitorios asociados a estas acciones y minimizando aquellos elementos que puedan interferir negativamente, mientras que para PC los datos deben de contener información relativa al estado emocional del sujeto.

El procesamiento de los datos es un elemento esencial para obtener unos resultados satisfactorios. A lo largo de la presente tesis se han expuesto dos técnicas de procesamiento basadas en la aplicación de envolventes inferiores, para eliminar o destacar transitorios en forma de campanas cóncavas/convexas de las señales EOG y ECG, y se han analizado las variaciones de las mismas junto a los datos de EEG ante situaciones de estrés y control de un teclado virtual.

En lo referente a los datos de EOG:

1. Se ha desarrollado una nueva técnica para el filtrado de pestañeos y sobredisparos, así como una versión en tiempo real.

2. Los resultados se han comparado con un filtro de mediana de 300ms, al ser uno de los más usados por su simplicidad, capacidad de conservar las pendientes de los transitorios y reducción de artefactos. No obstante, su eficacia en la eliminación de pestañeos y sobredisparos se reduce considerablemente con la duración de éstos, con parpadeos situados en torno a una sacada o con una secuencia de pestañeos.

3. El procesamiento de datos EOG logra resultados notablemente mejores que el filtro de mediana (>97% de reducción frente al 40% en el peor de los casos), viéndose menos afectado por la duración de los parpadeos y sobredisparos.

4. La relación señal-ruido obtenida es superior a 10dB.

5. Las pendientes de los transitorios asociados a las sacadas se ven reducidas, cosa que no se observa con el filtro de mediana.

6. La aplicabilidad en interfaces HCI basadas en sacadas está limitada a periodos de fijaciones superiores a 500ms, debido a la atenuación de las pendientes de las sacadas que acontece con este procedimiento, lo que podría afectar negativamente a los sistemas HCI y los clasificadores de tareas.

7. La alta capacidad de la técnica de extraer los pestañeos facilita que éstos puedan emplearse en HCI. Únicamente se precisa de un proceso adicional que permita diferenciar entre parpadeos y sobredisparos.

8. Los resultados obtenidos por la implementación en tiempo real son similares a los obtenidos por la version offline. No obstante, las pendientes de las sacadas se ven más atenuadas.

9. Los sistemas HCI, como el descrito en Merino et al (2010b), pueden reducir su complejidad, al no tener que considerar estas interferencias.

10. Se ha desarrollado un modelo de la señal EOG que permite valorar los resultados de la técnica presentada en este documento. Además puede ser usada para validar otros procesamientos, como por el ejemplo el descrito en Merino et al (2010b).

En lo referente a los datos de ECG:

1. Se ha desarrollado una nueva técnica para la detección de los complejos QRS, así como una versión en tiempo real.

2. La técnica no requiere establecer ningún parámetro, al contrario de otras técnicas en las que hay que definir umbrales iniciales de decisión fijos/adaptativos o realizar sesiones de entrenamiento.

3. Los resultados obtenidos por ambas versiones son similares, con una sensibilidad, predicción positiva y precisión superiores al 99.7%.

4. La precisión en la detección del máximo de la onda R, y por tanto en el cálculo de los segmentos RR, es muy alta. La desviación modal en la localización es 0 (aproximadamente el 78% de los complejos), y el intervalo [-8, +8]ms recoge el 99.89% de éstas.

5. La carga computacional obtenida de los datos experimentales es lineal.

6. El procesamiento es robusto respecto a la longitud del buffer, obteniéndose un alto grado de similitud entre los datos de los expertos y

los generados por la técnica desarrollada en esta tesis. Asimismo, se observa una pequeña mejora en el rendimiento cuando la longitud de la ventana es superior a 1.05 segundos.

7. Se ha evaluado el efecto de dos contextos diferentes sobre diversos parámetros, observando variaciones significativas. Así, es posible diferenciar entre situaciones en la que el sujeto está relajado, sin realizar ninguna actividad relevante, frente a situaciones de estrés o que requieren una mayor atención e interacción por su parte, como son tareas de aritmética/memoria o durante la escritura de un texto con interfaces HCI basadas en EMG y EOG.

8. Los parámetros Mrr, pNN50 y HF son los que mejor marcan las modificaciones causadas por el nivel de estrés inducido y las actividades de aritmética y memoria.

9. El uso de teclados virtuales basados en escaneo y selección por eventos usando EOG y EMG producen modificaciones significativas en el ECG que pueden ser usadas para adaptar el comportamiento de ésta al estado del usuario (frustración/fatiga).

Por último, las modificaciones que acontecen en el EEG cuando se someten a los sujetos a actividades cognitivas bajo estrés reflejan que:

1. El lóbulo frontal (posiciones F) concentra los principales cambios asociados a las tareas realizadas.

2. El número de parámetros afectados por la acción de memorizar es mucho mayor que los afectados por realizar cálculos aritméticos.

3. Al contrario de lo que ocurre con los datos de ECG, las características del EEG que se comportaron según lo previsto no reflejaron un efecto a causa del estrés. De manera que, 4 minutos de tarea es suficiente para distinguir entre reposo y actividad, pero insuficiente ante situaciones estresantes. Asimismo, hay que considerar que este hecho se puede deber a un efecto de acomodación en los sujetos.

4. Las variaciones inducidas por la tarea aritmética muestran mayoritariamente un ascenso durante la actividad frente a los reposos.

5. La tarea de memoria produce, en general, un incremento de los parámetros en las posiciones frontales, observándose un comportamiento inverso entre las bandas θ y β.

Las técnicas desarrolladas tienen definidas una implementación online, lo que permite su uso en sistemas de tiempo real. Así, pueden ser usadas en interfaces HCI y/o en sistemas que modifiquen su comportamiento en

función del estado emocional del individuo. Es común que las interfaces PC usen varias bioseñales para determinar el estado emocional del sujeto. Junto a la información extraída de los datos de ECG y EEG, se puede obtener la duración de las sacadas, el ritmo de parpadeos y su anchura, con el objetivo de detectar somnolencia, concentración, estrés y/o nivel de excitación del sujeto, pudiéndose modificar el comportamiento de una aplicación en función de cómo estos parámetros varíen.

Esta tesis se ha enfocado en tres bioseñales, dado el amplio espectro de alternativas existentes. De esta manera, una línea de ampliación sería el estudio de otras señales como EMG, presión sanguínea, actividad electrodermal, etc., en interfaces HCI y PC, tratando de dotar al sistema de la inteligencia suficiente para detectar las acciones voluntarias del usuario y ser capaz de adaptarse a su estado emocional. Por ejemplo, adaptar la velocidad de escaneo de un teclado virtual según el nivel de frustración del sujeto, de manera que si la velocidad de escaneo no permite al usuario seleccionar la opción que desea, éste se frustrará, con lo que se disminuirá la velocidad de barrido para que tenga tiempo suficiente de poder seleccionar la opción que busca. Para ello, habrá que analizar qué parámetros de las diferentes bioseñales marcan mejor los cambios ante diferentes contextos, estudiar y/o desarrollar técnicas de procesamiento que permitan reducir las interferencias que perjudiquen la extracción correcta de las características, y destacar aquellos cambios que sean ventajosos para el objetivo deseado.

Por otro lado, el desarrollo del módulo de actuación no ha sido detallado en esta tesis, quedando pendiente su especificación. Por ello, habrá que estudiar cuáles son las mejores técnicas a la hora de determinar las acciones a realizar, ya sea mediante redes neuronales, support vector machine, gaussian mixture model, lógica difusa u otros algoritmos que permitan clasificar la actividad del sujeto y su estado emocional.

Anexo A

A method of EOG signal processing to detect the direction of eye movements

A Method of EOG Signal Processing to Detect the Direction of Eye Movements

Manuel Merino, Octavio Rivera, Isabel Gómez, Alberto Molina, Enrique Dorronzoro
Electronic Technology Department.
University of Seville.
Seville, Spain.
manmermon@dte.us.es; octavio@dte.us.es; igomez@us.es; almolina@us.es; enriquedz@dte.us.es

***Abstract*— In this paper, a signal processing algorithm to detect eye movements is developed. The algorithm works with two kinds of inputs: derivative and amplitude level of electrooculographic signal. Derivative is used to detect signal edges and the amplitude level is used to filter noise. Depending of movement direction, different kinds of events are generated. Events are associated with a movement and its route. A hit rate equal to 94% is reached. This algorithm has been used to implement an application that allows computer control using ocular movement.**

Keywords: computer control; EOG signal processing: handicapped.

I. INTRODUCTION

Development of interfaces adapted to the user physical skills is necessary in some situations where users have different diseases. In most cases, some residual user movements are used to interact with these interfaces. Biosignals are useful to detect these movements, such as electrooculography (EOG) or electromyography (EMG) that are used in [1], where the aim is handled a computer through event and a virtual keyboard. An algorithm to manage the computer mouse based on EOG signal is discussed in [2]. Also the EOG signal has been used to handle a wheelchair [3].

In other cases, interfaces do not require user's movement. This kind of interfaces is based on the concept brain computer interaction (BCI), where electroencephalography is used. A system to type text based on the P300 paradigm is described in [4, 5] is described, while Mattiocco et al. described how is possible move a cursor through the mu-rhythm paradigm [6].

This paper describes an algorithm for processing EOG signal that allows the extraction of features in it to detect the direction of eye movement. This is separated in seven parts. The main properties of EOG signal are described in Section II. Section III focuses the preprocessing summary. The algorithm to detect the direction of eye movement is established in the Section IV. The next Section describes the tests realized. Finally, in Sections VI and VII are shown the results of tests and the conclusions.

II. FOUNDATIONS

EOG signal is based on electrical potential difference between the cornea and retina when eye movement is realized. The amplitude of this signal ranges between [50, 3500] μV and its frequency components go from 0 to 100Hz. On the other hand, the EOG signal is interfered by others, such as electroencephalography, electromyography, electrical network, speech, blink, etc. For these reasons, it is important the interference of noise is dimmed and the user is calm and relaxed.

An eye movement is related to a rise/fall of EOG signal amplitude. Two voltage levels, "low" and "high", can be defined in order to distinguish between a deliberate movement and a non deliberate one. Both, the "low" level and the "high" level, can be identified by a threshold value defined by equation 1, where "value" represents an absolute value of amplitude.

$$\text{classify(value)}\begin{cases}\text{value} \geq \text{Amplitude}_{\text{Threshold}} \cdot \textit{Tolerance} \rightarrow \textit{High} \\ \text{value} < \text{Amplitude}_{\text{Threshold}} \cdot \textit{Tolerance} \rightarrow \textit{Low}\end{cases} \quad (1)$$

In general, an event is made using two eye movements, one is used to generate the event and the other one is used to return a neutral position. Both movements are the same direction, but their senses are opposite. During these movements, three different stages can be recognized using EOG signals: the signal amplitude rises from the "low" level to the "high" level, then it stabilizes in the "high" level and finally, it fades until the "low" level (Figure 1).

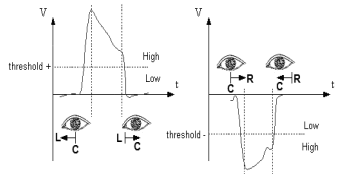

Figure 1. Eye movement components.

In this way, four different components could be identified: initial edge, final edge, area between edges and errors. This fact allows removing noise from the signals. For example, although the three stages are presented during a blink, the width of area between edges is much smaller. In this sense, a timer can be used in order to classify and remove blinks. A pulse is classified as a blink if the width of this area is smaller than 250ms.

III. PRE-PROCCESS

EOG signal information is mainly contained in low frequencies. For this reason a bandpass filter with a range

between 0.1 and 30 Hz is applied and a sample rate of 128 Hz. Then an average filter is applied in order to remove some noise components.

Eye movements are detected using an algorithm based on edge. The edges are detected through the derivative of the EOG signal. This one is calculated using discrete values of signal amplitude (eq. 2). So, two values are used, one represents the preceding value of amplitude (n samples before), e(t – n), and the other one represents the current value, e(t).

$$e'(t) = e(t) - e(t-n) / n \in N, n > 1 \quad (2)$$

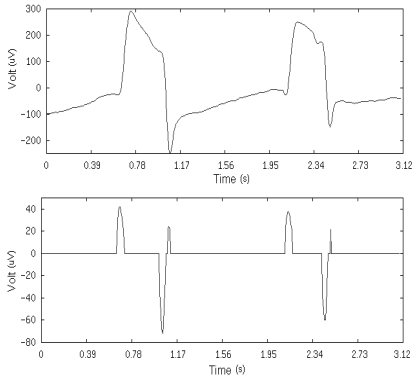

Figure 2. Filter Processing Result. (a) EOG signal. (b) Derivative.

A filter is applied to the signal derivative in order to remove some components without information. In Figure 2, the two steps of preprocessing are shown: first a smoothing filter is applied and in a second phase derivative is calculated.

IV. PROCCESS

Next, the algorithm to detect the direction of eye movements is described. The section is separated in two parts: the initial edge and final edge of them.

A. Procedure

A complex algorithm can be used to control the process. A flowchart representing the part of this algorithm associated with a pulse having positive amplitude is shown in Annex I. The states are described in table I.The input of this algorithm is the derivative of EOG signal that can have three different values: a value greater than 0, a value smaller than 0 and a value equal to 0. The values that are not equal to 0 are related to initial and final edges of a pulse having positive amplitude. The value equal to 0 is associated with the area between edges (no-activity area). State transitions are led by the values of signal amplitude at current moment and previous one, and by the value of the signal derivative.

TABLE I. STATES FROM A PULSE HAVING POSITIVE AMPLITUDE.

State	Description
INITIAL	Waiting an initial edge.
InitialEdge+	Initial edge detects.
Error-	Error.
FinalEdgeWait-	Waiting final edge.
FinalEdge-	Final edge detects.

The process starts in the INITIAL state. In this one, a non-zero input is waited. As mentioned above, this value can be related to an initial edge or a final edge. Next, the behaviour is described in detail. First, the part of algorithm associated with an initial edge is shown. Then, a final edge is considered.

B. Initial Edge

When an eye movement is started (Figure 3) the value of signal amplitude changes from the "low" level to the "high" level, obtaining a value of signal derivative that is greater than 0. At this moment, a transition from INITIAL state to InitialEgde+ state occurs. When area between edges is reached (derivative equal to 0), a transition to FinalEdgeWait- happens. It is necessary to consider some possible disturbances that could occur. Next, these ones are described.

Figure 3. Initial edge.

1) Horizontal initial edge

In this situation a small area where the slope of signal is brought nearer to 0 is presented (Figure 4). Therefore two peaks are shown in the signal derivative. In this case there are two options:

a) The maximum value of signal amplitude in this area is lower than the value of set threshold. In this situation the first peak is rejected because the "high" level is not reached yet, so the machine is in INITIAL state. However the second one happens when the "high" level has been reached, therefore the transition from INITIAL state to InitialEdge+ state occurs.

b) The maximum value of signal amplitude in this area is higher than the value of set threshold. In this situation a transition from INITIAL state to InitialEdge+ state occurs because of the first peak. After that, the value of input is equal to 0 due to the horizontal noise and this fact causes a transition to FinalEdgeWait- state. When the second peak arrives, the preceding value, e(t – n), is set to the "high" level, so although the slope of signal derivative is positive, a change from the "low" level to the "high" level does not occur, this means a state transition does not occur. Therefore the second peak is rejected.

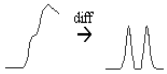

Figure 4. Horizontal initial edge.

On the other hand, the effects of horizontal initial edge can be attenuated because the signal derivative is calculated by subtracting two non-consecutive components as mentioned above.

2) Overlapped amplitude peak in the initial edge

In this case three peaks are shown in the signal derivative (Figure 5). The behaviour is similar to the one shown in the previous section. If the amplitude of first peak does not overcome the set threshold, then a transition does not occur and the second peak is rejected. In this situation a transition from INITIAL state to InitialEdge+ state occurs when the "high" level has been reached.

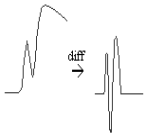

Figure 5. Overlapped amplitude peak in the initial edge.

On the other hand, if the amplitude of first peak overcomes the set threshold, then a transition to InitialEdge+ state occurs. When the second peak is received a transition to Error- state happens, meaning that it is probably an error. In this situation, the third peak tries to generate a transition to InitialEdge+ state; however that is only possible if the amplitude of this peak overcomes the "high" level.

3) Single edge

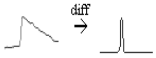

Figure 6. Single edge.

A single edge is an amplitude step like is shown in Figure 6. This causes a transition to InitialEdge+ state if the "high" level has been reached; else the single edge is rejected without effects. After the rise, the signal amplitude falls down. When the derivative is equal to 0, a transition to FinalEdgeWait- state occurs. In this situation two cases are studied: the single edge is followed by a pulse having positive amplitude; and the single edge is followed by a pulse having negative amplitude (Figures 7-8).

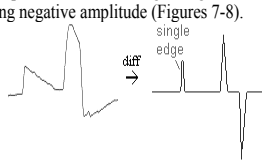

Figure 7. Single edge followed by a pulse having positive amplitude.

In the first case (Figure 7), the effect of the single edge depends on the value of preceding item, e(t – n):

a) If e(t – n) is associated to the "high" level: this means that the fall of single edge is not quick enough to reach the "low" level. So, the ascending slope of following pulse does not take effects, but the state of machine is correct. However, timer is reset when a transition to InitialEdge+ state is done, and this occurs with the single edge. Therefore, the timer value is not adequate and a misinterpretation could be made, e. g. if the second pulse is related to a blink and the timer value would be greater than 250 ms. This case is known as crest in the final edge which is described below.

b) If e(t – n) is associated to the "low" level: this means that the fall of single edge is relatively quick. In this case, a transition to InitialEdge+ state could be done when e(t) is related to the "high" level.

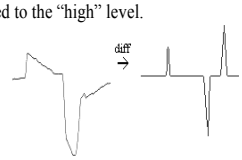

Figure 8. Single edge followed by a pulse having negative amplitude.

In the second case (Figure 8), the sign of initial edge is different to one of single edge. A transition to FinalEdge- state could be done. However, it is not an EOG movement. So before the transition occurs, it is necessary to check the preceding and current amplitude value.

On the other hand, a transition from FinalEdge- state to INITIAL state occurs when the value of signal derivative is equal to 0.

4) Abrupt fall before initial edge

Two examples of abrupt falls are shown in the Figure 9. In both cases, if the threshold value in negative case is reached then a transition from INITIAL state to InitialEdge- state occurs.

When the fall is abrupt as one that is shown in Figure 9.a, a transition to Error+ state occurs because the sign of second peak derivative is opposite to the one of first peak. Then, the area between edges is reached and the value of derivative is equal to 0. In such situation, two cases are possible: the pulse is a single peak of amplitude, leading to a transition to INITIAL state, or the second peak is a real initial edge. So if the current amplitude value is the "low" level (for a positive case), then a transition to INITIAL state (it is a single peak of amplitude) occurs. In the other case, a transition to FinalEdgeWait- state occurs.

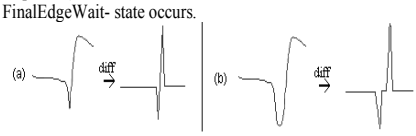

Figure 9. Abrupt fall before initial edge. (a) Pointed. (b) Round.

When the fall is not abrupt as one that is shown in Figure 9.b, the behaviour is similar to one that is shown when a blink is done. However, when the area between edges is reached, a transition from FinalEdge+ state to INITIAL state occurs. If current amplitude value is related to the "high" level, then a transition to FinalEdgeWait- state occurs. In other case, a transition to INITIAL state occurs.

5) Single peaks of amplitude

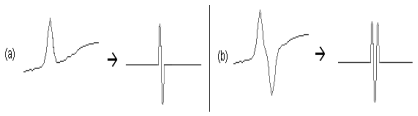

Figure 10. Single peaks of amplitude. (a) Even peaks. (b) Odd peaks.

There are two different cases:

a) Even number of peaks in the signal derivative (Figure 10.a). The final state is Error- when the processing of all peaks is completed.

b) Odd number of peaks in the signal derivative (Figure 10.b). The final state is Error- when the last peak is received. At this moment, the current amplitude value is checked in order to detect an overlapped amplitude peak. However, in this case a transition from Error- state to InitialEdge- state does not occur because the current amplitude value is related to the "low" level.

6) Crest in the initial edge

A crest is a rise of amplitude in the end of an edge. If this one is rounded (Figure 11.a) the pulse derivative is similar to one of a blink. However, the current amplitude value is related to the "high" level in the second peak, so there is not a state transition, i.e., the current state is FinalEdgeWait-. The problem is solved.

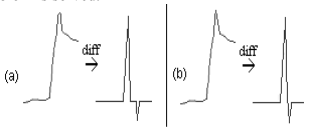

Figure 11. Crest in the initial edge. (a) Round. (b) Pointed.

On the other hand, if the crest is pointed (Figure 11.b) the signal derivative has an even number of peaks; such situation is similar to one shown in previous section. However, the pulse is a real movement. So, first it is necessary to check if the current amplitude value is related to the "low" level. In the considered case, the current amplitude value is related to the "high" level, and therefore a transition to FinalEdgeWait- state occurs. In other case, it is a single peak and a transition to INITIAL state occurs.

C. Final Edge

The end of an eye movement leads to a falling edge due to change from the "high" level to the "low" level. A negative peak is shown in the signal derivative. This fact can be used to detect the end of an EOG movement (Figure 12).

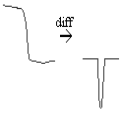

Figure 12. Final edge.

1) Horizontal final edge

This disturbance is similar to one presented in subsection 1, but in final edge. As then, there are two options:

a) The maximum value of signal amplitude in this area is higher than the value of set threshold. Both, the current and previous amplitude value, are related to the "high" level, so the state does not change. A transition to FinalEdge- state occurs when the next peak arrives, because the preceding amplitude value is related to the "high" level and the current amplitude value is related to the "low" level. So the pulse is associated with an EOG movement if the duration of pulse is greater than 250ms. In other case it is associated with a short pulse (noise).

b) The maximum value of signal amplitude in this area is lower than the value of set threshold. The current amplitude value is related to the "low" level in the first peak of signal derivative, and the preceding amplitude value is related to the "high" level, so a transition to FinalEdge- state occurs, obtaining an output value equal to 1 if the width of pulse is adequate. Now, a transition to INITIAL state occurs because of horizontal noise. Finally, the second peak could be identified as an initial edge. However, current amplitude value is related to the "low" level and therefore, a transition does not occur.

2) Overlapped amplitude peak in the final edge

This disturbance is shown in Figure 13. A single peak of amplitude is overlapped with the final edge of the pulse. An odd number of peaks are presented in the signal derivative. If the current value of amplitude of the first peak is related to the "high" level a transition does not occurs. The next two peaks are identified as a crest in the final edge which is processing using the method described in the next subsection.

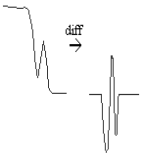

Figure 13. Overlapped amplitude peak in the final edge.

On the other hand, if the current value of amplitude of the first peak is related to the "low" level a transition to FinalEdge- state occurs. This state is kept until the values of signal derivative are equal to 0. So, the next two peaks are filtered without problems.

3) Crest in the final edge

There are two cases in this disturbance that are shown in Figure 14. The processing is the same in both cases. A transition from FinalEdgeWait- state to InitEdge+ state does not occur when the first peak of signal derivative is received because the current and preceding amplitude values are the same (the "high" level), so the process is in FinalEdgeWait- state. Then, a transition to FinalEdge- state occurs when the second peak is received due to the current amplitude value is related to the "low" level and the preceding amplitude value is related to the "high" level.

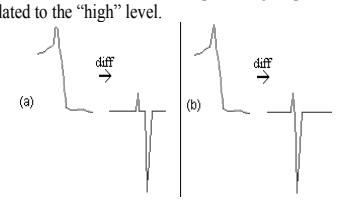

Figure 14. Crest in the final edge. (a) Round. (b) Pointed.

V. EXPERIMENT DESIGN

The algorithm was tested through different kinds of tests. Next, these tests are described.

A. Participants

Some tests were made to the system. Three users without visual disabilities between 25 and 42 years old participated on these trials.

B. Tests

We used BCI2000 [7] and the amplifier gUSBamp of g.tec [8]. The EOG signal was recorded through four sensors of Ag/AgCl placed around the eyes (Figure 15). The difference between the sensors 1 and 3 was used to register the vertical eye movements, and the difference between sensors 2 and 3 was used to register the horizontal eye movements.

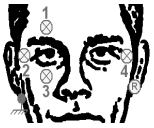

Figure 15. Sensors.

Four targets were placed around the computer screen (Figure 16). Users were asked to move their eyes from central position (C) to one of the extreme side (right (R), left (L), up (U) or down (D)) and then the eyes returned the initial position (C). This is shown in Figure 17.

Six tests were completed by each user. First of them was used to calibrate the system. In this one 12 movements were done (R - U- L - D - R - U- L - D - R - U- L - D). The users were asked to move 6 times their eyes in a unique direction in the followed four tests. In the last one, they had to move their eyes in different directions that were set previously.

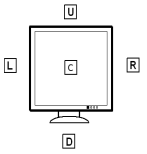

Figure 16. Targets of eyes movements.

Figure 17. Eye movements.

VI. RESULTS

Test results are shown in Table II. Average hit rate is of 94.11%. This high hit rate shows that the people with disability could handle a computer through events detected for the system when he/she does an eye movement.

TABLE II. TEST RESULTS.

Character	Correct (%)
Individual 1	100
Individual 2	95.83
Individual 3	86.49

VII. CONCLUSION AND FUTURE WORK

A system used to detect eye movement based on the EOG signal is proposed. So the system objective is to detect when a movement of eyes is realized and the route described. The main goal of this algorithm is reduce both initial calibration and detection errors. In this form, events generated for the system when an eye movement is done can be used to handle computer applications causing as less fatigue as possible to the user. This allows handicapped people are able to access the computer in an easy and comfortable form. So, in the future, we will use the EOG signal as communication interface to handle an application based on augmentative and alternative communication. Also, we will detect the stress and fatigue of user in order to use these results in ambient living application.

ACKNOWLEDGEMENTS

This project has been carried out within the framework of a research program: (p08-TIC-3631) – Multimodal Wireless interface funded by the Regional Government of Andalusia.

REFERENCES

[1] Hari Singh Dhillon, Rajesh Singla, Navleen Singh Rekhi, and Rameshwar Jha. "EOG and EMG Based Virtual Keyboard: A Brain-Computer Interface". Computer Science and Information Technology, 2009. ICCSIT 2009. 2nd IEEE International Conference on. 2009.

[2] B. Estrany, P. Fuster, A. Garcia and Y. Luo. "EOG signal processing, and analysis for controlling computer by eye movements". PETRA'09, June 2009.

[3] Yathunanthan, S. Chandrasena, L.U.R. Umakanthan, A. Vasuki, and V. Munasinghe, S.R. "Controlling a Wheelchair by Use of EOG Signal". Information and Automation for Sustainability, 2008. ICIAFS 2008. 4th International Conference on. 2008 .

[4] Chang S. Nam, Yongwoong Jeon, Yuequing Li, Young-Joo Kim, and Hoon-Yong Yoon. "Usability of the P300 Speller: Towards a More

Sustainable Brain-Computer Interface". International Journal on Human-Computer Interaction, Vol. 1, No. 5. 2009.

[5] D.S. Klobassa,T.M. Vaughan, P. Brunner, N.E. Schwartz, J.R. Wolpawa, C. Neuper, and E.W. Sellers. "Toward a high-throughput auditory P300-based brain–computer interface". Clinical Neurophysiology. 2009.

[6] M. Mattiocco, F. Babiloni, D. Mattia, S. Bufalari, S. Sergio, S.Salinari, M.G. Marciani, and F. Cincotti. "Neuroelectrical source imaging of mu rhythm control for BCI applications". Engineering in Medicine and Biology Society, 2006. EMBS '06. 28th Annual International Conference of the IEEE p.980-983. 2006.

[7] Gerwin Schalk, Member, IEEE, Dennis J. McFarland, Thilo Hinterberger, Niels Birbaumer, and Jonathan R. Wolpaw. "BCI2000: A General-Purpose Brain-Computer Interface (BCI) System". IEEE Transactions on Biomedical Engineering, vol. 51, NO. 6, p. 1034-1043. June 2004.

[8] Available from: <http://www.gtec.at/content.htm> 13.04.2010.

ANNEX I: COMPLETE FLOWCHART OF A PULSE HAVING POSITIVE AMPLITUDE

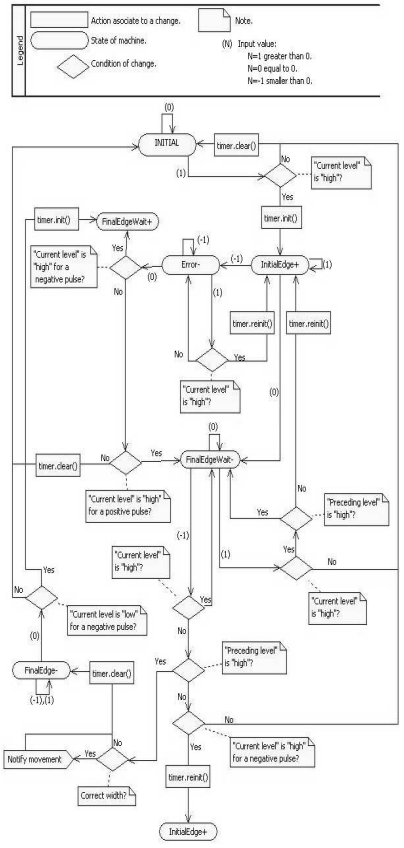

Anexo B

Customizable Software Interface for Monitoring Applications

Customizable Software Interface for Monitoring Applications

Manuel Merino, Isabel Gómez, Octavio Rivera, and Alberto J. Molina

Electronic Technology Department, University of Seville,
Avd. Reina Mercedes s/n,
41012, Seville, Spain
{Manmermon,Octavio}@dte.us.es {igomez,almolina}@us.es
http://matrix.dte.us.es/grupoimyt/

Abstract. In this paper we propose an application based on virtual keyboard and automatic scanning to communicate with a PC and the others people. The aim users are the people with disabilities. A high degree of customization is possible in the software. So the user can selected the color of buttons, position of system on screen, the kind of scanning, timer, the interface of communication, etc. Five people without disabilities tested our system. The results of the tests show the application reduce the fatigue of user and increased the text entry rate.

Keywords: interface, prediction system, control system, disability.

1 Introduction

Communication is a fundamental quality for human beings. People use different ways of Communication in their diary life. Communication skills are necessary in order to get a social integration. Nevertheless degenerative diseases, accidents, psychological disorders and others reason can make difficult the human communication. So, according to the Eurostat [1], the total population in Europe was 362 million in 1996 which 14.8% of the population between 6 and 64 years old have physical, psychological or sensorial disabilities. Therefore, assistive and adapted systems have to be developed. The aim of these ones is to help users in their diary tasks, letting them to live in a more comfortable way.

The development of a general purpose system is a complex task because every people have different skills and preferences. These systems have a degree of flexibility and customizable. However the limitations of these systems are heightened when people have severe disabilities.

Nowadays there are several tools and devices that allow disabled people to use specific applications. This paper describes a system located among three research main areas: Human-Computer Interface (HCI), Augmentative and Alternative Communication (AAC) y Assistive Technology (AT). A user can interact with this system using keyboard-handled software applications. An appropriate device which is adapted to user needs is only required to interact with it. The developed system can be

K. Miesenberger et al. (Eds.): ICCHP 2010, Part I, LNCS 6179, pp. 147–153, 2010.

handled with several kinds of input devices which increases the number of potential users. In our tests are performed using electromyography signal (EMG).

2 Related Work

Development of interfaces adapted to the user physical skills is necessary because the users can have different diseases. In most cases, some residual user movements are required to interact with these interfaces, like adapted switches or eye-tracker. Electric biosignals are used in some of these ones, such as electrooculography [2] or electromyography [2]. There exists another kind of interfaces that a user movement is not required to interact with it, like one is used in Brain Computer Interaction (BCI) [3]. This one is based on detecting some electric biosignals (electroencephalogram).

In addition to these input interfaces, an application to make possible the interaction between user and computer/PDA is necessary. Text entry is one of the most common features of this kind of applications. The main aim must be to reduce the numbers of user actions when users have some physical disabilities. To get this goal, prediction systems are used, like character prediction, word prediction or sentence prediction. Examples of this kind of applications are shown in [4, 5]. Both applications are virtual keyboards (VKs). First one [4] is a commercial application based on Windows Operative System. Different kinds of extended VKs can be selected but reduced VKs are not implemented. It uses an automatic scanning method and word prediction. On the other hand, the position of keys in the VK is not suitable to scan through column-rows or serial method. Prediction list length is setting to six words so it is not customizable. Configuration options (such as the color or size of buttons, position or size of application, etc.) cannot be changed by a handicapped.

Second one [5] is a fluctuating VK that uses a manual scanning method and character prediction. When a character is selected, the buttons around of this are changed based on the character prediction system. This property provokes the user fatigue is increased.

Dasher [6] is a different text input method using a character prediction. This one is based on a mouse pointer tracking system to select the wished character from a shown set. This is a text input system that allows a high rate character/minute. The selected text can be used by a voice synthesizer, but is not possible to send to another application. Also the operative system cannot be handled by this application.

3 Methodology

3.1 Software Description

The proposed application is an automatic scanning based VK using a prediction system. It runs on Windows XP and was implemented using Java 1.5. The prediction system requires a dictionary which is a database that was implemented using SQLite. Special features were implemented using C# 2.0.

Our software works like a daemon, it means that it is always visible in foreground and never catches the focus (fig. 1). Different input events can be generated by user to

interact with the system. When an input event is received, it is processed by the Application Handler, and a set action is done depending on the state of the system. Computer applications can be handled by keyboard [7] and this software uses this fact. So, the selected action is send to Operative System like a real keystroke on a conventional keyboard, letting user to open/close computer applications, to send/receive e-mails, to browse the Internet, to enter texts, etc.

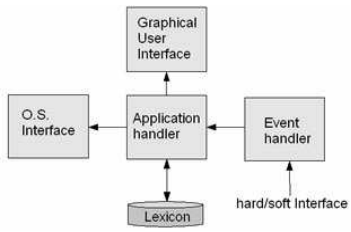

Fig. 1. Functional description

The Graphical User Interface (GUI) is composed of five different automatic scanning based VKs: a numeric VK (from 0 to 9), a punctuation mark VK, a command VK (including alt, shift, ctrl, enter, tab, f1, f2, etc., buttons), and an advanced command VK (this one can be customized setting on each button a sequence of commands, for example alt + f4, or alt + c), an application VK (is equivalent to start menu of Windows XP – fig. 3), and a letter VK (can be a reduced VK or an extend VK – fig. 2). Two alternatives have been implemented: a row-column scanning method or a serial scanning method.

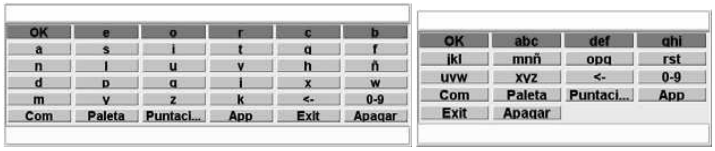

Fig. 2. GUI – Extend/reduced letter VK

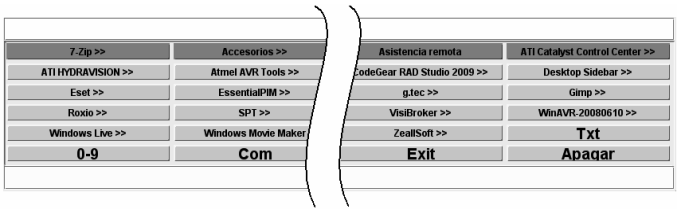

Fig. 3. GUI – Application VK

On the other hand, a personal VK can be defined by the user. This VK is based on an xml file and its structure is:

```
<teclado teclasPorFila="number of buttons in a row">
  <boton tipoBoton="button type" texto="text">
    <letra orden = "position"> letter </letra>
    ...
    <letra orden = "position"> letter </letra>
  </boton>
  <boton ...>
  ...
  </boton>
  ...
</teclado>
```

The maximum number of buttons in a row is indicated in the property *teclasPorFila* in <*teclado* ...>...</*teclado*>. The labels <*boton*...>...</*boton*> have two properties. One is *tipoBoton* that discriminates between letter, number, punctuation mark and command keys. The other property is *texto* that is used to descriptor text in the key. The last label is <*letra*...>*letter*</*letra*> where the *orden* indicates the position of the letter, number, command or punctuation mark.

Three text entry methods have been incorporated. One of them consists on a conventional text entry method. Characters of the wished word are entered one by one in this method. Other ones are word prediction systems. A study of different prediction systems is presented in [8, 9], in which we can check word prediction systems are the most commonly used. First of these ones is called NT and is only available when an ambiguous VK (more than one character per key) is used. NT is a modification of NT predictor system. When a key of VK is selected a new prediction list is made. In the new list, the words of the previous one whose characters match with those typed orderly so far are remained. Second one is called K-Word. In this method, first characters of the wished word have to be selected before a prediction is made. After that, K-Word predictor builds a list of suggestion using a k-gram algorithm with selected characters.

The user-application communication is realized by the user control interface. It has to be able to adapt dynamically to the user context. This dynamic adaptability and costumer of application are contained in the concept of plasticity [10]. Thus our application has been development to enable that the user personalizes the appearance of GUI, so the user can choose the color of scanned and no-scanned buttons, the color of button's text, the size of buttons, the position of application in the screen, the scanned time, selected/no-select special VK, configure special VK, select and configure prediction system, select the type of scanned system, etc. A configure application allows to personalize the properties described before. The options of the configure application are automatic scanning to allow to person with disability can personalize the software. When an option is chosen a VK is shown which allows the user selects the new value of the actual option.

Otherwise, two log files are generated by the application. These files can be used in research tasks. The user events are registered by one of them. The prediction words are stored by the other log file. This saves the selected prediction word and its different lists of prediction, the time, the number of automatic reset of system and the number

interaction by rows, columns and letters. The files allow study the advantages of a kind of VK and/or a prediction system.

3.2 User Control Interface

Three kinds of communication ports were designed: parallel/serial port and TCP/IP. In the future usb port will be added. These ports allow a lot different types of interface. At least an event has to be generated by the interface. Two different events are allowed. One is the selection event to select current option (mandatory) and the other is the change event to advance to next option (optional). These events are evaluated in [11, 12]. Events are distinguished based on time. The parallel port was tested by a stick switch based on the select event. The serial port was used by a button switch based on selection and change events and a microphone based on selection event. The TCP/IP was tested by EMG interface. In addition the system could be handled by control and/or shift button of conventional keyboard.

Any interface that generates input events based on user actions can be used to interact with this software. At the moment, it has been tested using different switches and an electromyography based device. The last one uses three electrodes placed on the user's arm. Hence, a movement of his/her hand can be detected and an adequate event can be generated. The signal processing procedure splits the electromyography signal on non-overlapping windows that are 100 samples width. An absolute value operation is applied on each window and the result is integrated. The signal is interpreted as a selection when obtained value is above a set threshold.

3.3 Procedure

Some trials focused on text input system have been done. Five users without disabilities between 25 and 35 years old participated in these trials. They had not used the application before. Results using conventional text entry, K-Word and NT prediction system are compared between each in order to obtain time savings. Also penalization time due to user errors is calculated. Maximum prediction list length is set to 14 words. The list of suggestions in K-Word predictor is displayed when user has selected three first characters of the wished word. The main objective of these trials is to entry text without mistakes. The application implements a functionality that let user to fix errors. Some tests with handicapped people must be done in the future.

4 Work and Results

The trial results were stored in two log files. Time measurements included increments due to penalization sources. These sources were: wrong character selections (in this case, time was required to set them); wrong word selections from prediction list; selections using more than one user input (users was not able to choose the desired row, column, letter or word); reset of system due to time out, etc. Besides time measurements, information about different types of mistakes can be found in the aforementioned log files.

Trial results are shown in tables 1 and 2. The table 2 shows the gain using the predictor systems. The K-Word predictor gain about text entry conventional is 27.58%,

which means a time saving of 192.537 seconds. So, the gain using NT predictor is 52.02% about text entry conventional, which is 353.04 seconds. On the other hand, NT predictor is 34.36% faster than K-Word.

Table 1. Times in text entry systems

User	KWord	NT	Conventional
1	*475.05*	*318.79*	*572.68*
2	*501.21*	*356.38*	*580.48*
3	*357.15*	*238.14*	*522.87*
4	*512.76*	*335.20*	*868.18*
5	*501.02*	*296.15*	*765.65*

Table 2. Gains of text entry systems

User	KWord vs. Conventional (%)	NT vs. KWord(%)	NT vs. Conventional (%)
1	*17.05*	*33.06*	*44.33*
2	*13.66*	*29.90*	*38.61*
3	*31.70*	*33.32*	*54.46*
4	*40.94*	*34.63*	*61.39*
5	*34.56*	*40.89*	*61.32*

5 Conclusion and Planned Lines of Research

It has been presented an application that is easy to use and it does not require any training. The operative system can be handled, and text can be written. It must be mentioned that users must have knowledge in handling computer using control keys of a standard keyboard. So, it is not operating system dependent, because it is based on Java.

All its possibilities are included in graphical interface that is shown permanently on the computer screen. The design of this application is flexible in respect of main keyboard displayed on screen and the used input signal. It is possible to change among several configurations of keyboard during execution time. Also, three different prediction systems have been implemented. Furthermore, the inputs which handle the software come from several devices (parallel port, serial port or TCP/IP).

On the other hand, the application is a research tool. Two log files are made. They both store information about a using session. Therefore, different kinds of results can be extracted, such as penalize due to wrong character selections, wrong word selections from prediction list, selections using more than one user input (users was not able to choose the desired row, column, letter or word), reset of system due to time out, etc.

Acknowledgements

This project has been carried out within the framework of a research program: (p08-TIC-3631) – Multimodal Wireless interface funded by the Regional Government of Andalusia.

References

1. Eurostat. Health Statistics. Luxembrourg: Office for Official Publications of the European communities (2002) ISBN: 92-894-3730-8, http://epp.eurostat.ec.europa.eu (Retrieved on December 2009)
2. Dhillon, H.S., Singla, R., Rekhi, N.S., Rameshwar, J.: EOG and EMG Based Virtual Keyboard: A Brain-Computer Interface. In: 2nd IEEE International Conference on Computer Science and Information Technology, ICCSIT 2009 (2009)
3. Nam, C.S., Jeon, Y., Li, Y., Kim, Y.-J., Yoon, H.-Y.: Usability of the P300 Speller: Towards a More Sustainable Brain-Computer Interface. International Journal on Human-Computer Interaction 1(5) (2009)
4. Wivik on-screen keyboard software, http://www.wivik.com/ (Retrieve on December 2009)
5. Merlin, B., Raynal, M.: Increasing Software Keyboard Key by Recycling Needless Ones. In: Assistive Technology from Adapted Equipment to Inclusive Environments - AAATE 2009, vol. 25, pp. 139–143 (2009) ISBN: 978-1-60750-042-1
6. Ward, D.J., Blackwell, A.F., MacKay, D.J.C.: Dasher - a Data Entry Interface Using Continuous Gestures and Language Models. In: UIST 2000 (2000), http://www.inference.phy.cam.ac.uk/dasher (Retrieve on December 2009)
7. Gómez González, I.M., Molina Cantero, A.J., Romero, O.R.: Multi Purpose Interface for Handling General Computer Applications. In: 9th European Conference for the Advancement of Assistive Technology in Europe (AAATE 2007), San Sebastián, España, pp. 7–8 (2007)
8. Garay-Vitoria, N., Abascal, J.: Text prediction: a survey. Univ. Access Inf. Soc. 4, 188–203 (2006)
9. Rivera, O., Molina, A.J., Gómez, I., Sánchez, G.: Evaluation of Unambiguous Virtual Keyboards with Character Prediction. In: Conference of the Association for the Advance of Assistive Technology in Europe (AAATE 2009), Florence, Italy, vol. 25, pp. 144–149 (2009) ISBN: 978-1-60750-042-1
10. Sendín, M., López Juan, M.: Contributions of Dochtomic View of plasticity to seamlessly embed accessibility and adaptivity support in user interfaces. In: Advances in Engineering Software, pp. 1261–1270 (2009)
11. Rivera, O., Molina, A.J., Gómez, I., Merino, M.: A Study of Two-inputs Scanning Methods to Enhance the Communication Rate. In: Conference of the Association for the Advance of Assistive Technology in Europe (AAATE 2009), Florence, Italy, vol. 25, pp. 132–137 (2009) ISBN: 978-1-60750-042-1
12. Rivera, O., Molina, A.J., Gómez, I.: Two-Input Based Procedures Using a Single Device. In: Conference of the Association for the Advance of Assistive Technology in Europe (AAATE 2009), Florence, Italy, vol. 25, p. 881 (2009) ISBN: 978-1-60750-042-1

Bibliografía

Agrawal S, Gupta A (2013) Fractal and EMD based removal of baseline wander and powerline interference from ECG signals. Computers in Biology and Medicine 43(11):1889–1899, DOI 10.1016/j.compbiomed.2013.07.030

Ahern GL, Schwartz GE (1985) Differential lateralization for positive and negative emotion in the human brain: EEG spectral analysis. Neuropsychologia 23(6):745–755, DOI 10.1016/0028-3932(85)90081-8

Akselrod S, Gordon D, Ubel FA, Shannon DC, Berger AC, Cohen RJ (1981) Power spectrum analysis of heart rate fluctuation: a quantitative probe of beat-to-beat cardiovascular control. Science (New York, NY) 213(4504):220–222, DOI 10.1126/science.6166045

Amirian I, Toftegård Andersen Lr, Rosenberg J, Gögenur I (2014) Decreased heart rate variability in surgeons during night shifts. Canadian journal of surgery Journal canadien de chirurgie 57(5):300–4

App E, Debus G (1998) Saccadic velocity and activation: development of a diagnostic tool for assessing energy regulation. Ergonomics 41(5):689–697, DOI 10.1080/001401398186856

Ashtiani B, Mackenzie IS (2010) BlinkWrite2 : An Improved Text Entry Method Using Eye Blinks. In: ETRA, vol 1, pp 339–346, DOI doi: 10.1145/1743666.1743742

Babloyantz A, Destexhe A (1988) Is the normal heart a periodic oscillator? Biological Cybernetics 58(3):203–211, DOI 10.1007/BF00364139

Bahill AT, Clark MR, Stark L (1975) Dynamic overshoot in saccadic eye movements is caused by neurological control signed reversals. Experimental neurology 48(1):107–122, DOI 10.1016/0014-4886(75)90226-5

Barea R, Boquete L, Mazo M, Lopez E, Bergasa L (2000) EOG guidance of a wheelchair using neural networks. Proceedings 15th International Conference on Pattern Recognition ICPR-2000 4, DOI 10.1109/ICPR.2000.903006

Benitez DS, Gaydecki PA, Zaidi A, Fitzpatrick AP (2000) A new QRS detection algorithm based on the Hilbert transform. Computers in Cardiology 2000 27:379–382, DOI 10.1109/CIC.2000.898536

Birnbaum GD, Birnbaum I, Birnbaum Y (2014) Twenty years of ECG grading of the severity of ischemia. Journal of electrocardiology 47(4):546–55, DOI 10.1016/j.jelectrocard.2014.02.003

Bocca ML, Denise P (2006) Total sleep deprivation effect on disengagement of spatial attention as assessed by saccadic eye movements. Clinical Neurophysiology 117(4):894–899, DOI 10.1016/j.clinph.2006.01.003

Bolton MP, Wytch R (1992) Mouse emulator for tetraplegics. Medical and Biological Engineering and Computing 30(6):665–668, DOI 10.1007/BF02446802

Bova SM, Giovenzana A, Signorini S, La Piana R, Uggetti C, Bianchi PE, Fazzi E (2008) Recovery of visual functions after early acquired occipital damage. Developmental Medicine and Child Neurology 50(4):311–315, DOI 10.1111/j.1469-8749.2008.02044.x

Bradley MM, Hamby S, Löw A, Lang PJ (2007) Brain potentials in perception: Picture complexity and emotional arousal. Psychophysiology 44(3):364–373, DOI 10.1111/j.1469-8986.2007.00520.x

Brown M, Marmor M, Vaegan, Zrenner E, Brigell M BMI (2006) ISCEV Standard for Clinical Electro-oculography (EOG) 2006. Documenta Ophthalmologica 113(3):205–212, DOI 10.1007/s10633-006-9030-0

Bulling A, Ward Ja, Gellersen H, Tröster G (2008) Robust recognition of reading activity in transit using wearable electrooculography. Lecture Notes in Computer Science (including subseries Lecture Notes in Artificial Intelligence and Lecture Notes in Bioinformatics) 5013 LNCS:19–37, DOI 10.1007/978-3-540-79576-6_2

Bulling A, Ward JA, Gellersen H, Tröster G (2009) Eye movement analysis for activity recognition. Proceedings of the 11th ... pp 41–50, DOI 10.1109/TPAMI.2010.86

Bulling A, Ward JA, Gellersen H, Tröster G (2011) Eye movement analysis for activity recognition using electrooculography. IEEE Transactions on Pattern Analysis and Machine Intelligence 33(4):741–753, DOI 10.1109/TPAMI.2010.86

Bustamante Ca, Duque SI, Orozco-Duque a, Bustamante J (2013) ECG delineation and ischemic ST-segment detection based in wavelet transform and support vector machines. Pan American Health Care Exchanges, PAHCE DOI 10.1109/PAHCE.2013.6568279

Cacioppo JT, Crites SL, Gardner WL, Bernston GG (1994) Bioelectrical echoes from evaluative categorizations: I. A late positive brain potential that varies as a function of trait negativity and extremity. Journal of personality and social psychology 67(1):115–125, DOI 10.1037/0022-3514.68.6.997

Caffier PP, Erdmann U, Ullsperger P (2003) Experimental evaluation of eye-blink parameters as a drowsiness measure. Tech. Rep. 3-4, DOI 10.1007/s00421-003-0807-5

Calvo RA, D'Mello S (2010) Affect detection: An interdisciplinary review of models, methods, and their applications. IEEE Transactions on Affective Computing 1(1):18–37

Cannon WB (1929) Bodily Changes in Pain, Hunger, Fear and Rage. DOI 10.1097/00007611-192909000-00037

Cardona G, Quevedo N (2014) Blinking and driving: the influence of saccades and cognitive workload. Current eye research 39(3):239–44, DOI 10.3109/02713683.2013.841256

Carretié L (1995) An ERP study on the specificity of facial expression processing. International Journal of Psychophysiology 19(3):183–192, DOI 10.1016/0167-8760(95)00004-C

Carretié Arangüena L, Iglesia Dorado J (2000) Psicofisiología. Fundamentos metodológicos. Pirámide

Chan FHY, Yang YS, Lam FK, Zhang YT, Parker Pa (2000) Fuzzy EMG classification for prosthesis control. IEEE Transactions on Rehabilitation Engineering 8(3):305–311, DOI 10.1109/86.867872

Chanel G, Rebetez C, Bétrancourt M, Pun T (2011) Emotion assessment from physiological signals for adaptation of game difficulty. IEEE Transactions on Systems, Man, and Cybernetics Part A:Systems and Humans 41(6):1052–1063, DOI 10.1109/TSMCA.2011.2116000

Chatrian GE, Lettich E, Nelson PL (1985) Ten percent electrode system for topographic studies of spontaneous and evoked EEG activity. American Journal Of Eeg Technology 25:83–92, DOI 10.1080/00029238.1985.11080163

Chen D, Vertegaal R (2004) Using Mental Load for Managing Interruptions In Physiologically Attentive User Interfaces. Extended Abstract of the 2004 Conference on human Factors in computing Systems, CHI 2004

Chikh MA, Ammar M, Marouf R (2012) A neuro-fuzzy identification of ECG beats. Journal of Medical Systems 36(2):903–914, DOI 10.1007/s10916-010-9554-4

Conjeti S, Singh RR, Banerjee R (2012) Bio-inspired wearable computing architecture and physiological signal processing for on-road stress monitoring. Proceedings - IEEE-EMBS International Conference on Biomedical and Health Informatics: Global Grand Challenge of Health Informatics, BHI 2012 25(C):479–482, DOI 10.1109/BHI.2012.6211621

Cooper R, Osselton JW (1980) EEG technology. Butterworths, London

Cooper R, Osselton JW, Shaw JC (1974) EEG Technology. Butterworth-Heinemann, London

Das M, Ari S (2013) Analysis of ECG signal denoising method based on S-transform. Irbm 34(6):362–370, DOI 10.1016/j.irbm.2013.07.012

Davidson RJ, Fox NA (1982) Asymmetrical brain activity discriminates between positive and negative affective stimuli in human infants. Science (New York, NY) 218(4578):1235–1237, DOI 10.1126/science.7146906

Dawson GD (1947) CEREBRAL RESPONSES TO ELECTRICAL STIMULATION OF PERIPHERAL NERVE IN MAN. Journal of neurology, neurosurgery, and psychiatry 10(3):134–40

De Gennaro L, Ferrara M, Urbani L, Bertini M (2000) Oculomotor impairment after 1 night of total sleep deprivation: A dissociation between measures of speed and accuracy. Clinical Neurophysiology 111(10):1771–1778, DOI 10.1016/S1388-2457(00)00393-X

De Gennaro L, Ferrara M, Curcio G, Bertini M (2001) Visual search performance across 40 h of continuous wakefulness: Measures of speed and accuracy and relation with oculomotor performance. Physiology and Behavior 74(1-2):197–204, DOI 10.1016/S0031-9384(01)00551-0

De Gennaro L, Devoto A, Lucidi F, Violani C (2005) Oculomotor changes are associated to daytime sleepiness in the multiple sleep latency test. Journal of Sleep Research 14(2):107–112, DOI 10.1111/j.1365-2869.2005.00444.x

Dedovic K, Renwick R, Mahani NK, Engert V, Lupien SJ, Pruessner JC (2005) The Montreal Imaging Stress Task: Using functional imaging to investigate the effects of perceiving and processing psychosocial stress in the human brain. Journal of Psychiatry and Neuroscience 30(5):319–325

Denney D, Denney C (1984) The eye blink electro-oculogram. The British journal of ophthalmology 68(4):225–228, DOI 10.1136/bjo.68.4.225

Dhillon H, Singla R, Rekhi NS, Jha R (2009) EOG and EMG based virtual keyboard: A brain-computer interface. In: Proceedings - 2009 2nd IEEE International Conference on Computer Science and Information Technology, ICCSIT 2009, pp 259–262, DOI 10.1109/ICCSIT.2009.5234951

Dohare AK, Kumar V, Kumar R (2014) An efficient new method for the detection of QRS in electrocardiogram. Computers and Electrical Engineering 40(5):1717–1730, DOI 10.1016/j.compeleceng.2013.11.004

Dorrian J, Tolley C, Lamond N, van den Heuvel C, Pincombe J, Rogers AE, Drew D (2008) Sleep and errors in a group of Australian hospital nurses at work and during the commute. Applied Ergonomics 39(5):605–613, DOI 10.1016/j.apergo.2008.01.012

Duchowski A (2007) Eye tracking methodology: Theory and practice. DOI 10.1007/978-1-84628-609-4

Duke M (1975) Isolated U wave-inversion in acute myocardial infarction. DOI 10.1159/000169720

Ekman P, Friesen WV, O'Sullivan M, Chan A, Diacoyanni-Tarlatzis I, Heider K, Krause R, LeCompte WA, Pitcairn T, Ricci-Bitti PE, Scherer K, Tomita M, Tzavaras A (1987) Universals and Cultural Differences in the Judgments of Facial Expressions of Emotion. Journal of personality and social psychology 53(4):712–717

El Kaliouby R, Picard R, Baron-Cohen S (2006) Affective computing and autism. DOI 10.1196/annals.1382.016

Electrophysiology TFotESoCtNAS (1996) Heart Rate Variability : Standards of Measurement, Physiological Interpretation, and Clinical Use. Circulation 93(5):1043–1065, DOI 10.1161/01.CIR.93.5.1043

Estrany B, Fuster P, Garcia A, Luo Y (2009) EOG signal processing and analysis for controlling computer by eye movements. In: Proceedings of the 2nd International Conference on Pervasive Technologies Related to Assistive Environments, pp 1–4, DOI 10.1145/1579114.1579132

Etevenon P (1986) Applications and perspectives of EEG cartography. In: Duffy FH (ed) Topographic mapping of brain electrical activity, Butterworths, pp 113–141

Ewing DJ, Neilson JM, Travis P (1984) New method for assessing cardiac parasympathetic activity using 24 hour electrocardiograms. British heart journal 52(4):396–402, DOI 10.1136/hrt.52.4.396

Fabbri M, Pizza F, Magosso E, Ursino M, Contardi S, Cirignotta F, Provini F, Montagna P (2010) Automatic slow eye movement (SEM) detection of sleep onset in patients with obstructive sleep apnea syndrome (OSAS): Comparison between multiple sleep latency test (MSLT) and maintenance of wakefulness test (MWT). Sleep Medicine 11(3):253–257, DOI 10.1016/j.sleep.2009.05.020

Fairclough SH (2009) Fundamentals of physiological computing. Interacting with Computers 21(1-2):133–145, DOI 10.1016/j.intcom.2008.10.011

Fernández T, Harmony T, Rodríguez M, Reyes A, Marosi E, Bernal J (1993) Test-retest reliability of EEG spectral parameters during cognitive tasks: I. Absolute and relative power. The International journal of neuroscience 68(3-4):255–261

Fernández T, Harmony T, Rodríguez M, Bernal J, Silva J, Reyes A, Marosi E (1995) EEG activation patterns during the performance of tasks involving different components of mental calculation. Electroencephalography and clinical neurophysiology 94(3):175–182, DOI 10.1016/0013-4694(94)00262-J

Findlay JM, Walker R (1999) A model of saccade generation based on parallel processing and competitive inhibition. The Behavioral and brain sciences 22(4):661–674; discussion 674–721, DOI 0140-525X/99

Freudenthaler N, Neuf H, Kadner G, Schlote T (2003) Characteristics of spontaneous eyeblink activity during video display terminal use in healthy volunteers. Graefe's Archive for Clinical and Experimental Ophthalmology 241(11):914–920, DOI 10.1007/s00417-003-0786-6

Galley N (1989) Saccadic eye movement velocity as an indicator of (de)activation. A review and some speculations

Galley N (1998) An enquiry into the relationship between activation and performance using saccadic eye movement parameters. Ergonomics 41(5):698–720, DOI 10.1080/001401398186865

Galley N, Schleicher R, Galley L (2004) Blink parameter as indicators of driver's sleepiness - possibilities and limitations. Vision in vehicles Amsterdam Elsevier pp 1–8, DOI 10.2307/20033668

Gevins A, Smith ME, McEvoy L, Yu D (1997) High-resolution EEG mapping of cortical activation related to working memory: Effects of task difficulty, type of processing, and practice. Cerebral Cortex 7(4):374–385, DOI 10.1093/cercor/7.4.374

Gevins A, Smith ME, Leong H, McEvoy L, Whitfield S, Du R, Rush G (1998) Monitoring working memory load during computer-based tasks with EEG pattern recognition methods. Human factors 40(1):79–91, DOI 10.1518/001872098779480578

Giakoumis D, Tzovaras D, Moustakas K, Hassapis G (2011) Automatic recognition of boredom in video games using novel biosignal moment-based features. IEEE Transactions on Affective Computing 2(3):119–133

Glass A (1966) Comparison of the effect of hard and easy mental arithmetic upon blocking of the occipital alpha rhythm. The Quarterly journal of experimental psychology 18(2):142–52, DOI 10.1080/14640746608400021

Godijn R, Theeuwes J (2002) Programming of endogenous and exogenous saccades: evidence for a competitive integration model. Tech. Rep. 5, DOI 10.1037/0096-1523.28.5.1039

Goldberger AL, Amaral LA, Glass L, Hausdorff JM, Ivanov PC, Mark RG, Mietus JE, Moody GB, Peng CK, Stanley HE (2000) PhysioBank, PhysioToolkit, and PhysioNet: components of a new research resource for complex physiologic signals. Circulation 101(23):E215–E220, DOI 10.1161/01.CIR.101.23.e215

Gómez I, Anaya P, Cabrera R, Molina AJ, Rivera O, Merino M (2010) Augmented and alternative communication system based on dasher application and an accelerometer. In: Lecture Notes in Computer Science (including subseries Lecture Notes in Artificial Intelligence and Lecture Notes in Bioinformatics), vol 6180 LNCS, pp 98–103, DOI 10.1007/978-3-642-14100-3_16

Gould KS, Hirvonen K, Koefoed VF, Rø ed BK, Sallinen M, Holm A, Bridger RS, Moen BE (2009) Effects of 60 hours of total sleep deprivation on two methods of high-speed ship navigation. Ergonomics 52(12):1469–1486, DOI 10.1080/00140130903272611

Graham FK, Hackley SA (1991) Passive and Active Attention to Input

Greenwood JP, Batin PD, Nolan J (1997) Assessment of cardiac autonomic function

Gruber T, Müller MM, Keil A, Elbert T (1999) Selective visual-spatial attention alters induced gamma band responses in the human EEG. Clinical Neurophysiology 110(12):2074–2085, DOI 10.1016/S1388-2457(99)00176-5

Guidera SA, Steinberg JS (1993) The signal-averaged P wave duration: a rapid and noninvasive marker of risk of atrial fibrillation. Journal of the American College of Cardiology 21(7):1645–1651, DOI 10.1016/0735-1097(93)90381-A

Han J, Ji X, Hu X, Guo L, Liu T (2015) Arousal Recognition Using Audio-Visual Features and FMRI-based Brain Response. IEEE Transactions on Affective Computing p 1, DOI 10.1109/TAFFC.2015.2411280

Harrison Y, Horne JA (2000) Sleep loss and temporal memory. Tech. Rep. 1, DOI 10.1080/713755870

Hasan J (1996) Past and future of computer-assisted sleep analysis and drowsiness assessment. Journal of clinical neurophysiology : official publication of the American Electroencephalographic Society 13(4):295–313, DOI 10.1097/00004691-199607000-00004

Himebaugh NL, Begley CG, Bradley A, Wilkinson JA (2009) Blinking and tear break-up during four visual tasks. Optometry and vision science : official publication of the American Academy of Optometry 86(2):E106–E114, DOI 10.1097/OPX.0b013e318194e962

Hirvonen K, Puttonen S, Gould K, Korpela J, Koefoed VF, Müller K (2010) Improving the saccade peak velocity measurement for detecting fatigue. Journal of Neuroscience Methods 187(2):199–206, DOI 10.1016/j.jneumeth.2010.01.010

Höhne W (1974) Zur Auswertung des Elektrookulogramms. Albrecht von Graefes Archiv fr Klinische und Experimentelle Ophthalmologie 192(1):35–47, DOI 10.1007/BF00411318

Hori T (1982) Electrodermal and electro-oculographic activity in a hypnagogic state. Psychophysiology 19(6):668–672

Horne JA, Reyner LA (1995) Sleep related vehicle accidents. BMJ (Clinical research ed) 310(6979):565–567, DOI 10.1136/bmj.310.6991.1411b

Howorka K, Pumprla J, Jirkovska A, Lacigova S, Nolan J (2010) Modified orthostatic load for spectral analysis of short-term heart rate variability improves the sensitivity of autonomic dysfunction assessment. Journal of diabetes and its complications 24(1):48–54, DOI 10.1016/j.jdiacomp.2008.10.003

Huigen E, Peper A, Grimbergen CA (2002) Investigation into the origin of the noise of surface electrodes. Medical & biological engineering & computing 40(3):332–338, DOI 10.1007/BF02344216

Iwanaga K, Saito S, Shimomura Y, Harada H, Katsuura T (2000) The effect of mental loads on muscle tension, blood pressure and blink rate. Journal of physiological anthropology and applied human science 19(3):135–141, DOI 10.2114/jpa.19.135

Janssen JH, Van Den Broek EL, Westerink JHDM (2012) Tune in to your emotions: A robust personalized affective music player. User Modelling and User-Adapted Interaction 22(3):255–279, DOI 10.1007/s11257-011-9107-7

Järvenpää J, Oikarinen L, Korhonen P, Väänänen H, Toivonen L, Viitasalo M (2007) Changing Capacity of Electrocardiographic Ventricular Repolarization in Post-Myocardial Infarction Patients With and Without Nonfatal Cardiac Arrest. American Journal of Cardiology 99(3):295–299, DOI 10.1016/j.amjcard.2006.08.027

Jasper HH (1958) The ten-twenty electrode system of the International Federation. Electroencephalography and Clinical Neurophysiology 10(2):371–375, DOI 10.1016/0013-4694(58)90053-1

Johnson R (1993) On the neural generators of the P300 component of the event-related potential. Psychophysiology 30(1):90–97, DOI 10.1111/j.1469-8986.1993.tb03208.x

Juhola M (1991) Median filtering is appropriate to signals of saccadic eye movements. Computers in biology and medicine 21(1-2):43–49, DOI 10.1016/0010-4825(91)90034-7

Kappas A (2010) Smile when you read this, whether you like it or not: Conceptual challenges to affect detection. IEEE Transactions on Affective Computing 1(1):38–41

Khushaba RN, Kodagoda S, Takruri M, Dissanayake G (2012) Toward improved control of prosthetic fingers using surface electromyogram (EMG) signals. Expert Systems with Applications 39(12):10,731–10,738, DOI 10.1016/j.eswa.2012.02.192

Kim EYKEY, Kang SKKSK, Jung KJK, Kim HJKHJ (2005) Eye mouse: mouse implementation using eye tracking. 2005 Digest of Technical Papers International Conference on Consumer Electronics, 2005 ICCE DOI 10.1109/ICCE.2005.1429790

Kim KH, Bang SW, Kim SR (2004) Emotion recognition system using short term monitoring of physiological signals. Medical and Biological Engineering and Computing computing 42(3):419–427

Kleiger RE, Stein PK, Bosner MS, Rottman JN (1992) Time domain measurements of heart rate variability. Cardiology clinics 10(3):487–498

Klimesch W (1997) EEG-alpha rhythms and memory processes. In: International Journal of Psychophysiology, vol 26, pp 319–340, DOI 10.1016/S0167-8760(97)00773-3

Klimesch W (1999) EEG alpha and theta oscillations reflect cognitive and memory performance: a review and analysis. Brain research Brain research reviews 29(2-3):169–195, DOI 10.1016/S0165-0173(98)00056-3

Klobassa DS, Vaughan TM, Brunner P, Schwartz NE, Wolpaw JR, Neuper C, Sellers EW (2009) Toward a high-throughput auditory P300-based brain-computer interface. Clinical Neurophysiology 120(7):1252–1261, DOI 10.1016/j.clinph.2009.04.019

Köhler BU, Hennig C, Orglmeister R (2002) The principles of software QRS detection. IEEE Engineering in Medicine and Biology Magazine 21(1):42–57, DOI 10.1109/51.993193

Korhonen P, Husa T, Konttila T, Tierala I, Mäkijärvi M, Väänänen H, Toivonen L (2009) Complex T-wave morphology in body surface potential mapping in prediction of arrhythmic events in patients with acute myocardial infarction and cardiac dysfunction. Europace 11(4):514–520, DOI 10.1093/europace/eup051

Krupiński R, Mazurek P (2009a) Estimation of eye blinking using biopotentials measurements for computer animation applications. Lecture Notes in Computer Science (including subseries Lecture Notes in Artificial Intelligence and Lecture Notes in Bioinformatics) 5337 LNCS:302–310, DOI 10.1007/978-3-642-02345-3_30

Krupiński R, Mazurek P (2009b) Median filters optimization for electrooculography and blinking signal separation using synthetic model. In: IFAC Proceedings Volumes (IFAC-PapersOnline), vol 14, pp 326–331

Krupiński R, Mazurek P (2010) Towards to real-time system with optimization based approach for EOG and blinking signals separation for human computer interaction, Lecture Notes in Computer Science, vol 6179. Springer Berlin Heidelberg, Berlin, Heidelberg, DOI 10.1007/978-3-642-14097-6

Kurisu S, Watanabe N, Ikenaga H, Shimonaga T, Higaki T, Iwasaki T, Mitsuba N, Ishibashi K, Dohi Y, Kihara Y (2014) Effects of eplerenone on P-wave signal-averaged electrocardiogram in hypertensive patients with coronary artery disease. International journal of cardiology 172(1):e180–1, DOI 10.1016/j.ijcard.2013.12.154

Lacey JI (1967) Somatic response patterning and stress: Some revisions of activation. In: Appley MH, Trumbell R (eds) Psychological Stres: Issues in Research, Appleton-Century-Crofts, New York, pp 14–37

Laparra-Hernández J, Belda-Lois JM, Medina E, Campos N, Poveda R (2009) EMG and GSR signals for evaluating user's perception of different types of ceramic flooring. International Journal of Industrial Ergonomics 39(2):326–332, DOI 10.1016/j.ergon.2008.02.011

Levenson RW (1992) Autonomic Nervous System Differences Among Emotions. DOI 10.1111/j.1467-9280.1992.tb00251.x

Li CL, Jasper H (1953) Microelectrode studies of the electrical activity of the cerebral cortex in the cat. The Journal of physiology 121(1):117–40

Lorente De Nó R (1947) Action potential of the motoneurons of the hypoglossus nucleus. Journal of Cellular and Comparative Physiology 29(3):207–287, DOI 10.1002/jcp.1030290303

Lorenzo I, Ramos J, Arce C, Guevara MA, Corsi-Cabrera M (1995) Effect of total sleep deprivation on reaction time and waking EEG activity in man. Sleep 18(5):346–354

Luttmann A, Schmidt KH, Jäger M (2010) Working conditions, muscular activity and complaints of office workers. International Journal of Industrial Ergonomics 40(5):549–559

Lutzenberger W, Elbert T, Rockstroh B (1987) A brief tutorial on the implications of volume conduction for the interpretation of the EEG

MacKenzie IS, Ashtiani B (2011) BlinkWrite: Efficient text entry using eye blinks. Universal Access in the Information Society 10(1):69–80, DOI 10.1007/s10209-010-0188-6

Madeiro JaPV, Cortez PC, Marques JaaL, Seisdedos CRV, Sobrinho CRMR (2012) An innovative approach of QRS segmentation based on first-derivative, Hilbert and Wavelet Transforms. Medical Engineering and Physics 34(9):1236–1246, DOI 10.1016/j.medengphy.2011.12.011

Magosso E, Ursino M, Zaniboni a, Provini F, Montagna P (2007) Visual and computer-based detection of slow eye movements in overnight and 24-h EOG recordings. Clinical Neurophysiology 118(5):1122–1133, DOI 10.1016/j.clinph.2007.01.014

Malliani A (1994) Editorial Power spectrum analysis of heart rate variability : a tool to explore neural regulatory mechanisms. British Heart Journal 71:1–2, DOI 10.1126/science.6166045

Malliani A, Pagani M, Lombardi F, Cerutti S (1991) Cardiovascular neural regulation explored in the frequency domain. Circulation 84(2):482–492, DOI 10.1161/01.CIR.84.2.482

Manganotti P, Formaggio E, Storti SF, De Massari D, Zamboni a, Bertoldo a, Fiaschi a, Toffolo GM (2012) Time-frequency analysis of short-lasting modulation of EEG induced by intracortical and transcallosal paired TMS over motor areas. Journal of Neurophysiology 107(9):2475–2484, DOI 10.1152/jn.00543.2011

Manganotti P, Formaggio E, Del Felice A, Storti SF, Zamboni A, Bertoldo A, Fiaschi A, Toffolo GM (2013) Time-frequency analysis of short-lasting modulation of EEG induced by TMS during wake, sleep deprivation and sleep. Frontiers in human neuroscience 7(November):767, DOI 10.3389/fnhum.2013.00767

Manikandan MS, Soman KP (2012) A novel method for detecting R-peaks in electrocardiogram (ECG) signal. Biomedical Signal Processing and Control 7(2):118–128, DOI 10.1016/j.bspc.2011.03.004

Manor BR, Gordon E (2003) Defining the temporal threshold for ocular fixation in free-viewing visuocognitive tasks. Journal of Neuroscience Methods 128(1-2):85–93, DOI 10.1016/S0165-0270(03)00151-1

Martinez M, Soria E, Magdalena R, Martínez M, José A, Martín JD, Vila J (2008) Comparative study of several Fir Median Hybrid Filters for blink noise removal in Electrooculograms. WSEAS Transactions on Signal Processing 4(3):53–59

Mattiocco M, Babiloni F, Mattia D, Bufalari S, Sergio S, Salinari S, Marciani MG, Cincotti F (2006) Neuroelectrical source imaging of mu rhythm control for BCI applications. In: Annual International Conference of the IEEE Engineering in Medicine and Biology - Proceedings, pp 980–983, DOI 10.1109/IEMBS.2006.260128

Mehta SS, Shete Da, Lingayat NS, Chouhan VS (2010) K-means algorithm for the detection and delineation of QRS-complexes in Electrocardiogram. Irbm 31(1):48–54, DOI 10.1016/j.irbm.2009.10.001

Merino M, Gómez I, Rivera O, Molina AJ (2010a) Customizable Software Interface for Monitoring Applications. In: Lecture Notes in Computer Science (including subseries Lecture Notes in Artificial Intelligence and Lecture Notes in Bioinformatics), ICCHP 2010, Part I, LNCS 6179, pp 148–153

Merino M, Rivera O, Gómez I, Molina A, Dorronzoro E (2010b) A method of EOG signal processing to detect the direction of eye movements. In: Proceedings - 1st International Conference on Sensor Device Technologies and Applications, SENSORDEVICES 2010, pp 100–105

Merino M, Gómez I, Molina AJ, Guzman K (2012) Assessment of Biosignals for Managing. In: Lecture Notes in Computer Science (including subseries Lecture Notes in Artificial Intelligence and Lecture Notes in Bioinformatics), ICCHP 2012, Part II, LNCS 7383, pp 331–337

Merino M, Gómez IM, Molina AJ (2015a) Envelope filter sequence to delete blinks and overshoots. Biomedical Engineering Online 14:1–23, DOI 10.1186/s12938-015-0046-0

Merino M, Gómez IM, Molina AJ (2015b) Envelopment filter and K-means for the detection of QRS waveforms in electrocardiogram. Medical Engineering & Physics 37(6):605–609, DOI 10.1016/j.medengphy.2015.03.019

Merino M, Gómez I, Molina AJ (in press 2015) EEG Feature Variations under Stress Situations. In: 37th Annual International Conference of the IEEE Engineering in Medicine and Biology Society

Molnár M (1994) On the origin of the P3 event-related potential component. International journal of psychophysiology : official journal of the International Organization of Psychophysiology 17(2):129–144, DOI 10.1016/0167-8760(94)90028-0

Monge MM, Gomez I, Molina A (2014) Stress and heart rate : significant parameters and their variations Article Type : original article. Exp Clin Cardiol 20(8):3509–3517

Morris TL, Miller JC (1996) Electrooculographic and performance indices of fatigue during simulated flight. In: Biological Psychology, vol 42, pp 343–360, DOI 10.1016/0301-0511(95)05166-X

Nam CS, Jeon Y, Li Y, Kim Yj, Yoon Hy (2009) Usability of the P300 Speller : Towards a More Sustainable Brain-Computer Interface. eMinds: International Journal on Human-Computer Interaction I(5):111–125

Nasoz F, Lisetti CL, Vasilakos AV (2010) Affectively intelligent and adaptive car interfaces. Information Sciences 180(20):3817–3836, DOI 10.1016/j.ins.2010.06.034

Neejärvi J, Värri A, Fotopoulos S, Neuvo Y (1993) Weighted FMH filters. DOI 10.1016/0165-1684(93)90064-H

Nikara T, Sato S, Takamatsu T, Sato R, Mita T (1976) A new wave (2nd c-wave) on corneoretinal potential. Experientia 32(5):594–596, DOI 10.1007/BF01990182

Norman DA (2007) The Design of Future Things, vol 18. DOI 10.1002/hfm.20127

Nunez PL, Srinivasan R (2006) Electric Fields of the Brain: The Neurophysics of EEG, vol 4

Nussbaum G, Veigl C, Miesenberger K (2009) EMG signal controlled pneumatic gripper for mouthsticks. In: Assistive Technology Research Series, vol 25, pp 36–40, DOI 10.3233/978-1-60750-042-1-36

Nygårds ME, Sörnmo L (1983) Delineation of the QRS complex using the envelope of the e.c.g. Medical & Biological Engineering & Computing 21(5):538–547, DOI 10.1007/BF02442378

Oberman LM, Hubbard EM, McCleery JP, Altschuler EL, Ramachandran VS, Pineda JA (2005) EEG evidence for mirror neuron dysfunction in autism spectrum disorders. Cognitive Brain Research 24(2):190–198, DOI 10.1016/j.cogbrainres.2005.01.014

Obrist PA (1976) The Cardiovascular-Behavioral Interaction?As It Appears Today. Psychophysiology 13(2):95–107, DOI 10.1111/j.1469-8986.1976.tb00081.x

Olson GM, Olson JS (2003) Human-computer interaction: psychological aspects of the human use of computing. Annual review of psychology 54:491–516, DOI 10.1146/annurev.psych.54.101601.145044

Oostenveld R, Praamstra P (2001) The five percent electrode system for high-resolution EEG and ERP measurements. Clinical Neurophysiology 112(4):713–719, DOI 10.1016/S1388-2457(00)00527-7

Ozkan G, Adar A, Ulusoy S, Bektaş H, Kırış A, Fidan M, Celik S (2014) Presence of fragmented QRS and its correlation with myocardial performance index in patients with nephrotic syndrome. Anadolu kardiyoloji dergisi : AKD = the Anatolian journal of cardiology 14(5):450–5, DOI 10.5152/akd.2014.4886

Pal S, Mitra M (2012) Empirical mode decomposition based ECG enhancement and QRS detection. Computers in Biology and Medicine 42(1):83–92, DOI 10.1016/j.compbiomed.2011.10.012

Pan J, Tompkins WJ (1985) A Real-Time QRS Detection Algorithm. IEEE Transactions on Biomedical Engineering 32(3):230–236

Parini S, Maggi L, Turconi AC, Andreoni G (2009) A robust and self-paced BCI system based on a four class SSVEP paradigm: Algorithms and protocols for a high-transfer-rate direct brain communication. Computational Intelligence and Neuroscience 2009, DOI 10.1155/2009/864564

Pastor MC, Bradley MM, Löw A, Versace F, Moltó J, Lang PJ (2008) Affective picture perception: Emotion, context, and the late positive potential. Brain Research 1189(1):145–151, DOI 10.1016/j.brainres.2007.10.072, 0402594v3

Pellicori P, Joseph AC, Zhang J, Lukaschuk E, Sherwi N, Bourantas CV, Loh H, Clark AL, Cleland JG (2015) The relationship of QRS morphology with cardiac structure and function in patients with heart failure. Clinical research in cardiology : official journal of the German Cardiac Society DOI 10.1007/s00392-015-0861-0

Petrantonakis PC, Hadjileontiadis LJ (2009) EEG-based emotion recognition using hybrid filtering and higher order crossings. In: 2009 3rd International Conference on Affective Computing and Intelligent Interaction and Workshops, ACII 2009, Affiliation: Department of Electrical and Computer Engineering, Aristotle University of Thessaloniki, GR-54124 Thessaloniki, Greece; Correspondence Address: Petrantonakis, P. C.; Department of Electrical and Computer Engineering, Aristotle University of T

Petrantonakis PC, Hadjileontiadis LJ (2010a) Emotion recognition from brain signals using hybrid adaptive filtering and higher order crossings analysis. IEEE Transactions on Affective Computing 1(2):81–97

Petrantonakis PC, Hadjileontiadis LJ (2010b) Emotion recognition from EEG using higher order crossings. IEEE Transactions on Information Technology in Biomedicine 14(2):186–197

Petsche H, Pockberger H, Rappelsberger P (1986) EEG Topography and Mental Performance. In: Duffy F (ed) Topographic mapping of the brain, Butterworths-Heinemann, Stoneham, pp 63–98

Pfister T, Robinson P (2011) Real-time recognition of affective states from nonverbal features of speech and its application for public speaking skill analysis. IEEE Transactions on Affective Computing 2(2):66–78, DOI 10.1109/T-AFFC.2011.8

Pfurtscheller G, Grabner RH, Brunner C, Neuper C (2007) Phasic heart rate changes during word translation of different difficulties. Psychophysiology 44(5):807–813

Picard RW (1997) Affective Computing, vol 136. DOI 10.1007/BF01238028

Picton TW, Hillyard S (1988) Endogenous event-related potentials. In: Handbook of Electroencephalography and Clinical Neurophysiology, Revised Series, Vol. 3: Human Event Related Potentials, pp 361–426

Pomeranz B, Macaulay RJ, Caudill MA, Kutz I, Adam D, Gordon D, Kilborn KM, Barger AC, Shannon DC, Cohen RJ (1985) Assessment of autonomic function in humans by heart rate spectral analysis. The American journal of physiology 248(1 Pt 2):H151–3

Porcu S, Ferrara M, Urbani L, Bellatreccia a, Casagrande M (1998) Smooth-Pursuit and Saccadic Eye-Movements as Possible Indicators of Nighttime Sleepiness. Physiology & Behavior 65(3):437–443

Pumprla J, Howorka K, Groves D, Chester M, Nolan J (2002) Functional assessment of heart rate variability: Physiological basis and practical applications. DOI 10.1016/S0167-5273(02)00057-8

Radach R, Heller D, Inhoff A (1999) Occurrence and function of very short fixation durations in reading. Plenum Press, New York

Rajendra Acharya U, Rajendra Acharya U, Paul Joseph K, Paul Joseph K, Kannathal N, Kannathal N, Lim CM, Lim CM, Suri JS, Suri JS (2006) Heart rate variability: a review. Medical & biological engineering & computing 44(12):1031–51, DOI 10.1007/s11517-006-0119-0, s11517-006-0119-0

Ray WJ (1990) The electrocortical system. In: Cacioppo J, Tassinary L (eds) Principles of psychophysiology: Physical, social, and inferential elements, Cambridge University Press, New York, pp 385–412

Ray WJ, Cole HW (1985) EEG alpha activity reflects attentional demands, and beta activity reflects emotional and cognitive processes. Science (New York, NY) 228(4700):750–752, DOI 10.1126/science.3992243

Ritsema Van Eck HJ, Kors JA, Van Herpen G (2005) The U wave in the electrocardiogram: A solution for a 100-year-old riddle. Cardiovascular Research 67(2):256–262, DOI 10.1016/j.cardiores.2005.04.010

Rizzolatti G, Craighero L (2004) The mirror-neuron system. Annual review of neuroscience 27:169–192, DOI 10.1146/annurev.neuro.27.070203.144230

Rowland LM, Thomas ML, Thorne DR, Sing HC, Krichmar JL, Davis HQ, Balwinski SM, Peters RD, Kloeppel-Wagner E, Redmond DP, Alicandri E, Belenky G (2005) Oculomotor responses during partial and total sleep deprivation. Aviat Space Environ Med 76(7 Suppl):C104–13

Russo M, Thomas M, Thorne D, Sing H, Redmond D, Rowland L, Johnson D, Hall S, Krichmar J, Balkin T (2003) Oculomotor impairment during chronic partial sleep deprivation. Clinical Neurophysiology 114(4):723–736, DOI 10.1016/S1388-2457(03)00008-7

Sallinen M, Härmä M, Akila R, Holm A, Luukkonen R, Mikola H, Müller K, Virkkala J (2004) The effects of sleep debt and monotonous work on sleepiness and performance during a 12-h dayshift. Journal of Sleep Research 13(4):285–294, DOI 10.1111/j.1365-2869.2004.00425.x

Saul JP (1990) Beat-To-Beat Variations of Heart Rate Reflect Modulation of Cardiac Autonomic Outflow. Physiology 5(1):32–37

Saul JP, Rea RF, Eckberg DL, Berger RD, Cohen RJ (1990) Heart rate and muscle sympathetic nerve variability during reflex changes of autonomic activity. The American journal of physiology 258(3 Pt 2):H713–H721

Scerbo AS, Freedman LW, Raine A, Dawson ME, Venables PH (1992) A major effect of recording site on measurement of electrodermal activity. Psychophysiology 29(2):241–246, DOI 10.1111/j.1469-8986.1992.tb01693.x

Schiffman H (2001) Sensation and perception: An integrated approach . New York

Schleicher R, Galley N, Briest S, Galley L (2008) Blinks and saccades as indicators of fatigue in sleepiness warnings: looking tired? Ergonomics 51(7):982–1010, DOI 10.1080/00140130701817062

Setz C, Arnrich B, Schumm J, Marca RL, Tröster G, Ehlert U (2010) Discriminating stress from cognitive load using a wearable eda device. IEEE Transactions on Information Technology in Biomedicine 14(2):410–417

Shi Y, Ruiz N, Taib R, Choi E, Chen F (2007) Galvanic skin response (GSR) as an index of cognitive load. In: 25th SIGCHI Conference on Human Factors in Computing Systems 2007, CHI 2007, Affiliation: National ICT Australia, Technology Park, Bay 15, Eveleigh, NSW 1430, Australia; Correspondence Address: Shi, Y.; National ICT Australia, Technology Park, Bay 15, Eveleigh, NSW 1430, Australia; email: yu.shi@nicta.com.au, pp 2651–2656

Singh H, Singh J (2012) A Review on Electrooculography. International Journal of Advanced Engineering Technology 3(4):115–122

Singh RR, Conjeti S, Banerjee R (2011) An approach for real-time stress-trend detection using physiological signals in wearable computing systems for automotive drivers. In: 14th IEEE International Intelligent Transportation Systems Conference, ITSC 2011, Affiliation: Department of Electrical and Electronics Engineering, Birla Institute of Technology and Science (BITS) Pilani, Rajasthan, 333031, India; Affiliation: Department of Computer Science, Birla Institute of Technology and Science (BITS) Pilani, Raj, pp 1477–1482

Sirevaag EJ, Stern JA (2000) Ocular measures of fatigue and cognitive factors. Engineering psychophysiology: Issues and applications pp 269–287

Soleymani M, Chanel G, Kierkels JJM, Pun T (2008) Affective characterization of movie scenes based on multimedia content analysis and user's physiological emotional responses. In: Proceedings - 10th IEEE International Symposium on Multimedia, ISM 2008, pp 228–235, DOI 10.1109/ISM.2008.14

Song-kai Z, Jian-Tao W, Jun-Rong X (1988) The real-time detection of QRS-complex using the envelop of ECG. IEEE Engineering in Medicine and Biology Magazine 10(1):38

Sörnmo L, Laguna P, Emg T, Caton R, Berger H, Jacob ST, Reddy JK, Eps I, Sanei S, Chambers J, Waller A, Dutch T, Einthoven W, Prize N (2014) Bioelectrical Signal Processing in Cardiac and Neurological Applications. Gene expression 16:49, DOI 10.1002/9780470511923

Stemmler G (1989) The autonomic differentiation of emotions revisited: convergent and discriminant validation. Psychophysiology 26(6):617–632, DOI 10.1111/j.1469-8986.1989.tb03163.x

Steven A M, Matrhew Y, Camelia C, Burcu D (2010) The Effects of Acute Stress on Cognitive Performance

Sun Ft, Kuo C, Cheng Ht, Buthpitiya S, Collins P, Griss M (2012) Activity-Aware Mental Stress Detection Using Physiological Sensors. Mobile Computing, Applications, and Services pp 211–230, DOI 10.1007/978-3-642-29336-8_12

Surawicz B, Orr CM, Hermiller JB, Bell KD, Pinto RP (1997) QRS Changes During Percutaneous Transluminal Coronary Angioplasty and Their Possible Mechanisms. Journal of the American College of Cardiology 30(2):452–458, DOI 10.1016/S0735-1097(97)00165-4

Tamura A, Watanabe T, Nagase K, Mikuriya Y, Nasu M (1997) Significance of negative U waves in the precordial leads during anterior wall acute myocardial infarction. American Journal of Cardiology 79(7):897–900, DOI 10.1016/S0002-9149(97)00011-8

Thomas M, Sing H, Belenky G, Holcomb H, Mayberg H, Dannals R, Wagner J, Thorne D, Popp K, Rowland L, Et Al (2000) Neural basis of alertness and cognitive performance impairments during sleepiness. I. Effects of 24 h of sleep deprivation on waking regional brain activity. Journal of Sleep Research 9(4):335–352

Turpin G (1986) Effects of Stimulus Intensity on Autonomic Responding: The Problem of Differentiating Orienting and Defense Reflexes. Psychophysiology 23(1):1–14, DOI 10.1111/j.1469-8986.1986.tb00583.x

Uchida S, Maloney T, Feinberg I (1994) Sigma (12-16 Hz) and beta (20-28 Hz) EEG discriminate NREM and REM sleep. Brain research 659(1-2):243–248, DOI 10.1016/0006-8993(94)90886-9

Valentino DA, Arruda JE, Gold SM (1993) Comparison of QEEG and response accuracy in good vs poorer performers during a vigilance task. International Journal of Psychophysiology 15(2):123–133, DOI 10.1016/0167-8760(93)90070-6

Vila J, Fernández M (1989) The cardiac defense response in humans: Effects of predictability and adaptation period. Journal of Psychophysiology 3(3):245–258

Wang B, Korhonen P, Tierala I, Hänninen H, Väänänen H, Toivonen L (2013) U Wave Features in Body Surface Potential Mapping in Post-Myocardial Infarction Patients. Annals of Noninvasive Electrocardiology 18(6):538–546, DOI 10.1111/anec.12071

Wang Y, Deepu CJ, Lian Y (2011) A computationally efficient QRS detection algorithm for wearable ECG sensors. Proceedings of the 33rd Annual International Conference of the IEEE Engineering in Medicine and Biology Society, EMBS pp 5641–5644, DOI 10.1109/IEMBS.2011.6091365

Ward RD, Marsden PH (2004) Affective computing: Problems, reactions and intentions. Interacting with Computers 16(4):707–713, DOI 10.1016/j.intcom.2004.06.002

Weber RB, Daroff RB (1971) The metrics of horizontal saccadic eye movements in normal humans. Vision research 11(9):921–928, DOI 10.1016/0042-6989(71)90212-4

Wu D, Courtney CG, Lance BJ, Narayanan SS, Dawson ME, Oie KS, Parsons TD (2010) Optimal arousal identification and classification for affective computing using physiological signals: Virtual reality stroop task. IEEE Transactions on Affective Computing 1(2):109–118

Yan J, Lu L (2014) Improved Hilbert-Huang transform based weak signal detection methodology and its application on incipient fault diagnosis and ECG signal analysis. Signal Processing 98:74–87, DOI 10.1016/j.sigpro.2013.11.012

Yathunanthan S, Chandrasena LUR, Umakanthan A, Vasuki V, Munasinghe SR (2008) Controlling a wheelchair by use of EOG signal. In: Proceedings of the 2008 4th International Conference on Information and Automation for Sustainability, ICIAFS 2008, pp 283–288, DOI 10.1109/ICIAFS.2008.4783987

Ye C, Vijaya Kumar BVK, Coimbra MT (2012) Heartbeat classification using morphological and dynamic features of ECG signals. IEEE Transactions on Biomedical Engineering 59(10):2930–2941, DOI 10.1109/TBME.2012.2213253

Zils E, Sprenger A, Heide W, Born J, Gais S (2005) Differential effects of sleep deprivation on saccadic eye movements. Sleep 28(9):1109–1115

Fe de errores

Durante la redacción de esta tesis, al revisar los artículos que la constituye, han sido detectados los siguientes errores:

1. En la sección 4.2.4, en el punto "*4. Work and Results*" de la publicación Merino et al (2012): se dice erróneamente que el test psicológico STAI muestra que los sujetos estaban más excitados al inicio de la tarea que al final, cuando la realidad es que se observó un general incremento del nivel de excitación en los sujetos durante la realización de la actividad (los valores del test son menores en al finalizar la tarea que al inicio), excepto para dos individuos durante el uso de la señal EMG como interfaz de control.

2. En la sección 4.3.1, en el punto "*III. Result - B. Electroencephalogram*" en la publicación Merino et al (in press 2015): en él pone *"Second statistic analysis showed non-significant changes of all features respect to first activity phase, whereas, in memory, significant variations were obtained in Ac in P4 during second performance, and* $\overline{AS_\theta}$ *in FC3 and* $\overline{AS_\alpha}$ *in F3 during third activity phase"*. El texto debería decir "Second statistic analysis showed non-significant changes of all features respect to first activity phase ***during arithmetic task***, whereas, in memory, significant variations were obtained in *Ac* in P4 during second performance, and $\overline{AS_\theta}$ in FC3 and $\overline{AS_\alpha}$ in F3 during third activity phase".

3. En la sección 4.3.1, en el punto "*IV. Conclusion and Future Work*" en la publicación Merino et al (in press 2015): en la penúltima oración se dice que "Also, F3 is a common position[...]". Además de F3, hay que indicar que Fz también es una posición común, y que ambas localizaciones concentran una cantidad de variaciones significativas de parámetros respecto a las demás.

4. En la sección 4.3.1, en el punto "*IV. Conclusion and Future Work*" en la publicación Merino et al (in press 2015): en la penúltima oración se dice que "[...] P4 is mainly linked with memory performance". Falta añadir que la posición C3 está ligada a la actividad matemática.